

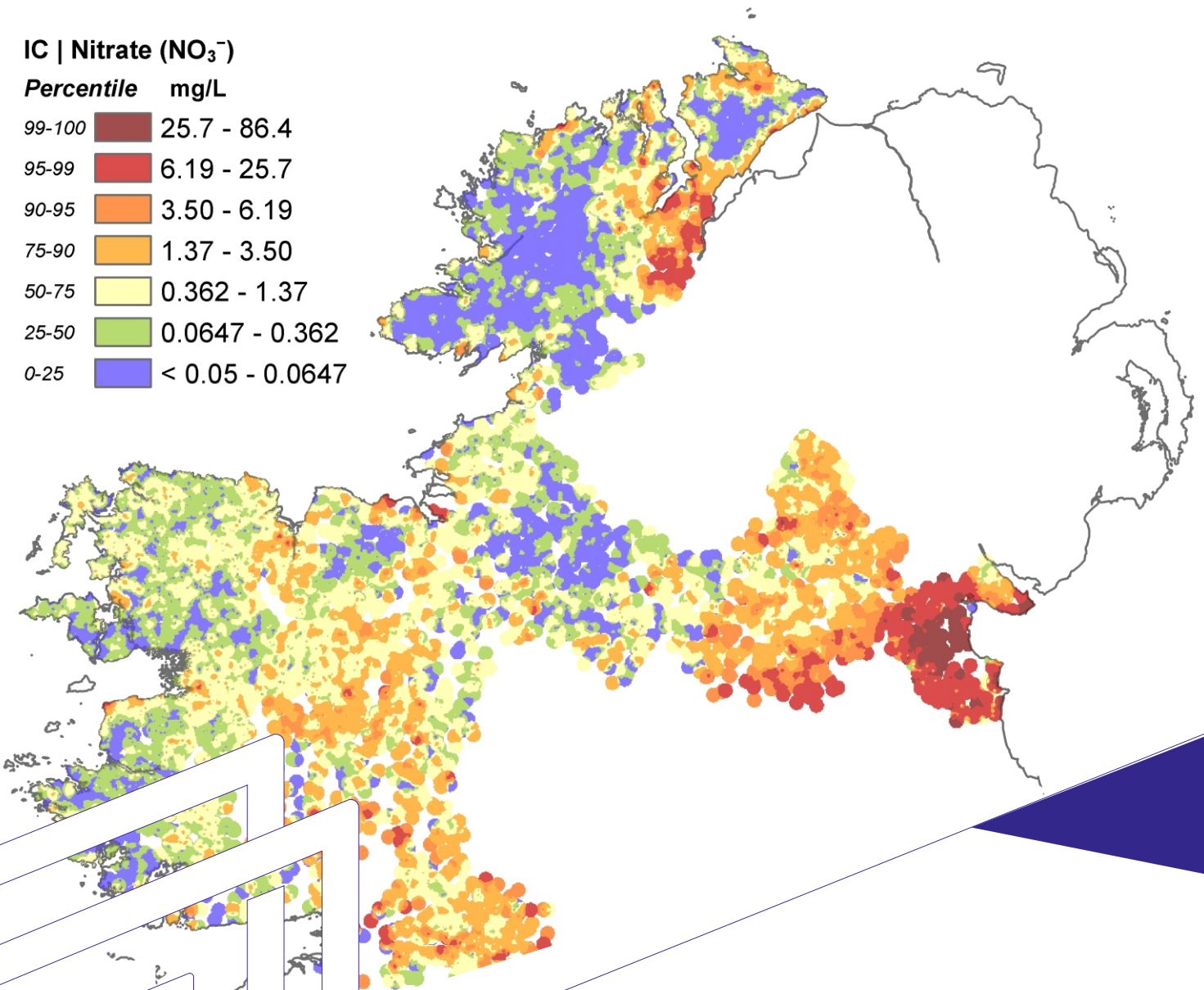


Tellus Border and West Stream Water Data Analysis and Interpretation

IC | Nitrate (NO_3^-)

Percentile mg/L

99-100	25.7 - 86.4
95-99	6.19 - 25.7
90-95	3.50 - 6.19
75-90	1.37 - 3.50
50-75	0.362 - 1.37
25-50	0.0647 - 0.362
0-25	< 0.05 - 0.0647



Geological Survey Ireland Report 2021

Version History

Ver. No.	Ver. Date	Comment	Revised By
1	03 November 2021	Version 1	

Disclaimer

The geochemical data presented in this report are from individual sites, which were sampled as part of a baseline geochemical survey. The results should only be used to set a regional context, not as the basis for interpretations concerning specific sites. Interpretations relating to specific sites should be based on follow-up site-specific investigations.

Although every effort has been made to ensure the accuracy of the material contained in this report, complete accuracy cannot be guaranteed. Neither Geological Survey Ireland nor the authors accept any responsibility whatsoever for loss or damage occasioned, or claimed to have been occasioned, in part or in full as a consequence of any person acting or refraining from acting, as a result of a matter contained in this report.

Reference:

Gallagher, V., Grunsky, E., Fitzsimons, M., Browne, M., Lilburn, S. and Symons, J. (2021) Tellus Border and West Stream Water Data Analysis and Interpretation. Geological Survey Ireland report.



Contents

Executive summary	4
1. Introduction	7
1.1 Background	7
1.2 Surface water geochemistry data in Ireland	8
1.3 Anthropogenic impacts on surface water chemistry	8
1.3.1 Potentially Harmful Substances	9
1.3.2 Nutrients: nitrate and phosphorus.....	9
1.4 Mineral exploration.....	11
1.5 Objectives.....	12
2. Dataset descriptions	13
2.1 Tellus data	13
2.2 Supporting datasets	14
3. Univariate mapping and statistical analysis	17
3.1 Geogenic controls	17
3.3. Potentially Harmful Substances	27
3.3.1 Background concentrations of metals in stream waters	29
3.3.2 EQS and water hardness.....	32
3.4 Stream Water Geochemistry and Mineralization	38
3.4.1 Review of mineralization in the region	38
3.4.2 Base metal mineralization and surface water geochemistry	39
3.4.3 Gold mineralization and stream water geochemistry.....	45
3.5. Anthropogenic impacts on stream water: nitrate and phosphorus	46



4. Multivariate statistical analysis.....	54
4.1 Data preparation for multivariate statistical analysis	54
4.2 Principal Component Analysis.....	55
4.2.1 Principal Components Associated with Rock Type.....	56
4.2.2 Principal Components Associated with Subsoil type	58
4.2.3 Principal Components Associated with SRF Geochemical Domains	60
4.2.4 Principal Components Associated with Land Cover classes	63
4.2.5 Principal Components: Mineralization	67
4.2.6 Multivariate assessment of selected elements/anions associated with anthropogenic activity.....	72
4.3 Cluster Analysis	77
4.3.1 Hierarchal Cluster Analysis.....	77
4.3.2 Other Methods of Clustering Tellus Waters Geochemistry	80
4.4 Random Forests Classification	81
4.4.1 Random Forests – Rock Type.....	81
4.4.2 Random Forests – Teagasc Subsoil.....	84
4.4.3 Random Forests – SRF Geochemical Domains	86
4.4.4 Random Forests – Land Cover	88
5. Summary and Conclusions	90
5.1 Geogenic control of stream water chemistry	90
5.2 Background stream water concentrations.....	91
5.3 Natural and anthropogenic processes influencing stream water	92
5.4 Mineralization signatures.....	94
6. References	95



Executive summary

Baseline geochemical analysis of stream water samples, collected from streams in the northern and western regions of Ireland, has been completed as part of the Tellus programme.

Data analysis has been carried out to explore spatial and statistical patterns in the data relating to geology and human activity. Univariate and multivariate analysis techniques, including Exploratory Data Analysis, Principal Component Analysis, Cluster Analysis and Random Forests have been undertaken and they demonstrate that there are coherent geochemical patterns related to underlying bedrock geology, subsoil composition and the influence of agriculture on water quality. The findings are relevant for the assessment of substances of concern in the environment, including Specific Pollutants, Priority Substances and nutrients. They also show that stream water chemistry has the potential to be employed in mineral exploration.

Geological signature

The geochemistry of stream waters reflects the contact that the water has with geological materials (soil, rock, sediment) as well as inputs from precipitation, groundwater and human activities. The Tellus survey targets first- and second-order streams, i.e. small up-catchment tributaries, and they are sampled during the drier summer months. As such, their chemical composition is considered to be influenced primarily by geology, i.e. bedrock and subsoil, since the sampling sites are typically upstream of significant human influences such as industry and urban environments. Multivariate analysis techniques show that there are strong associations between specific element assemblages in water geochemistry and particular rock and subsoil types, most notably limestone and granite, and tills derived from those rocks.

Nutrients

Data analysis shows that areas of intensive crop cultivation are characterized by higher nitrate and phosphorus concentrations than areas of other land uses. The median nitrate concentration for Tellus stream water draining arable land (21.2 mg/L) is over 18 times higher than for pastureland (1.19 mg/L) and almost 80 times higher than for other land uses. Similar, if less stark, distinctions were observed for phosphorus. Stream water draining well-drained soil had significantly higher concentration of both nitrate and phosphorus than stream water draining soil in other drainage classes. 4% of nitrate concentrations observed as part of this survey fall within the EPA's unsatisfactory category, compared to 47% of samples taken from larger watercourses as part of the EPA monitoring programme. Of these 'unsatisfactory' observations in the Tellus dataset, 96% occur in areas of agricultural land use, including pasture and arable types.

The association between agricultural activity and nitrate and phosphorus levels in stream waters is well known from EPA monitoring programmes. However, Tellus data provide a



more detailed picture of the impact of agriculture on water quality since the samples were collected from first- and second-order streams. They demonstrate that these impacts are pervasive, detectable even in the upper parts of catchments, with highest nutrient levels in areas of improved agricultural land (tillage and pasture).

Potentially harmful substances

In Ireland national monitoring programmes coordinated by the Environmental Protection Agency aim to support the reduction or elimination of contamination of surface water by Priority Substances, Priority Hazardous Substances and Specific Pollutants as listed in the Surface Water Regulations 2009 (European Commission 2009). Substances listed that are also part of the Tellus stream water data set are arsenic (As), cadmium (Cd), chromium (Cr), copper (Cu), fluoride (F-), lead (Pb), nickel (Ni) and zinc (Zn).

The environmental quality standards (EQSs) for metals are specified in relation to different levels of water hardness and natural background concentrations. To date in Ireland, in the absence of regional data for water hardness and background concentrations, the most conservative EQSs have been applied by default. Here Exploratory Data Analysis is used to assist with the derivation of natural background concentrations for As, Cr, Cu and Zn. For As, the estimated background concentration is 10 µg/L, for Cr 1.8 µg/L and for Cu 10 µg/L. In the case of Zn, the distribution is complex, reflecting its widespread dispersion in stream water across the region, and two threshold levels can be observed: one at 6.5 µg/L and a second at 34 µg/L that reflects widely dispersed samples in the 95-99th percentile range, which may be related to complexation by organic matter and mineralization, among other factors. Results indicate that there is good potential to use Tellus stream water data to compute background levels for relevant metals, allowing potential refinement of the EQSs at a national level when Tellus is complete.

The EQS values for Cd, Cu and Zn depend on the hardness of the water, reported as mg/L calcium carbonate (CaCO₃). Calculated water hardness derived from the Tellus data appears to be of high importance in assessing exceedances of Zn EQS values. Without hardness data it is likely that the degree of Zn exceedance of the EQS will be significantly overstated where the lowest EQS value is used as part of a conservative approach. The review of Tellus data for Cd and Cu suggest that for these elements, application of water hardness data would have a more limited impact on EQS assessment. Tellus high-resolution baseline stream water data allow reliable mapping of water hardness in areas where water monitoring stations are sampled.

Mineral exploration

Stream water chemistry has attracted attention in recent years as a potential mineral exploration tool. This analysis explores the potential of the stream waters dataset to identify existing base metal (zinc, lead) deposit locations and predict sites that may be of mineral exploration interest.



Base metal anomalies are evident in the Tellus waters data in the vicinity of known mineral deposit localities, both exploited and unworked. Not all of these observed anomalies occur downstream of the mines and thus may be reflective of the presence of bedrock mineralization in the general area rather than representing contamination by mining. Although waters in peat areas are relatively depleted with respect to many elements, apparent anomalies of Zn and Cd in those areas may reflect enrichment following complexation within organic-rich subsoils and sediments. Anomalous concentrations linked with known mineralization generally have low organic carbon concentrations – an observation which may be useful for base metal mineral exploration strategies.

Mineralization signatures in stream water chemistry are not confined to base metals. Gold pathfinder elements As and antimony (Sb) are enriched in streamwaters draining known gold deposits in counties Donegal, Monaghan and Mayo. Comparison of maps for stream sediment and stream water indicate that stream water geochemistry may identify known base metal and gold mineralization as readily as stream sediment geochemistry.

In addition, at a time of increased exploration interest in Rare Earth Elements (REEs), the possibility of using stream water data as a geochemical tool for critical element exploration is assessed. REEs are not readily mapped in Tellus soils and stream sediments owing to relatively high detection limits achieved in analysis but the stream water data provide a first insight into the spatial distribution of these elements in Ireland.

Conclusions

The nature of Tellus water samples, sampled at relatively high-density and collected up-catchment with minimal anthropogenic inputs, provides a unique opportunity to support the refinement of EQSs for certain metals and the use of waters data for mineral exploration in Ireland. This has been demonstrated for a limited region of Ireland and the methods used here may be extended to national coverage on completion of the Tellus survey.



1. Introduction

1.1 Background

Regional geochemical mapping has been conducted in parts of Ireland since the 1970s (Webb *et al.* 1973, O'Connor *et al.* 1988, O'Connor and Reimann 1993). Plans to cover the whole island began with the Resource and Environmental Survey of Ireland (RESI) (Bullock and Clinch 2001). As the island of Ireland is divided into two jurisdictions, the six counties of Northern Ireland (part of the UK) in the northeast and the remaining 26 counties of Ireland, RESI was intended as a collaboration between the Geological Survey of Northern Ireland (GSNI), the British Geological Survey (BGS) and Geological Survey Ireland (GSI). Its aim was to produce high-quality digital datasets of geochemical and geophysical parameters to support government planning and promote mineral exploration. RESI did not proceed but did lead directly to the original Tellus Project, which was carried out by GSNI and covered Northern Ireland only (Young and Donald 2013). The Tellus Border Project, covering the adjacent six counties in Ireland, was completed between 2011 and 2014 by GSI and GSNI (Young 2016, Gallagher *et al.* 2016a, 2016b). Since 2014, the Tellus Programme of GSI has continued as a Government of Ireland initiative undertaking geochemical and geophysical surveying over the remainder of the island of Ireland.

Geochemical samples collected for Tellus include topsoil, stream sediment and stream water. By 2021 topsoil had been collected and analysed from the entire northern half of the island (Young and Donald 2013; Gallagher *et al.* 2016b; Browne and Gallagher 2020; Browne *et al.* 2021) and this part of the programme is continuing with the aim of completing collection across the island by 2024. Stream sediment and stream water data are available for Northern Ireland (Young and Donald 2013) and parts of Ireland (Geological Survey Ireland, 2020a, 2020b, 2020c, 2020d).

This report describes the outcomes of analysis of the Tellus stream water dataset for the Border and West regions of Ireland. Initial univariate analysis, including geochemical mapping in a GIS environment, was followed by multivariate statistical analysis or Exploratory Data Analysis (EDA). The Tellus stream water data is of high quality, with low detection limits and a wide range of determinands (e.g. Geological Survey Ireland, 2020e), but it has not attracted the same attention as other Tellus datasets and so remains largely uninterpreted and under-utilized. Its limited uptake and impact may be partly related to the relatively restricted Tellus Border area coverage that was available until early 2020. With the addition of Tellus West data approximately 35 % of the country has now been completed. The aim of the project was to undertake detailed analysis of the currently available waters data in order to understand its potential utility to geological, mineral exploration and environmental objectives.



1.2 Surface water geochemistry data in Ireland

Surface water monitoring of rivers, lakes, transitional and coastal waters is conducted by the Environmental Protection Agency (EPA) under the EU Water Framework Directive (WFD). There are over 9,000 river monitoring sites in Ireland but only a proportion of these are monitored under the WFD. Some 1,500 river stations are being assessed under the current three-year programme (2019-2021) for physico-chemical parameters. Biological monitoring is carried out at 2,896 river stations over the same three-year interval. River monitoring sites include all the major rivers and their important tributaries. Key parameters of interest for assessing river water quality include biological quality, based on analysis of invertebrate populations, the levels of nutrients, such as nitrate and phosphate, and a range of potentially harmful substances, classified under EU regulations as Priority Substances and Specific Pollutants.

Apart from the EPA monitoring data, GSI's Tellus stream water dataset is one of the largest available in Ireland. Whereas most of the EPA monitoring sites are on third- or higher-order water courses, in the lower parts of catchments, over 99 % of the Tellus stream water samples were collected from first- (39.8 %), second- (52.1 %) and third-order (7.6 %) streams. By sampling in the upper parts of catchments the Tellus survey can provide a baseline for stream water chemistry in Ireland against which anthropogenic impacts can be measured. At an average sample density of 1 per 3.5 km², the Tellus data allow for a relatively detailed picture of the variation in physico-chemical parameters in any given region.

1.3 Anthropogenic impacts on surface water chemistry

The aim of the EU Water Framework Directive is to protect and enhance all waters, including surface waters, and to achieve “good” status for them. Key to these aims is (i) understanding the baseline chemistry of surface water in any given region, which contributes to an understanding of what “good” is, and (ii) measuring potential contaminant inputs through monitoring programmes. Contaminants can be seen as chemical inputs that cause the composition of the water to deviate from the baseline composition. Tellus can provide baseline stream water compositions for a range of chemical elements including potentially harmful metals and nutrients.

The chemical composition of any surface water sample depends on the composition of the source water and any chemical inputs that take place between the original water source and point of sampling. Chemical inputs come from natural materials such as rocks and soils that the water passes through or over and from anthropogenic activities that lead to discharges of chemicals to water courses. Natural sources contribute to the baseline chemistry whereas anthropogenic activities typically cause the surface water composition to deviate from the baseline. Nearly half of the surface waters in Ireland are failing to meet the legally binding water quality objectives set by the EU Water Framework Directive because of pollution and other human disturbance (Wall *et al.*



2020). Agriculture is the most common pressure affecting water quality, with one of the main problems damaging the quality of surface waters being nutrient pollution caused by too much nitrogen and phosphorus (Wall *et al.* 2020). Near towns and cities, sewage and industrial discharges can be significant. Mining is a source of elevated metal concentrations in some surface waters.

The issue of anthropogenic contaminants to surface waters is addressed in two strands, relating to (i) potentially harmful substances and (ii) nutrients.

1.3.1 Potentially Harmful Substances

EU Member States are required to monitor for a range of potentially harmful substances in water. These substances fall into two categories, **Priority Substances** and **Specific Pollutants**. Priority Substances, as listed in the Surface Water Regulations 2009 (European Commission 2009), are defined at a European level as substances posing a threat to the aquatic environment. National monitoring programmes are aimed at supporting the reduction or elimination of pollution of surface water by the substances on the list. The current list contains 48 substances or groups of substances, including herbicides, insecticides, polycyclic aromatic hydrocarbons (PAHs), solvents and various metals. The list is reviewed every six years at EU level to ensure that the WFD monitoring programme continues to be fit for purpose and that relevant substances of concern are included. Elements on the current list that are also part of the Tellus stream water dataset are **cadmium, nickel and lead**.

Member States must also identify Specific Pollutants of regional or local importance, set national Environmental Quality Standards (EQS) and establish national monitoring programmes for them. Sixteen substances, including metals, pesticides and hydrocarbons, are included in the current list of Specific Pollutants for Ireland. Of these, five have been analysed as part of Tellus (**fluoride, arsenic, chromium, copper and zinc**). In defining the EQS values for Specific Pollutants the regulations state that the values for all metals, except chromium VI, are as added values to background concentrations. A review of Ireland's current list of Specific Pollutants, and their associated EQSs, is underway by the EPA to determine whether they are still appropriate and to identify new candidate substances of concern for possible inclusion in a future revised list.

1.3.2 Nutrients: nitrate and phosphorus

The main aim of the EU Nitrates Directive (Nitrates Directive 1991) is to protect surface and ground water quality by preventing pollution from agricultural sources. The national Nitrates Action Programme includes a limit on the amount of livestock manure applied to land each year, set periods when manure spreading is prohibited and limits on livestock manure storage capacity. Yet, as stated in the latest EPA water quality report (Trodd and O'Boyle 2020), "the main problem damaging our waters is the presence of too much nutrients such as phosphorus and nitrogen which come primarily from agriculture and waste water". The most recent survey data for the period 2017 – 2019 (Trodd and O'Boyle 2020) indicate that 47% of river sampling sites sampled had



unsatisfactory nitrate concentrations ($> 8 \text{ mg/L NO}_3^-$). Moreover, 44 % of river sampling sites showed an increasing nitrate trend in the period 2013 to 2019 (Figure 1.1). The highest concentrations are observed in the south, southeast and east of the country where more intensive farming is coupled with freely draining soils and relatively low rainfall (Trodd and O'Boyle 2020).

The story for phosphorus (reported as phosphate) is similar (Figure 1.2). Phosphate in surface and ground waters comes mainly from sewage, industrial discharges and from animal manure and inorganic fertilizers spread on agricultural land. One third of river sampling sites assessed in 2017-2019 had unsatisfactory phosphate levels ($> 0.035 \text{ mg/L}$) while 26 % of river sites showed a trend of increasing phosphate levels (Trodd and O'Boyle 2020).

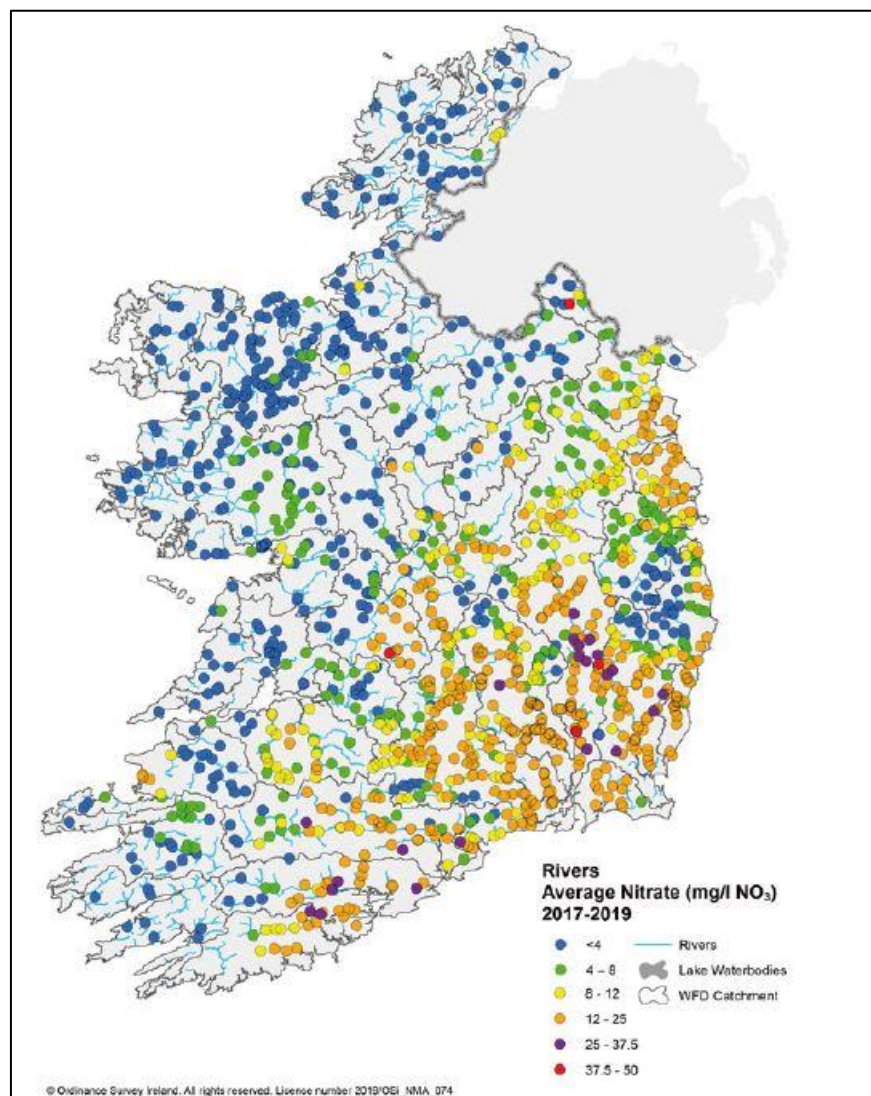


Figure 1.1 Nitrate in EPA river monitoring sites 2017 - 2019 (Trodd and O'Boyle 2020).



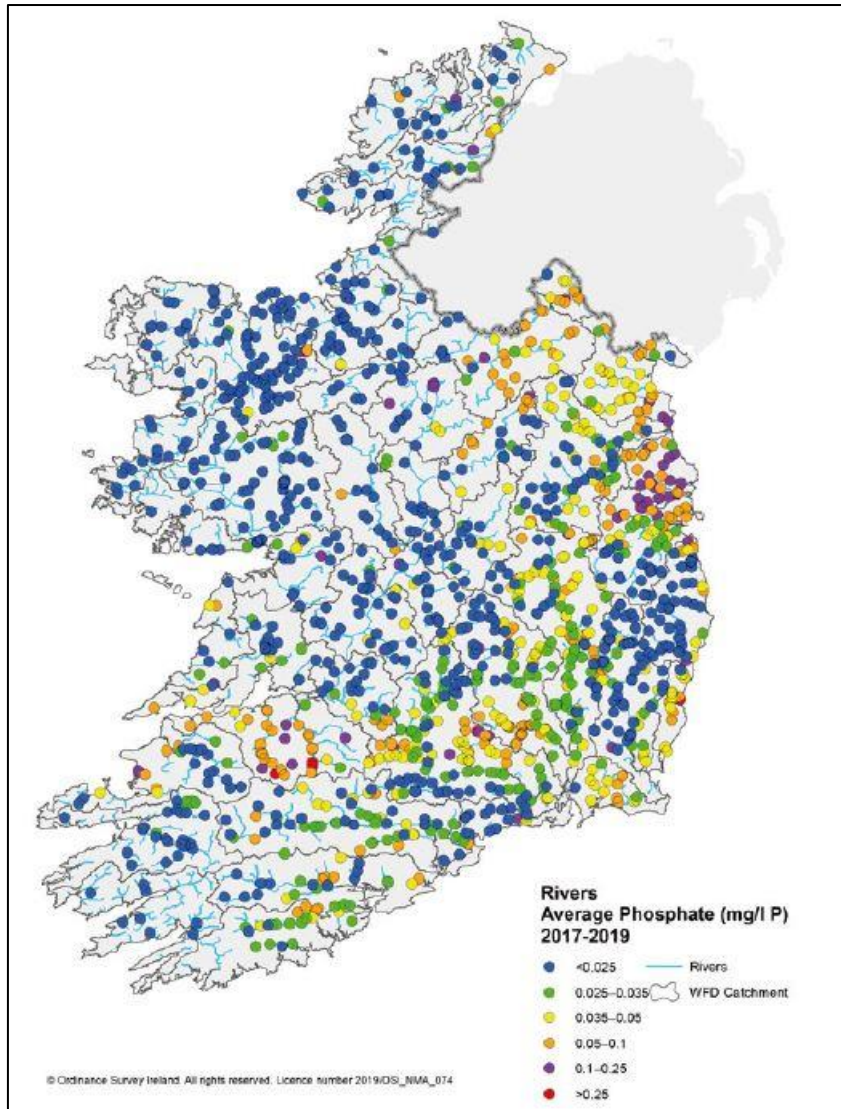


Figure 1.2 Phosphate in EPA river monitoring sites 2017 - 2019 (Trodd and O’Boyle 2020).

1.4 Mineral exploration

Hydrogeochemistry has attracted attention in recent years as a potential mineral exploration tool, particularly groundwater (e.g. Wallace *et al.* 2020) but also stream water (e.g. Simpson *et al.* 1993 and Wang *et al.* 2005). Advances in analytical techniques, specifically ICP-MS, leading to lower detection limits have facilitated the use of stream water in which element concentrations tend to be lower than in groundwater. The European Commission identifies a number of Critical Raw Materials (CRMs), reflecting increasing demand and supply risks for metallic minerals (European Commission 2020). Of these CRMs, the Tellus survey measures 32 and this report looks in detail at REEs as well as Zn and Pb, both which are economically important for Ireland.

Preliminary assessment by GSI of Tellus stream water geochemical data published to date (Gallagher *et al.* 2018) suggests that the water chemistry has a strong geogenic signature, reflecting the compositional variation in the bedrock geology. It also reflects at



least some known bedrock mineral occurrences, including base metal and gold deposits, and may be as proficient in this respect as stream sediment and soil geochemistry. However, there are other influences, both natural and anthropogenic, on the concentration of metals and other ore-related elements in stream water and a key task before attempting to utilize stream water geochemistry for exploration purposes is to identify the various factors or sources that contribute to elevated concentrations of elements associated with ore deposits in Ireland.

1.5 Objectives

The objectives for this work are to explore the Tellus stream water geochemistry data for the Border and West regions in order to:

- i. understand the extent to which the Tellus stream water geochemistry data reflect bedrock geology and other geological influences;
- ii. identify background concentrations for various chemical parameters where possible;
- iii. identify data populations for elements in stream waters in order to identify natural and anthropogenic processes, including inputs of nutrients and potentially harmful substances;
- iv. characterize mineralization signatures in stream water chemistry and identify potential exploration targets.



2. Dataset descriptions

2.1 Tellus data

Sample media: <0.45 µm filtered stream water 'W'

Coverage: Survey areas G1, G3 and G4, including counties Donegal, Sligo, Leitrim, Cavan, Monaghan, Louth, Mayo and parts of Galway, Roscommon and Clare (Figure 2.1).

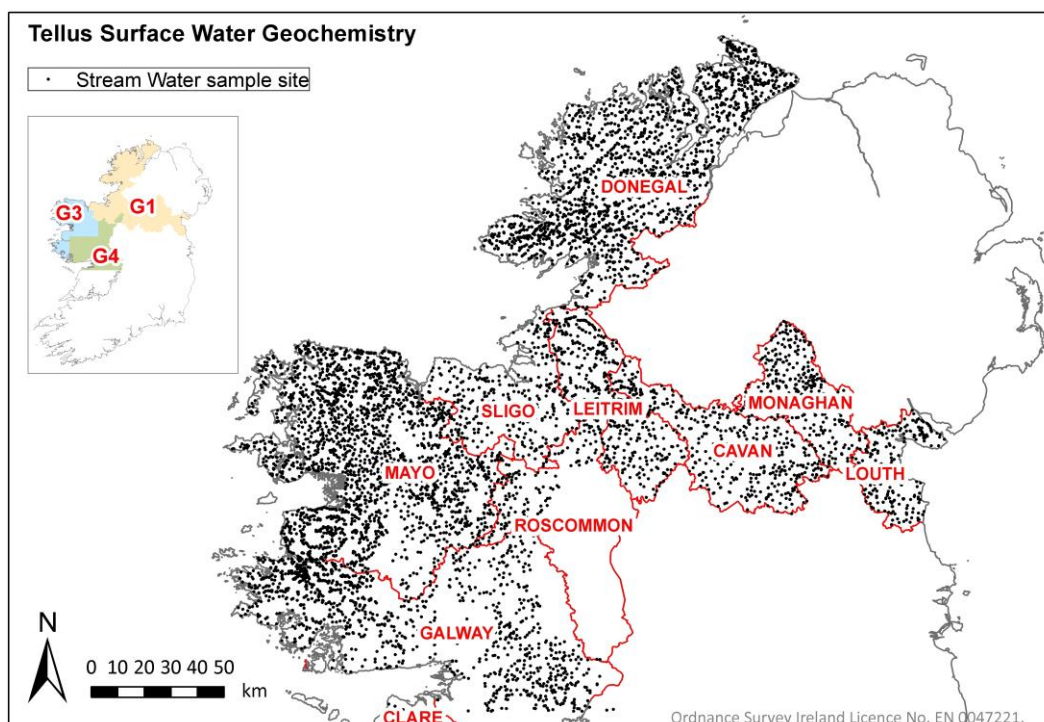


Figure 2.1 Stream water sampling sites, with counties. Inset shows Tellus survey areas.

Analytical methods: Field determinations are of pH, specific electrical conductance (SEC) and total alkalinity to assess bicarbonate concentration. Laboratory tests are for anions by ion chromatography (IC); multi-element major, minor and trace elements by inductively coupled plasma mass spectrometry (ICP-MS); and non-purgeable organic carbon (NPOC).

Survey years: 2011-2017. Table 2.1 lists the analytes included in the Tellus dataset and Table 2.2 lists the reporting units and lower limits of detection.

pH	SEC	HCO ₃ ⁻	NPOC	Cl ⁻	SO ₄ ²⁻	NO ₃ ⁻	Br ⁻	NO ₂ ⁻	HPO ₄ ²⁻
F ⁻	Ag	Al	As	B	Ba	Be	Bi	Ca	Cd
Ce	Co	Cr	Cs	Cu	Dy	Er	Eu	Fe	Ga
Gd	Hf	Ho	K	La	Li	Lu	Mg	Mn	Mo
Na	Nb	Nd	Ni	P	Pb	Pr	Rb	S	Sb
Se	Si	Sm	Sn	Sr	Ta	Tb	Th	Ti	Tl
Tm	U	V	W	Y	Yb	Zn	Zr		

Table 2.1 Analytes in Tellus stream water dataset.



pH	pH unit	0.01	Cs	$\mu\text{g L}^{-1}$	0.001	Pr	$\mu\text{g L}^{-1}$	0.002
SEC	$\mu\text{S cm}^{-1}$	0.001	Cu	$\mu\text{g L}^{-1}$	0.1	Rb	$\mu\text{g L}^{-1}$	0.01
HCO ₃	mg L^{-1}	0.00001	Dy	$\mu\text{g L}^{-1}$	0.002	S	mg L^{-1}	0.5
NPOC	mg L^{-1}	0.5	Er	$\mu\text{g L}^{-1}$	0.002	Sb	$\mu\text{g L}^{-1}$	0.005
Cl	mg L^{-1}	0.05	Eu	$\mu\text{g L}^{-1}$	0.002	Se	$\mu\text{g L}^{-1}$	0.04
SO ₄	mg L^{-1}	0.1	Fe	$\mu\text{g L}^{-1}$	1	Si	$\mu\text{g L}^{-1}$	50
NO ₃	mg L^{-1}	0.05	Ga	$\mu\text{g L}^{-1}$	0.01	Sm	$\mu\text{g L}^{-1}$	0.002
Br	mg L^{-1}	0.02	Gd	$\mu\text{g L}^{-1}$	0.002	Sn	$\mu\text{g L}^{-1}$	0.02
NO ₂	mg L^{-1}	0.01	Hf	$\mu\text{g L}^{-1}$	0.01	Sr	$\mu\text{g L}^{-1}$	0.01
HPO ₄	mg L^{-1}	0.1	Ho	$\mu\text{g L}^{-1}$	0.002	Ta	$\mu\text{g L}^{-1}$	0.02
F	mg L^{-1}	0.01	K	mg L^{-1}	0.02	Tb	$\mu\text{g L}^{-1}$	0.002
Ag	$\mu\text{g L}^{-1}$	0.05	La	$\mu\text{g L}^{-1}$	0.002	Th	$\mu\text{g L}^{-1}$	0.005
Al	$\mu\text{g L}^{-1}$	1	Li	$\mu\text{g L}^{-1}$	0.25	Ti	$\mu\text{g L}^{-1}$	0.05
As	$\mu\text{g L}^{-1}$	0.02	Lu	$\mu\text{g L}^{-1}$	0.002	Tl	$\mu\text{g L}^{-1}$	0.01
B	$\mu\text{g L}^{-1}$	5	Mg	mg L^{-1}	0.01	Tm	$\mu\text{g L}^{-1}$	0.002
Ba	$\mu\text{g L}^{-1}$	0.1	Mn	$\mu\text{g L}^{-1}$	0.2	U	$\mu\text{g L}^{-1}$	0.002
Be	$\mu\text{g L}^{-1}$	0.001	Mo	$\mu\text{g L}^{-1}$	0.03	V	$\mu\text{g L}^{-1}$	0.03
Bi	$\mu\text{g L}^{-1}$	0.01	Na	mg L^{-1}	0.2	W	$\mu\text{g L}^{-1}$	0.02
Ca	mg L^{-1}	0.3	Nb	$\mu\text{g L}^{-1}$	0.001	Y	$\mu\text{g L}^{-1}$	0.005
Cd	$\mu\text{g L}^{-1}$	0.001	Nd	$\mu\text{g L}^{-1}$	0.01	Yb	$\mu\text{g L}^{-1}$	0.002
Ce	$\mu\text{g L}^{-1}$	0.002	Ni	$\mu\text{g L}^{-1}$	0.1	Zn	$\mu\text{g L}^{-1}$	0.25
Co	$\mu\text{g L}^{-1}$	0.01	P	mg L^{-1}	0.001	Zr	$\mu\text{g L}^{-1}$	0.02
Cr	$\mu\text{g L}^{-1}$	0.05	Pb	$\mu\text{g L}^{-1}$	0.02			

Table 2.2 Analytes, reporting units and lower limits of detection.

2.2 Supporting datasets

Table 2.3 provides a list of supporting datasets that were utilized in this analysis.

Source	Dataset	Data Viewer	Metadata
Water			
EPA	WFD Catchments		
		https://gis.epa.ie/EPAMaps/Water	https://gis.epa.ie/geonetwork/srv/eng/catalog.search#/metadata/78b8def6-16fd-4934-bc2a-1d52380a2b34
	OSI Rivers and Lakes		
			https://gis.epa.ie/geonetwork/srv/eng/catalog.search#/metadata/c4040e19-38ec-4120-a588-8cd01ac94a9c
	OSI Geometric River Network		
			https://gis.epa.ie/geonetwork/srv/eng/catalog.search#/metadata/c4043e19-38ec-4120-a588-8cd01ac94a9c
Geology			



Source	Dataset	Data Viewer	Metadata
GSI	Bedrock 100k (scale 1:100,000)		
		https://dcenr.maps.arcgis.com/apps/webappviewer/index.html?id=de7012a99d2748ea9106e7ee1b6ab8d5&scale=0	https://dcenr.maps.arcgis.com/home/item.html?id=a40f6a8ca91f4340a86b12649d831d74
	Bedrock Outcrops		
			https://dcenr.maps.arcgis.com/home/item.html?id=a40f6a8ca91f4340a86b12649d831d74
	Bedrock 500k (scale 1:500,000)		
			https://dcenr.maps.arcgis.com/home/item.html?id=86317a8a90c845b59a0c6f58a2e28038
	Bedrock Geology 1 Million (scale 1:1,000,000)		
			https://dcenr.maps.arcgis.com/home/item.html?id=dc7bd3a02db24641bf3bf90d4a244730
	Geochemically Appropriate Levels for Soil Recovery Facilities		
		https://dcenr.maps.arcgis.com/apps/webappviewer/index.html?id=da71bb12d7f3439e9c6dcb906c9b98c1	https://dcenr.maps.arcgis.com/home/item.html?id=a41fcbf642774a6ca9713cbe703fb2e2
Mineral Localities			
	https://dcenr.maps.arcgis.com/apps/webappviewer/index.html?id=ebaf90ff2d554522b438ff313b0c197a&scale=0	https://dcenr.maps.arcgis.com/home/item.html?id=43d66cb2f2f24d81b7e03b8acda00c6a	
Quaternary Sediments			
	https://dcenr.maps.arcgis.com/apps/webappviewer/index.html?id=afa76a420fc54877843aca1bc075c62b	https://dcenr.maps.arcgis.com/home/item.html?id=1bbf22e9391c484db4b84e4150313bae	
Soil			
Teagasc / EPA	Subsoils		
		https://gis.epa.ie/EPAMaps/	https://gis.epa.ie/geonetwork/srv/eng/catalog.search#/metadata/5f1999f0-37e4-4c14-acf8-3b42bfdae894
	Irish Soil Information System		
	http://gis.teagasc.ie/soils/map.php https://gis.epa.ie/EPAMaps/		https://gis.epa.ie/geonetwork/srv/eng/catalog.search#/metadata/2cd0c5e9-83b2-49a9-8c3e-79675ffd18bf
Land Use			
EPA	Corine Landcover 2018		
		https://gis.epa.ie/EPAMaps/	https://gis.epa.ie/geonetwork/srv/eng/catalog.search#/metadata/fb5d2fa9-95fe-4d3f-8aed-e548348a40ea
Historic Mines Project			
EPA	Mine Districts		
		https://gis.epa.ie/EPAMaps/default?easting=?&northing=?&lid=EPA:LEMA_Facilities_Extractive_Facilities	https://gis.epa.ie/geonetwork/srv/eng/catalog.search#/metadata/dd4814fa-e4dc-4441-9f0b-3f6248fccbcf
	Mine Site Location		
			https://gis.epa.ie/geonetwork/srv/eng/catalog.search#/metadata/057633bc-562d-42d9-985c-aecca84b1f08d



Source	Dataset	Data Viewer	Metadata
	Mine Site Boundaries		
			https://gis.epa.ie/geonetwork/srv/eng/catalog.search#/metadata/237f3389-a20e-4503-897a-47e06828039c
	Mine Site Features		
			https://gis.epa.ie/geonetwork/srv/eng/catalog.search#/metadata/73c6d016-4d5c-4557-9ab0-7c12ebe0c59c
	Mine Linear Structures		
			https://gis.epa.ie/geonetwork/srv/eng/catalog.search#/metadata/7e478948-086e-4f67-bfa4-dd86235fd2f2
	Mine Spoil Heaps		
		https://gis.epa.ie/geonetwork/srv/eng/catalog.search#/metadata/d0e8497a-405d-40d3-9b63-a3db133e3a5b	
Industries			
EPA	EPA Licensed Facilities		
		https://gis.epa.ie/EPAMaps/	https://gis.epa.ie/geonetwork/srv/eng/catalog.search#/metadata/00750a6a-e2f4-451d-b41c-0f067a40c94c
Digital Terrain Model			
OSi	Digital Terrain Model (5m resolution)		
		https://www.osi.ie/	

Table 2.3 List of all supporting datasets utilized for this report, including data source and metadata. All data were accessed between September 2020 and January 2021.



3. Univariate mapping and statistical analysis

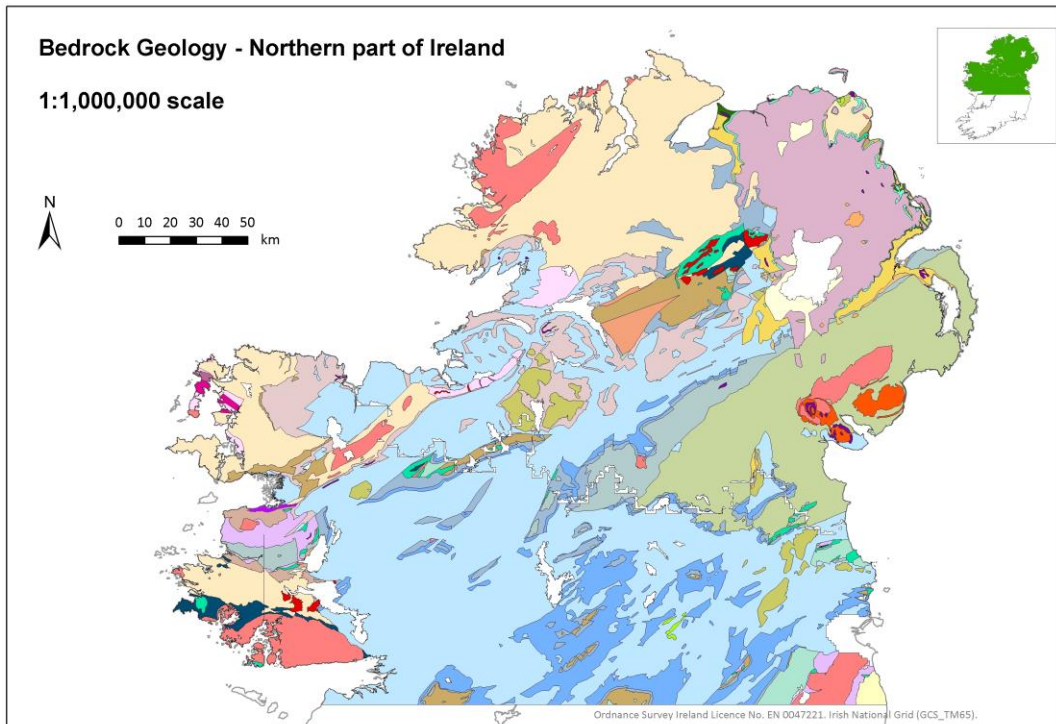
Univariate mapping and statistical analysis were carried out on the stream water data to provide an initial assessment of the controls on stream water chemistry, including bedrock composition and anthropogenic factors.

Quality control checks were carried out on the stream water data to ensure they were fit for the purpose of regional geochemical mapping (Geological Survey Ireland 2020e). The data were imported to ArcGIS and mapped as point data or as continuous surface maps based on interpolation using inverse distance weighting. These maps were classified using a standard Tellus classification scheme based on percentile breaks.

3.1 Geogenic controls

Figure 3.1 shows the distribution of bedrock geology in the northern half of Ireland, based on GSI's 1:1,000,000 bedrock geology map. Further context is provided by Figures 3.2–3.4. Figure 3.2 shows a simplified version of the Teagasc subsoil map and Figure 3.3 the main Corine Land Cover categories. Figure 3.4 shows GSI's SRF Domain map (Glennon et al. 2020). Univariate element maps (Figure 3.5–3.13) reveal patterns and correlations that reflect bedrock, subsoil, land cover and other controls on stream water chemistry. In each of the geochemical maps, the geological linework is included to allow comparison with Figure 3.1. Some examples are outlined below in relation to bedrock geology.





Legend

- | | |
|--|--|
| 83, Oligocene clay, sand & lignite | 42, Late Ordovician-Silurian deep marine greywacke, mudstone (Longford-Down) |
| 79, Palaeocene basalt lava | 41, Sedimentary melange |
| 77, Cretaceous chalk, flint, glauconitic sandstone | 40, Middle-Upper Ordovician slate, sandstone, greywacke, conglomerate |
| 76, Jurassic mudstone & limestone | 35, Lower-Middle Ordovician slate, sandstone, greywacke, conglomerate |
| 75, Triassic sandstone, mudstone, evaporite | 33, Ordovician volcanic rocks |
| 73, Permian sandstone, conglomerate, evaporite | 32, Cambrian greywacke, slate, quartzite |
| 72, Westphalian shale, sandstone, siltstone & coal | 29, Neoproterozoic metasedimentary rocks - Dalradian |
| 71, Namurian shale, sandstone, siltstone & coal | 20, Neoproterozoic schist and gneiss |
| 70, Visean to Westphalian redbed sandstone, conglomerate & mudstone | 15, Mesoproterozoic gneiss |
| 68, Visean sandstone, mudstone & evaporite | 12, Palaeoproterozoic gneiss |
| 64, Visean limestone & calcareous shale | 11, Palaeogene basic intrusive rocks |
| 61, Tournaisian limestone | 10, Palaeogene rhyolite |
| 60, Tournaisian sandstone, mudstone, limestone | 9, Palaeogene granitic rocks |
| 56, Carboniferous volcanic rocks | 8, Siluro-Devonian granitic rocks & appinite |
| 55, Up. Devonian sandstone & mudstone (Old Head Sandstone Fm) | 5, Lr Palaeozoic basic-intermediate intrusion |
| 52, ORS, sandstone, conglomerate & mudstone | 5, Lr Palaeozoic basic-intermediate intrusion (Connemara suite) |
| 51, Devonian volcanic rocks | 4, Ordovician granitic rocks |
| 49, Silurian deep marine mudstone, greywacke & conglomerate | 2, Serpentinite |
| 47, Silurian terrestrial - shallow marine sandstone, siltstone, conglomerate | |

Figure 3.1 Bedrock geology (1:1,000,000) of the northern half of Ireland.



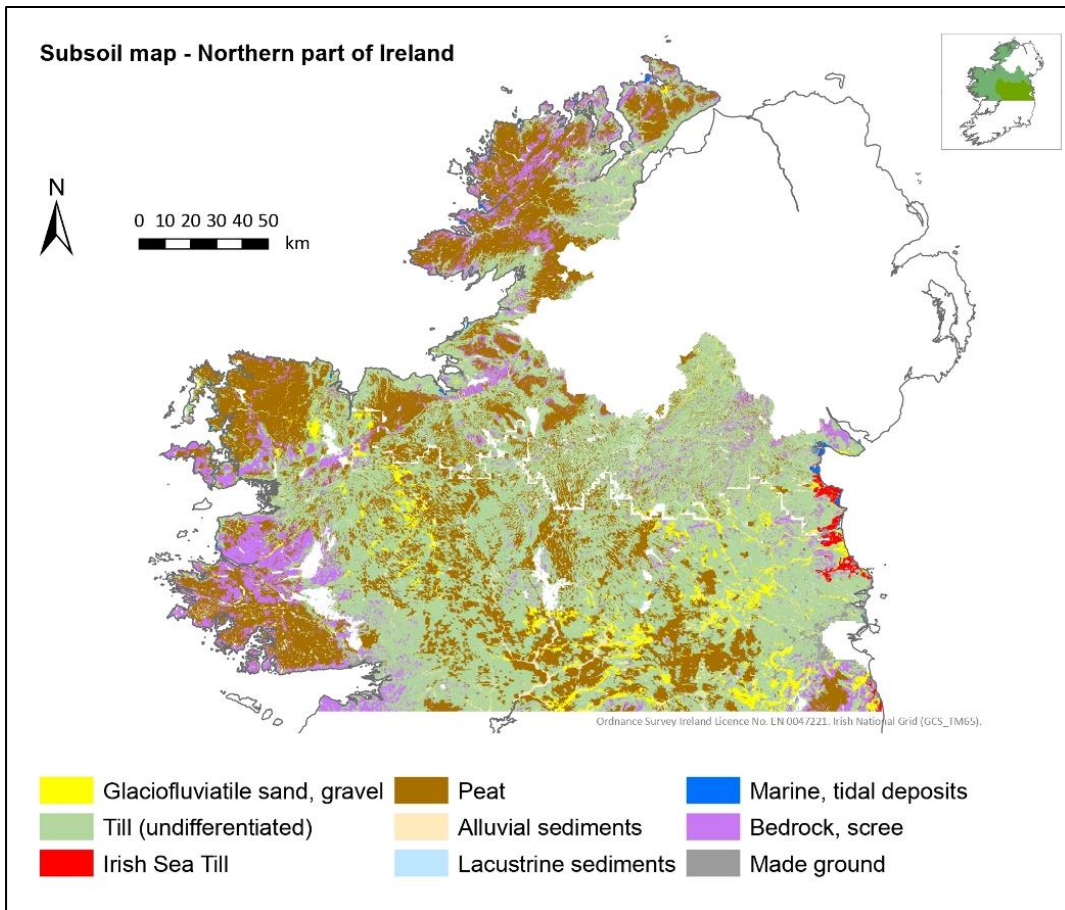


Figure 3.2 Subsoil map of northern part of Ireland, simplified from Teagasc subsoil map (Fealy *et al.* 2009).

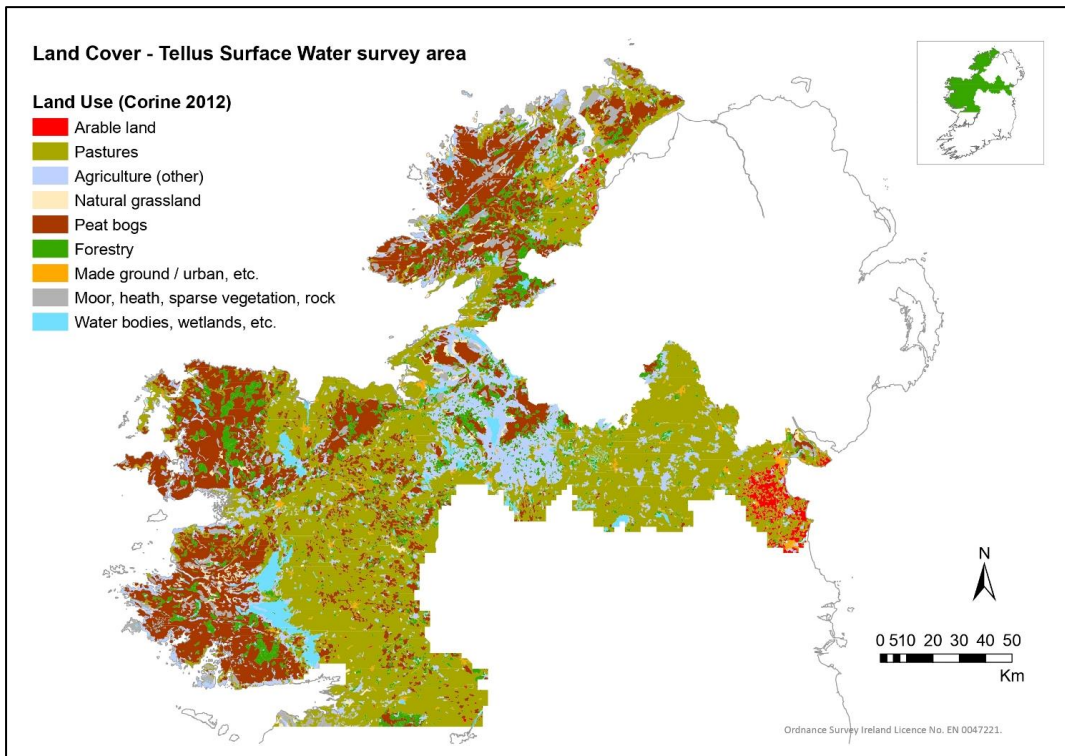


Figure 3.3 Simplified land cover map, northern part of Ireland (after Corine 2012).



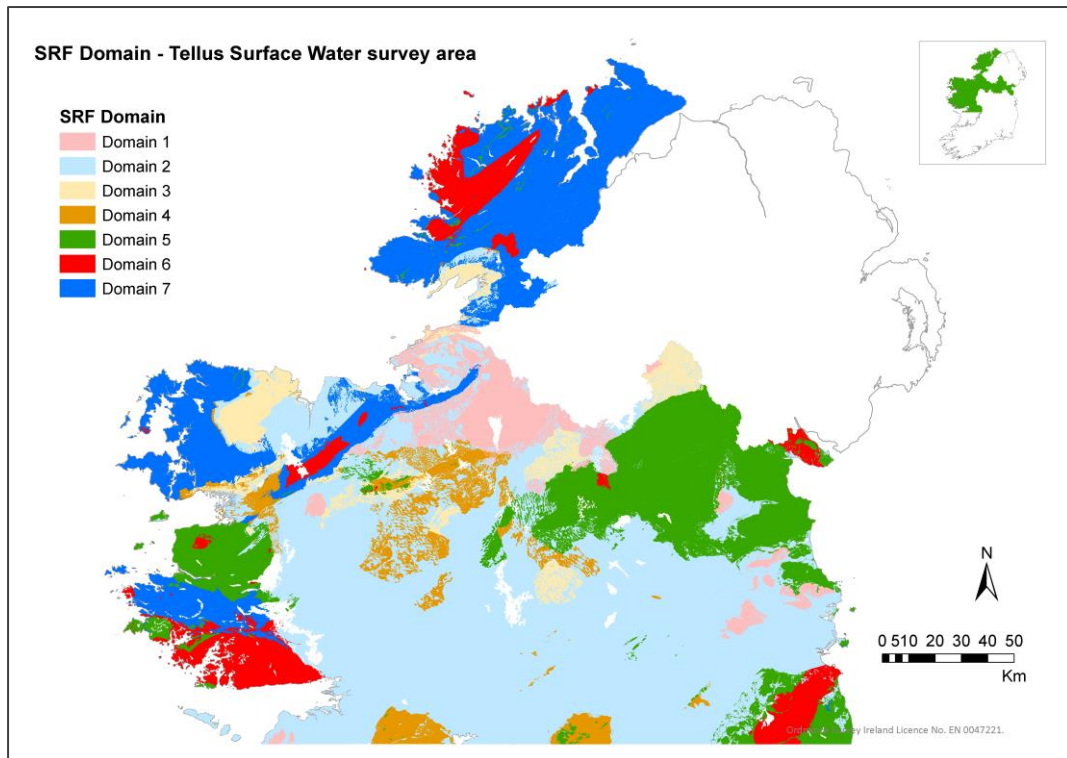


Figure 3.4 SRF Domain map (Glennon *et al.* 2020).

Figure 3.5 shows the distribution of calcium (Ca) in Tellus stream water samples. It strongly reflects the distribution of limestone-dominated Lower Carboniferous rocks in the region, except for much of County Louth, which is underlain by greywackes of the Longford-Down inlier. Here the high Ca concentrations mirror high concentrations of Mg, Ba, HCO_3^- , NO_3^- and U and appear to reflect agricultural activity, including liming and/or the application of fertilizers.



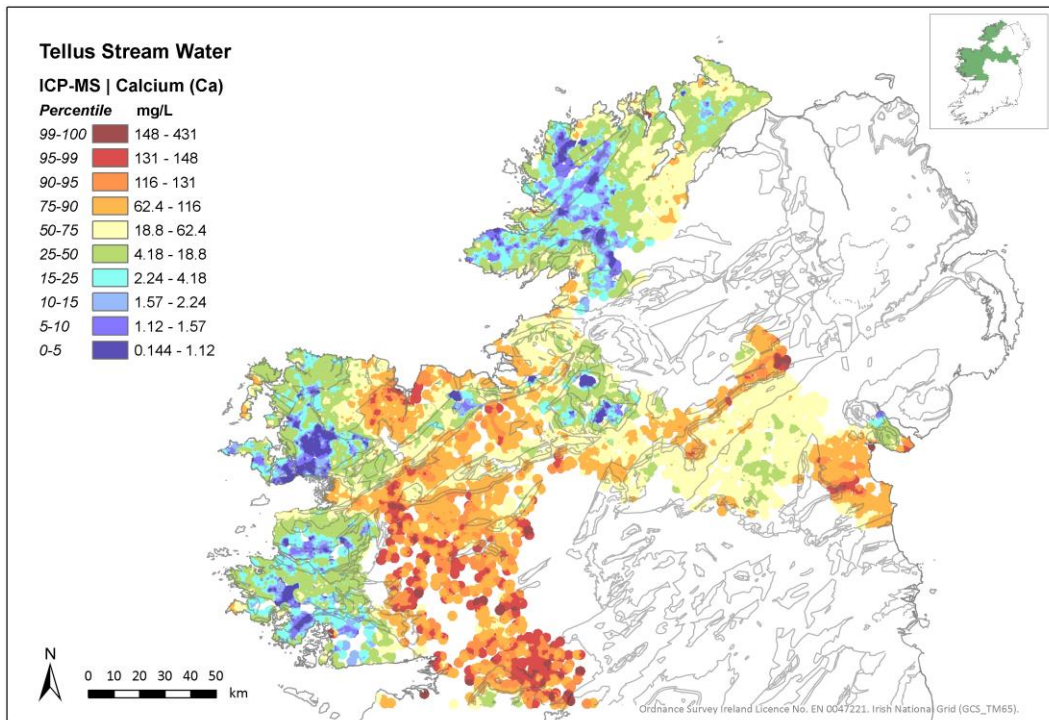


Figure 3.5 Distribution of calcium in Tellus stream water samples.

Chromium (Cr) in stream water (Figure 3.6) also strongly reflects known bedrock sources, including the Longford-Down inlier greywackes and the rocks of the South Mayo Trough, which include serpentinite and sediments containing Cr-bearing phases such as chromite and fuchsite.

Figure 3.7 shows an example of a rare earth element (REE) in stream water – the distribution of gadolinium (Gd) is also at least partly controlled by geology, with the boundary between the greywacke of the Longford-Down inlier and the Lower Carboniferous strata well defined. REEs are not readily mapped using Tellus soil and stream sediment data owing to relatively high detection limits achieved in analysis but the stream water data provide a first insight into the spatial distribution of these elements in Ireland.



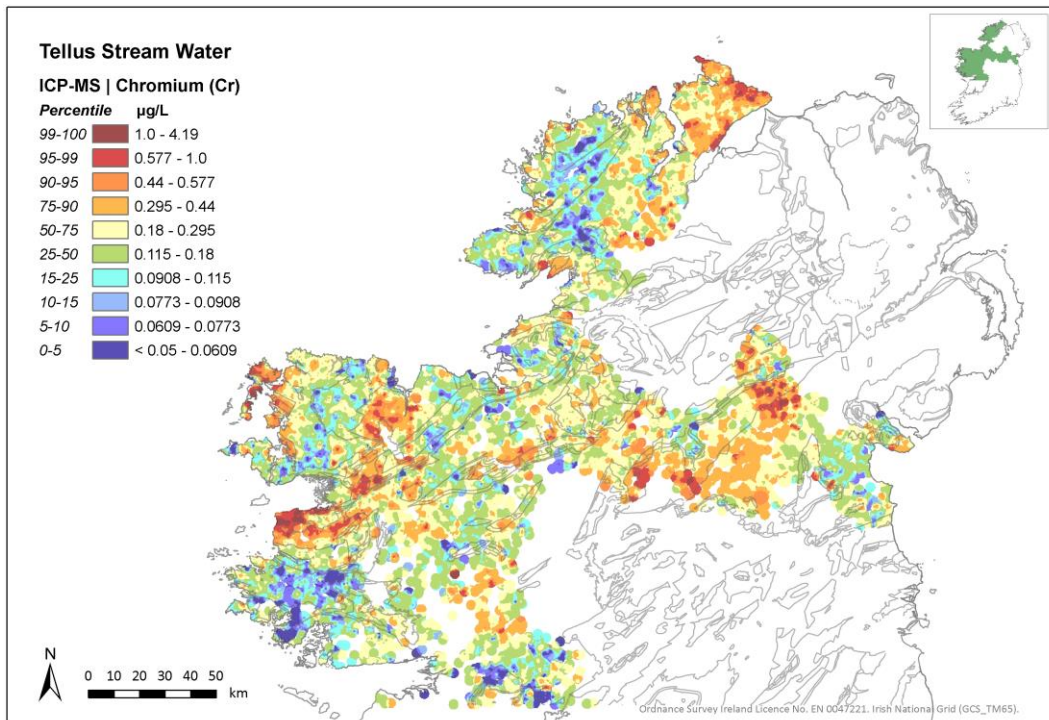


Figure 3.6 Distribution of chromium in Tellus stream water samples.

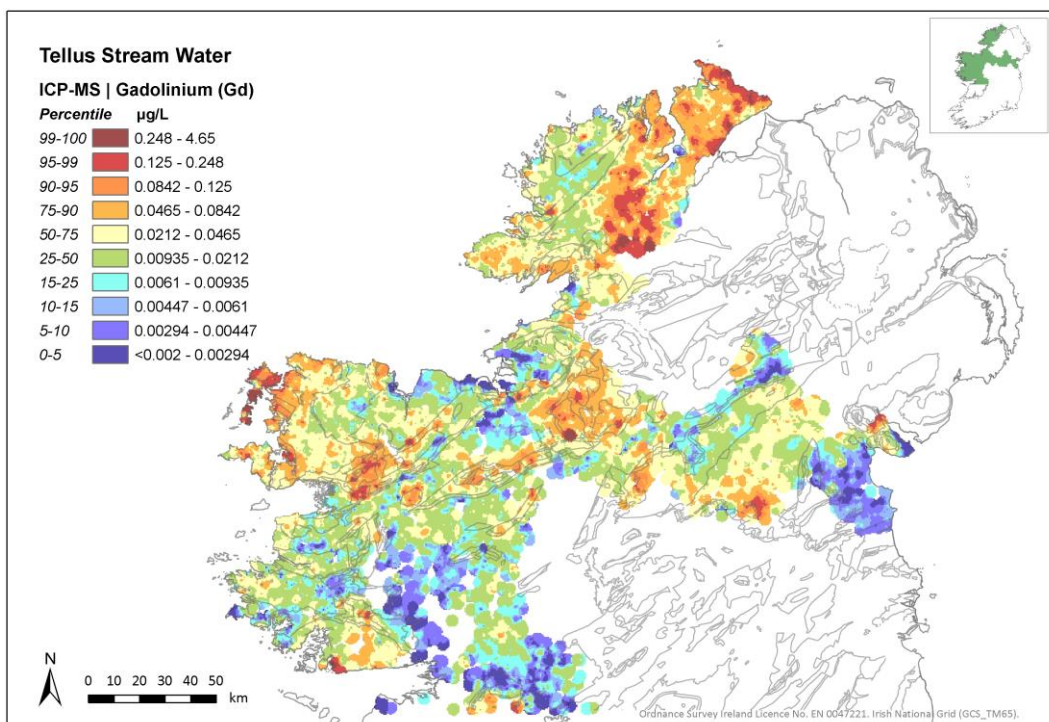


Figure 3.7 Distribution of gadolinium in Tellus stream water samples.



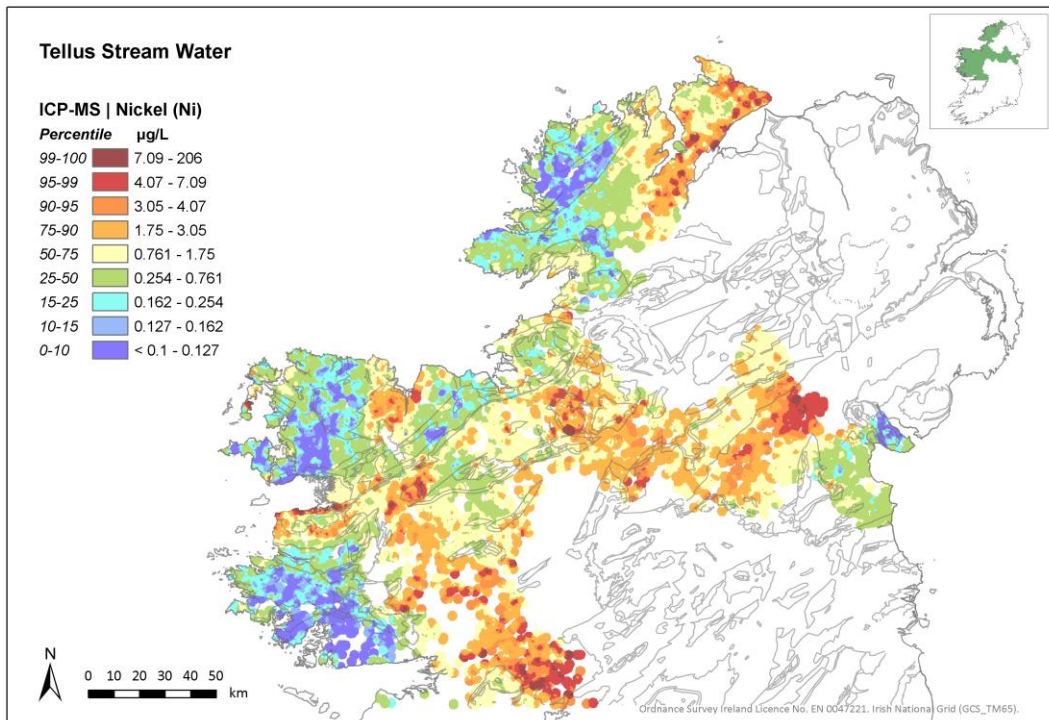


Figure 3.8 Distribution of nickel in Tellus stream water samples.

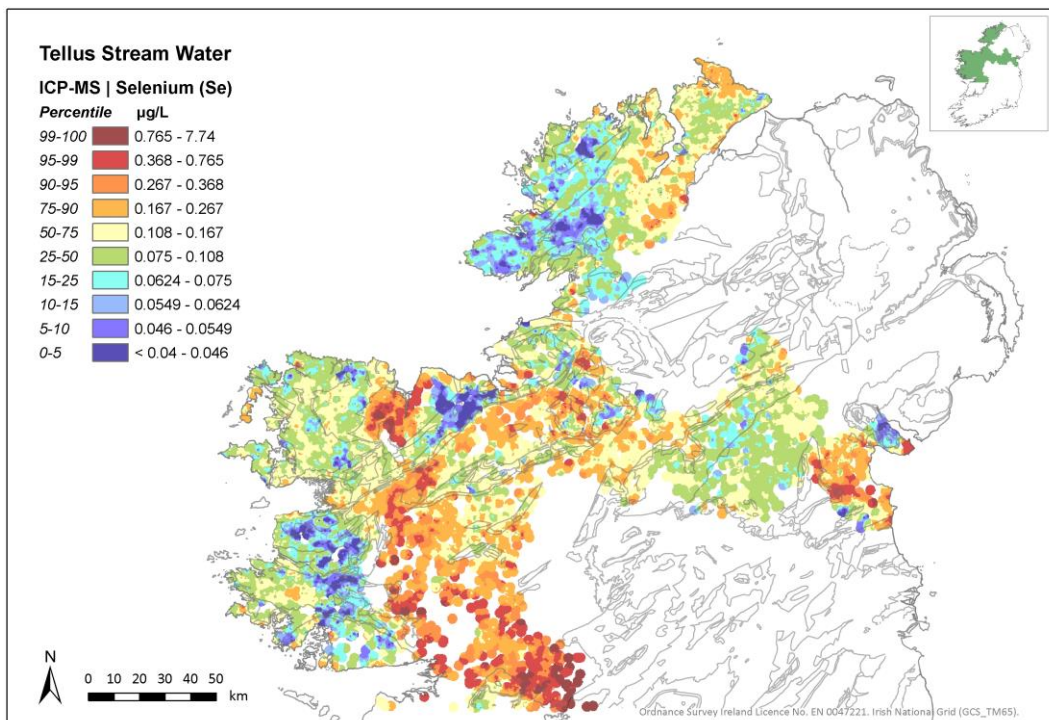


Figure 3.9 Distribution of selenium in Tellus stream water samples.

Nickel (Ni) in stream waters (Figure 3.8) has a similar distribution to chromium, albeit perhaps better defined in places. As with chromium, the Ni-enriched rocks of the Longford-Down inlier and the South Mayo Trough are well picked out but of particular interest are the relatively high concentrations recorded over the Lower Carboniferous



rocks of Mayo and east Galway. These rocks also show somewhat unexpected enrichments in other elements such as antimony (Sb), molybdenum (Mo), potassium (K), selenium (Se) (Figure 3.9), sulphur (S) (Figure 3.10) and uranium (U) (Figure 3.11). In the case of uranium, and perhaps other elements, the relatively high concentrations in streams draining limestone-dominated rock units may reflect the stability in solution of hexavalent uranium carbonates or bicarbonates (De Vivo *et al.* 2006). These high concentrations may mask U signatures associated with crystalline rocks such as granites, although the uraniferous Barnesmore Granite in Donegal has a prominent associated stream water U anomaly.

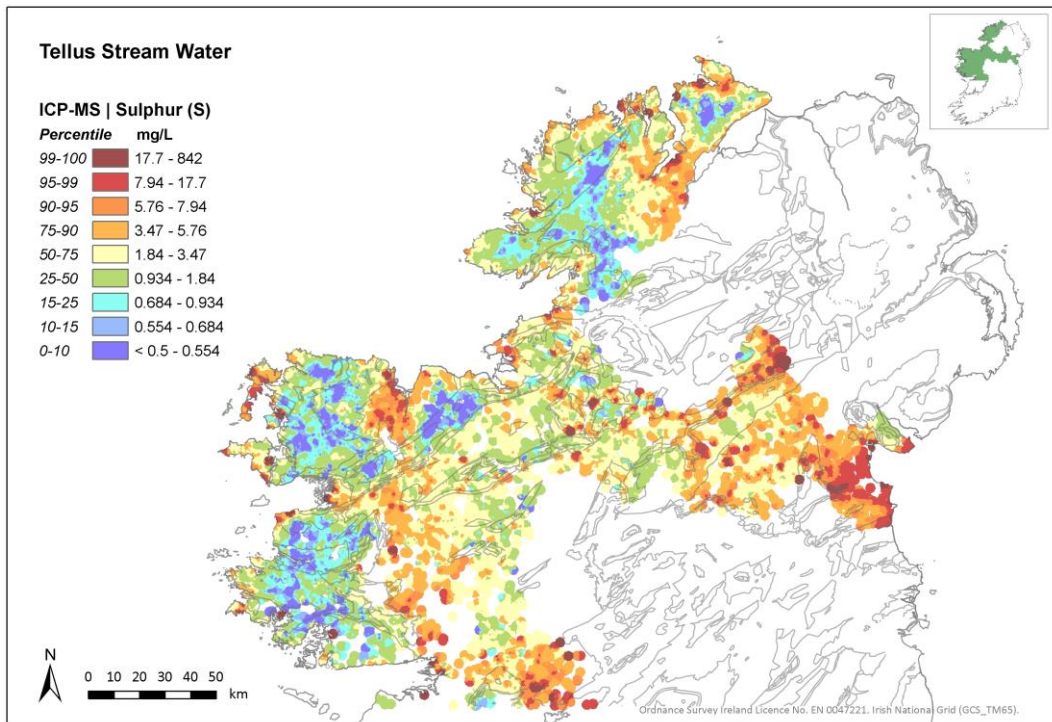


Figure 3.10 Distribution of sulphur in Tellus stream water samples.



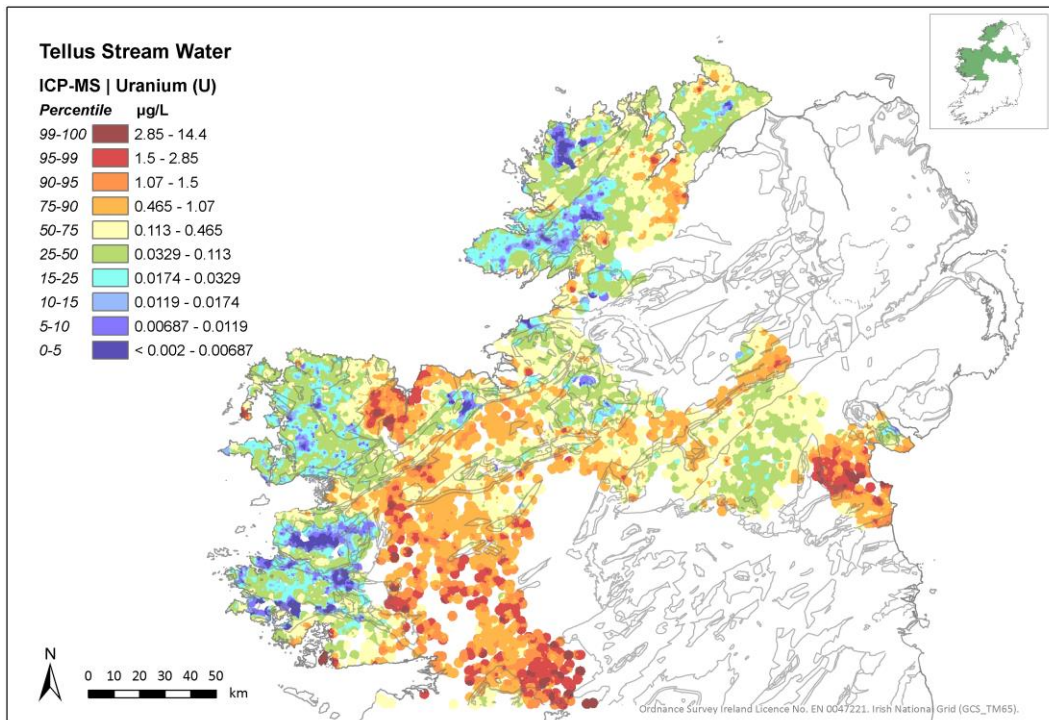


Figure 3.11 Distribution of uranium in Tellus stream water samples.

In contrast, sodium (Na) (Figure 3.12) shows the marine influence along the western and northern coasts, with enrichment in Na observed where on-shore winds and tides have affected freshwater systems. Similar patterns can be observed for other elements that are present in seawater, such as bromium (Br).

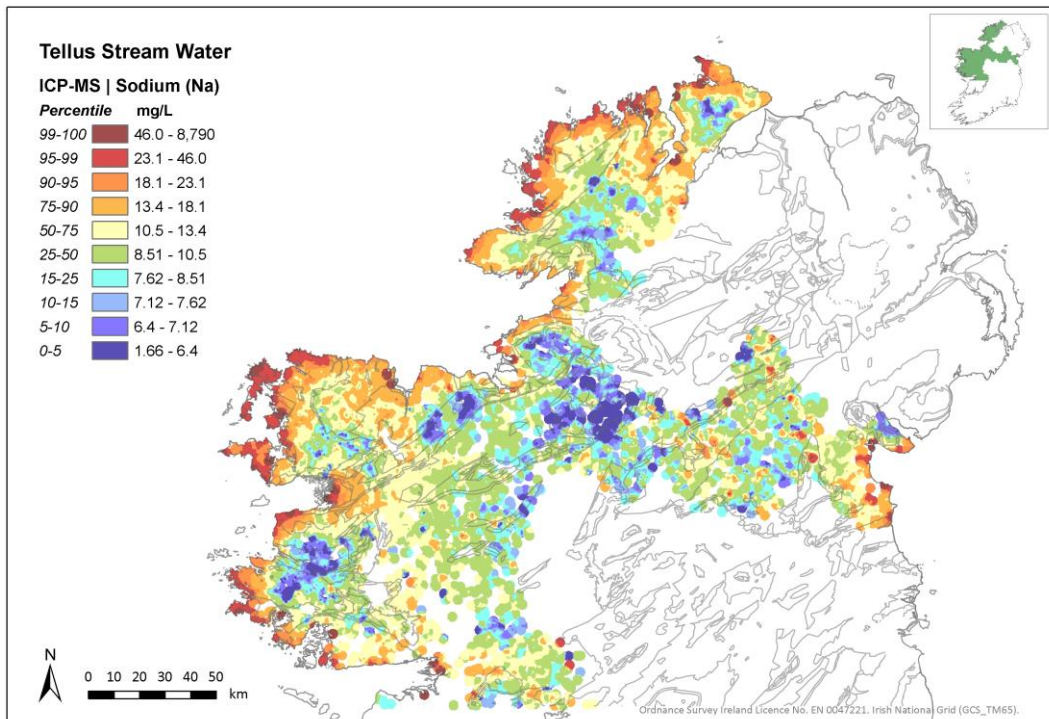


Figure 3.12 Distribution of sodium in Tellus stream water samples.



The distribution of zinc (Zn) in stream water (Figure 3.13) is strongly influenced by the presence of base metal mineralization, notably in County Monaghan where a large Zn anomaly coincides with widely dispersed mineralization that was exploited in numerous small mines in the 19th century. A Zn anomaly also marks Tynagh mine in south County Galway. Some of the other identified Zn anomalies also coincide with known mineral occurrences.

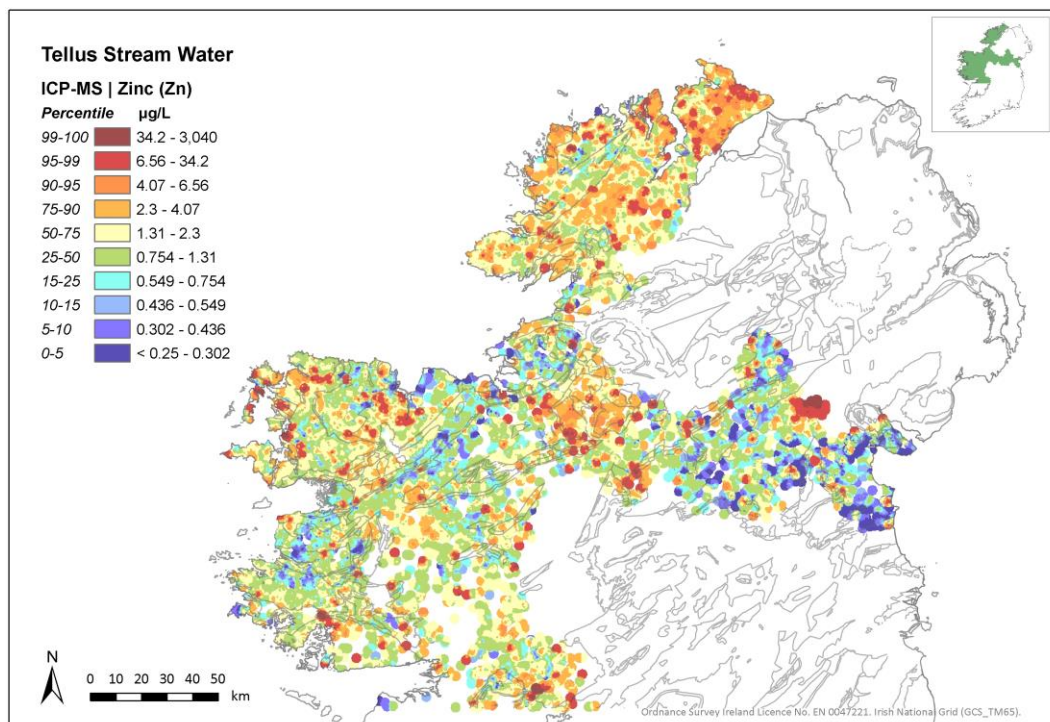


Figure 3.13 Distribution of zinc in Tellus stream water samples.

Finally, the map of pH distribution (Figure 3.14) demonstrates the influence of peat on stream water chemistry. Low pH characterizes the upland areas of Counties Donegal, Mayo, Galway, Leitrim and Roscommon where blanket bog is the predominant subsoil type. Relatively high pH is characteristic of arable land in County Louth and pasture around the midlands where it correlates with high Ca concentrations, reflecting the influence of limestone and agricultural practices, including fertilizer application.



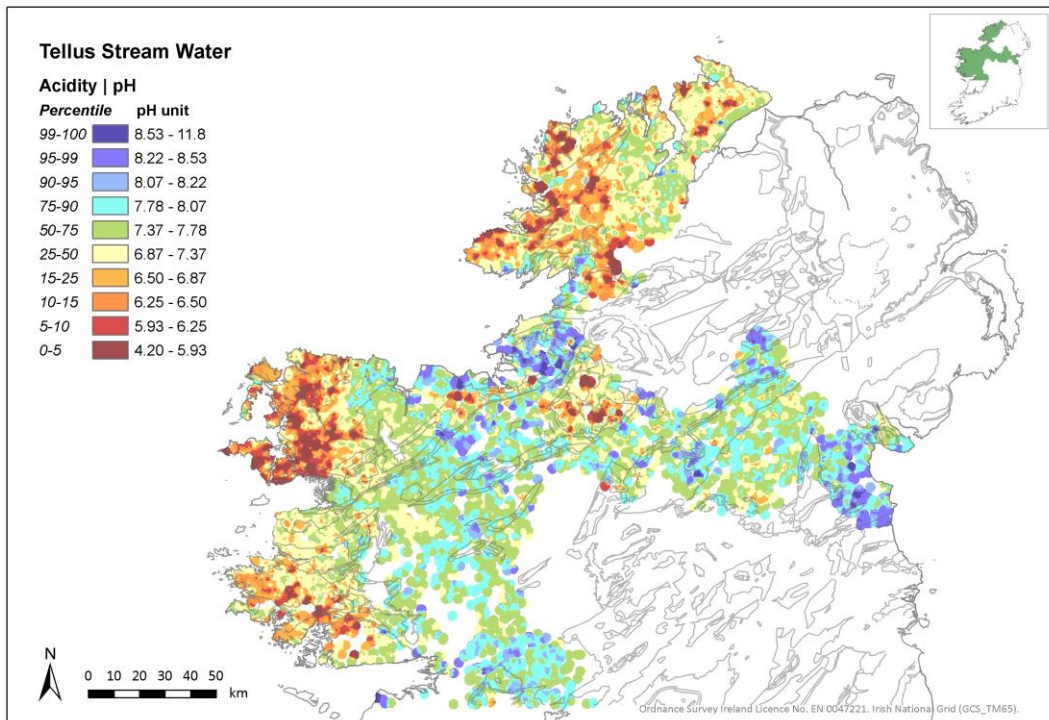


Figure 3.14 Distribution of pH in Tellus stream water samples.

3.3. Potentially Harmful Substances

As noted above, potentially harmful substances monitored in Ireland include **Priority Substances** and **Specific Pollutants**. The Environmental Quality Standards (EQS) for such elements and compounds are listed in the Environmental Objectives (Surface Waters) Regulations (European Commission 2009). These are listed in Table 3.1 for the elements that are included in the Tellus stream water dataset. For Cd, Cu and Zn, the EQS varies according to the water hardness.



Element	EQS value	Unit	Water hardness
As	25	µg/L	
Cr(III)	4.7	µg/L	
Cr(VI)	3.4	µg/L	
Cd	≤ 0.08	µg/L	< 40 mg/L CaCO ₃
Cd	0.08	µg/L	40 – < 50 mg/L CaCO ₃
Cd	0.09	µg/L	50 – < 100 mg/L CaCO ₃
Cd	0.15	µg/L	100 – < 200 mg/L CaCO ₃
Cd	0.25	µg/L	≥ 200 mg/L CaCO ₃
Cu	5	µg/L	≤ 100 mg/L CaCO ₃
Cu	30	µg/L	> 100 mg/L CaCO ₃
F ⁻	500	µg/L	
Ni	20	µg/L	
Pb	7.2	µg/L	
Zn	8	µg/L	≤ 10 mg/L CaCO ₃
Zn	50	µg/L	> 10 – ≤ 100 mg/L CaCO ₃
Zn	100	µg/L	> 100 mg/L CaCO ₃

Table 3.1 Environmental Quality Standards (EQS) for Specific Pollutants and Priority Substances included in Tellus stream water dataset.

In defining the EQS values for Specific Pollutants the regulations state that the values for As, Cr(III), Cu and Zn are as added values to background concentrations, i.e. that the EQS values are to be added for the background values for the given water source to give the working EQS, which therefore will exceed the EQS as listed in the regulations (Table 3.1). This approach is not used as part of current monitoring programmes in Ireland.

There are no current estimates of “background” values of metals in surface water in Ireland. Therefore in the national monitoring programme the EQS values that are applied are those as listed in the regulations, which are likely to be lower than values that would apply in many cases if background values were available. This could give rise to overly conservative limits being applied with more exceedances of the EQS than justified by the regulations.

An assessment of ambient background concentrations (ABCs) for metals in freshwaters in hydrometric areas and water bodies the UK, as defined under the Water Framework Directive, was carried out by Peters *et al.* (2012). They defined ABCs as concentrations representing low anthropogenic inputs, rather than natural backgrounds, as the monitoring data used to define them are considered likely to include contributions from natural and anthropogenic (point and diffuse) sources. They recommended that ABCs be based on individual hydrometric areas where sufficient data allowed and that the level be set at a low, conservative value such as the 5th or 10th percentile.



In contrast to monitoring sites, over 90 % of Tellus stream water sites are located on first- and second-order streams. The Tellus data are based on sampling in the upper parts of catchments with sites selected to minimize the risk of anthropogenic input of metals. In theory this should allow for an estimate of natural background concentrations.

Below, the potential use of Tellus data to estimate natural background concentrations of metals and to map water hardness is explored.

3.3.1 Background concentrations of metals in stream waters

Figure 3.15 shows Exploratory Data Analysis (EDA) plots for As, Cr, Cu and Zn for the entire Tellus dataset. All elements were transformed to log₁₀. All of the elements except Zn display log-normal distributions (straight lines in Quantile-Quantile (Q-Q) plots and symmetric histograms). Zn has a multimodal distribution with a small upper peak that is apparent as a steep ramp in the upper part of the Q-Q curve. Additional details on these elements are provided in Appendix E.

Figure 3.16 shows detailed Q-Q plots for these elements. The plots display the element concentrations on the Y-axis. Inflection points along the Q-Q curve can be used as “breakpoints” or “thresholds” that define the transition from one process to another. These inflection points can be used as estimations of background concentrations for each element. For As, the estimated break point occurs at 10 µg/L, for Cr 1.8 µg/L and for Cu 10 µg/L. The Zn Q-Q plot has several inflection points. That observed at the lower end of the range is an artefact related to censoring of values reported below the detection limit (0.25 µg/L). The Q-Q curve ramps upwards sharply at c. 6.5 µg/L and flattens out again at c. 34 µg/L. These inflection points cover the range of the small peak visible to the right of the main peak on the density plot. This ramp coincides with the 95–99th percentile range for Zn in stream water (Figure 3.13). Samples in this range are widely dispersed in the study area and, while some can be related to known mineral deposits, most have no clear association with mineralization. Some show a spatial association with peat bogs, e.g. in County Donegal, suggesting complexation by organic matter, whereas others may be linked to bedrock sources, such as Namurian shales in the Lough Allen area (Figure 3.1). A final inflection point at c. 55 µg/L Zn marks outliers of the data that in almost all cases reflect elevated Zn concentrations in streams draining former mine or mineralized areas.



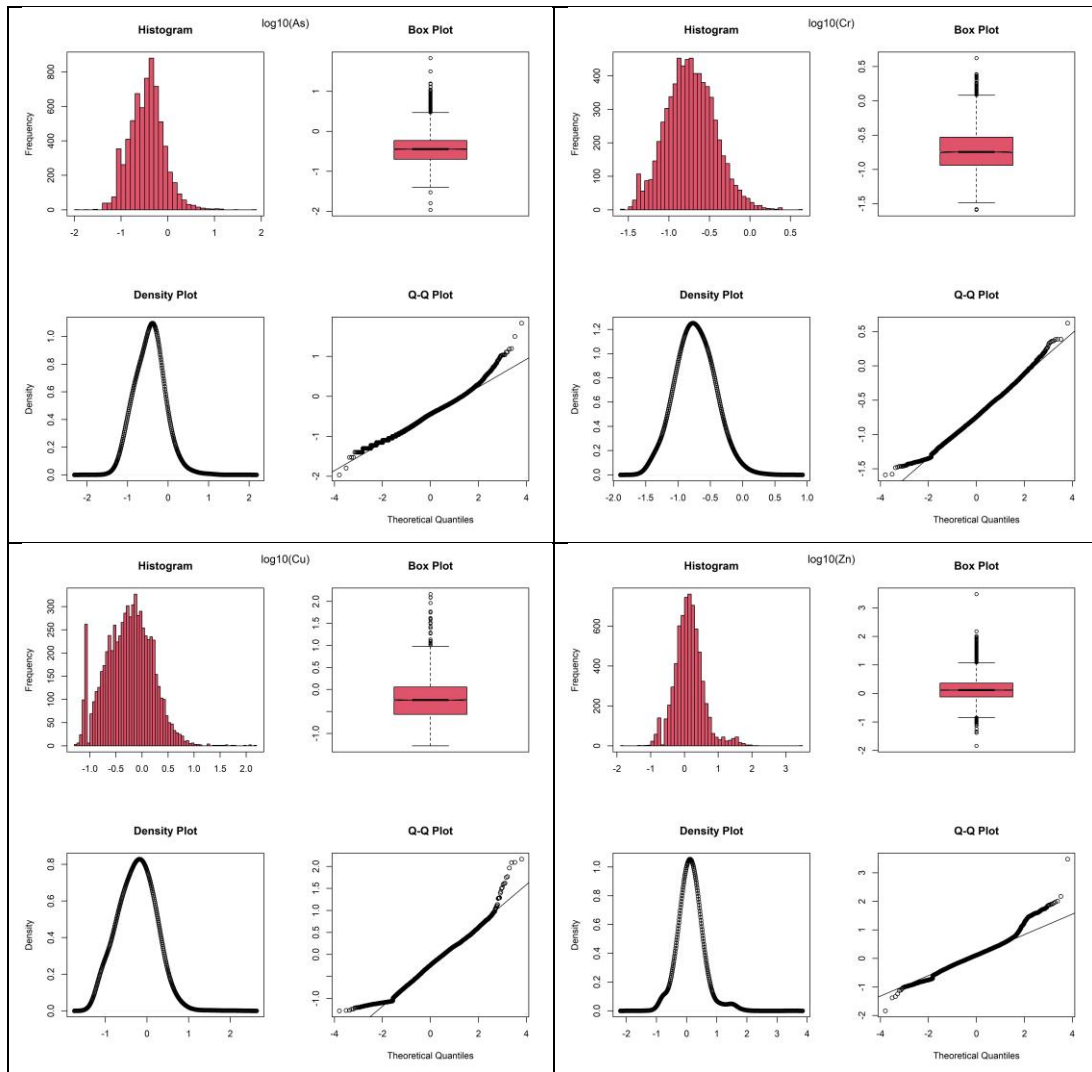


Figure 3.15 EDA plots for As, Cr, Cu and Zn.

These breaks provide estimates of the background concentrations in stream water for each of these elements in the area covered by the Tellus data (Table 3.2, “All”). Background values for As and Cr are well below the stated EQS limits (25 µg/L for As; 3.4 / 4.7 µg/L for Cr(III) / Cr(VI)). For Cu, the estimated background of 10 µg/L exceeds the stated 5 µg/L EQS for water with a hardness ≤ 100 mg/L CaCO₃ eq but is well below the corresponding 30 µg/L EQS for water with hardness exceeding 100 mg/L CaCO₃ eq. Adding any of these estimated background values to the EQS values to generate “corrected” EQS values would yield higher EQS values. For Zn, the higher estimated background of 34 µg/L exceeds the stated 8 µg/L EQS for water with a hardness < 10 mg/L CaCO₃ eq – adding this value to the stated EQS would eliminate many observed exceedances at the lower end of the scale.



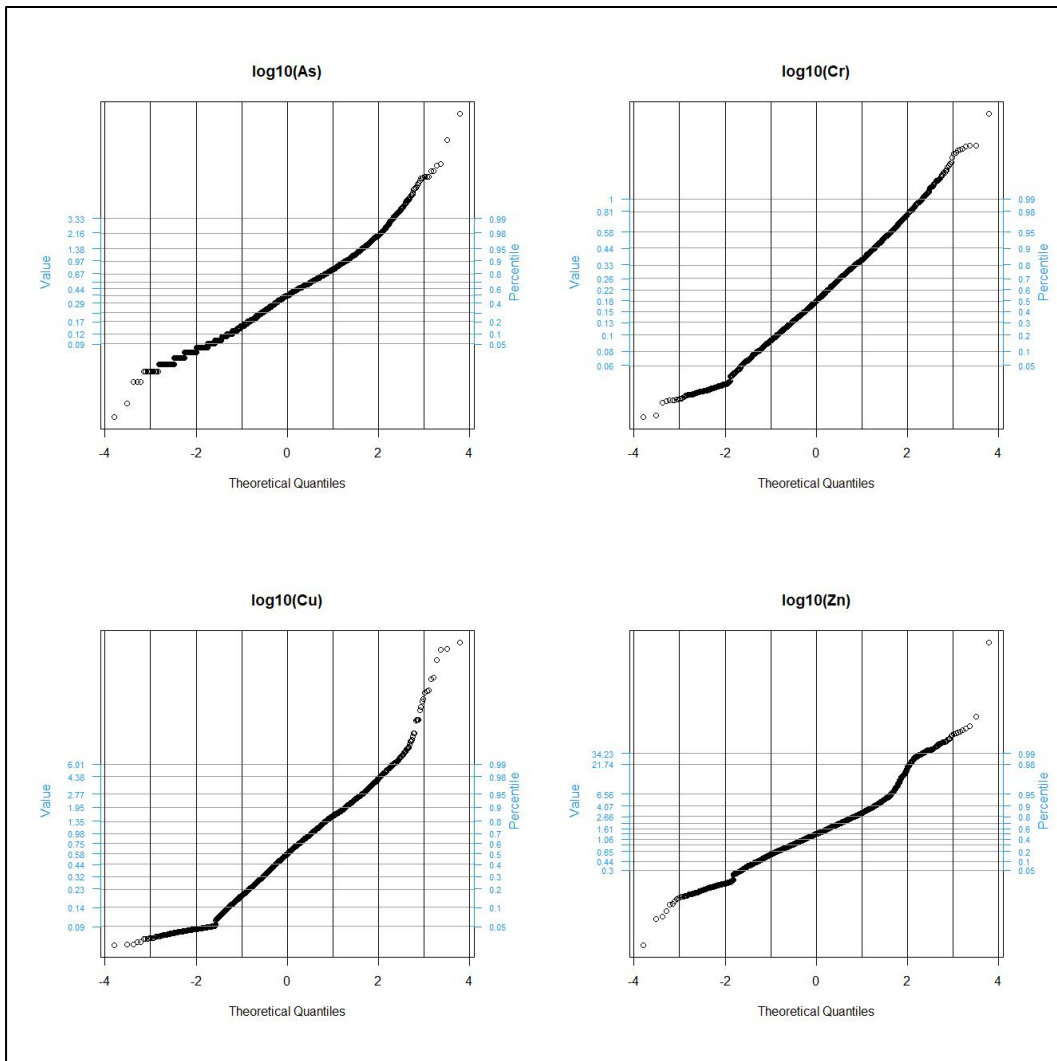


Figure 3.16. Quantile-Quantile plots for As, Cr, Cu and Zn

Domain	As $\mu\text{g/L}$	Cr $\mu\text{g/L}$	Cu $\mu\text{g/L}$	Zn $\mu\text{g/L}$
All	10	1.8	10	6.5 / 34
Domain 1	0.65	0.5	4, 6	7
Domain 2	3	1	5	9
Domain 3	1.9	0.8	2.1	4.8
Domain 4	1.8	0.7	1.9	4.7
Domain 5	5.6	1.5	4.4	13.8 / 44
Domain 6	0.95	0.93	1.24 / 1.82	4.7 / 7.7
Domain 7	6	1.14	13.5	14.2 / 53.5

Table 3.2 Estimated background concentrations of some elements in Tellus stream waters using Q-Q plot breaks. Data classified according to SRF Geochemical Domains. Some elements have more than one break point on Q-Q plot.



Table 3.2 summarizes the breakpoints observed on Q-Q plots for stream water samples classified by SRF Geochemical Domain (Appendix E). These domains provide a simplified bedrock / subsoil classification scheme that illustrates the influence of geogenic factors on stream water chemistry. As may be expected, there is considerable divergence between the estimated threshold or background values for individual elements among the SRF Domains, reflecting the diverse geology of the region. Using EQS concentrations for As, Cr (III), Cu and Zn in surface waters without correcting for background will likely lead to many apparent exceedances in monitoring data. Tellus regional stream water data is of sufficient resolution to allow estimates of natural background concentrations at regional or even sub-regional scale.

As stated above, current practice in Ireland is to apply the stated EQS values for metals As, Cr, Cu and Zn without correction for background. The above treatment suggests that there is good potential to use Tellus stream water data to compute “background” levels, at least for these four elements where the EQS is stated as being “added to background”. Different approaches are possible but the nature of Tellus samples, sampled at relatively high-density and collected up-catchment with, as far as can be assured, minimal anthropogenic inputs, provides a unique opportunity to make such estimations for Irish surface waters. Even if water bodies rarely have their status determined by their measured concentrations of Specific Pollutants, and addition of background values would only serve to reduce the incidence of such determinations further, it is nevertheless desirable to have an estimate of the background for these metals to ensure the correct EQS values are applied in all contexts.

3.3.2 EQS and water hardness

As specified in Table 3.1, the surface water EQS values for Cd, Cu and Zn depend on the hardness of the water, reported as mg/L CaCO₃. Lack of water hardness data for all monitoring stations has led to application of the most conservative EQS limits for screening purposes. Thus, the lowest EQS of 8 µg/L is used for Zn with the result that the surface water monitoring programme has flagged hundreds of EQS exceedances for Zn.

Water hardness can be calculated for Tellus stream water data from the reported concentrations of Ca²⁺ and Mg²⁺, as measured by ICP-MS. The relatively high spatial resolution of the data in turn allows extrapolated maps of stream water hardness to be generated, providing a basis for applying the appropriate EQS limits at any given site even if water hardness data are not available for that site.

This approach is outlined below for Cd, Cu and Zn for the area covered by Tellus data.



3.3.2.1 Zn EQS and water hardness

The Tellus stream water dataset includes baseline chemical data for 6835 sites spread across a geologically diverse region. While these data are not directly comparable to monitor-site data they do provide an insight into the possible impact that accounting for hardness would have on the outcomes of monitoring programmes.

Water hardness can be calculated for Tellus stream water data from the reported concentrations of Ca^{2+} and Mg^{2+} , as measured by ICP-MS. Given the robust nature of ICP analysis, this represents a reliable and consistent means of measuring stream water hardness. The equation to convert these concentrations to mole equivalent CaCO_3 concentrations is:

$$\text{Hardness (CaCO}_3 \text{ equivalent)} = [2.5 \times \text{Ca}^{2+}] + [4.1 \times \text{Mg}^{2+}]$$

The calculated hardness values have been interpolated to produce a map of stream water hardness in the study area, classified according to the EQS for Zn: $\leq 10 \text{ mg/L}$, $> 10 \text{ mg/L}$ and $\leq 100 \text{ mg/L}$ and $> 100 \text{ mg/L}$ $\text{CaCO}_3 \text{ eq.}$, for convenience labelled Category I, II and III, respectively.

Figure 3.17 shows the distribution of sites for which the measured Zn concentration in Tellus stream water exceeds $8 \text{ }\mu\text{g/L}$, the lowest EQS value and the one used to assess EPA monitoring data. Out of 6835 samples, 286 (4.2 %) exceed $8 \text{ }\mu\text{g/L}$ Zn. When allowance is made for hardness (Figure 3.18), 27 (0.4 %) exceed the EQS: three exceed the $100 \text{ }\mu\text{g/L}$ limit where hardness is greater than 100 mg/L CaCO_3 ; 12 exceed the $50 \text{ }\mu\text{g/L}$ limit where hardness is greater than 10 and less than 100 mg/L CaCO_3 ; 12 exceed the $8 \text{ }\mu\text{g/L}$ limit where hardness is less than 10 mg/L CaCO_3 .

Application of hardness data alone reduces the number of Zn exceedances observed by 90 %.



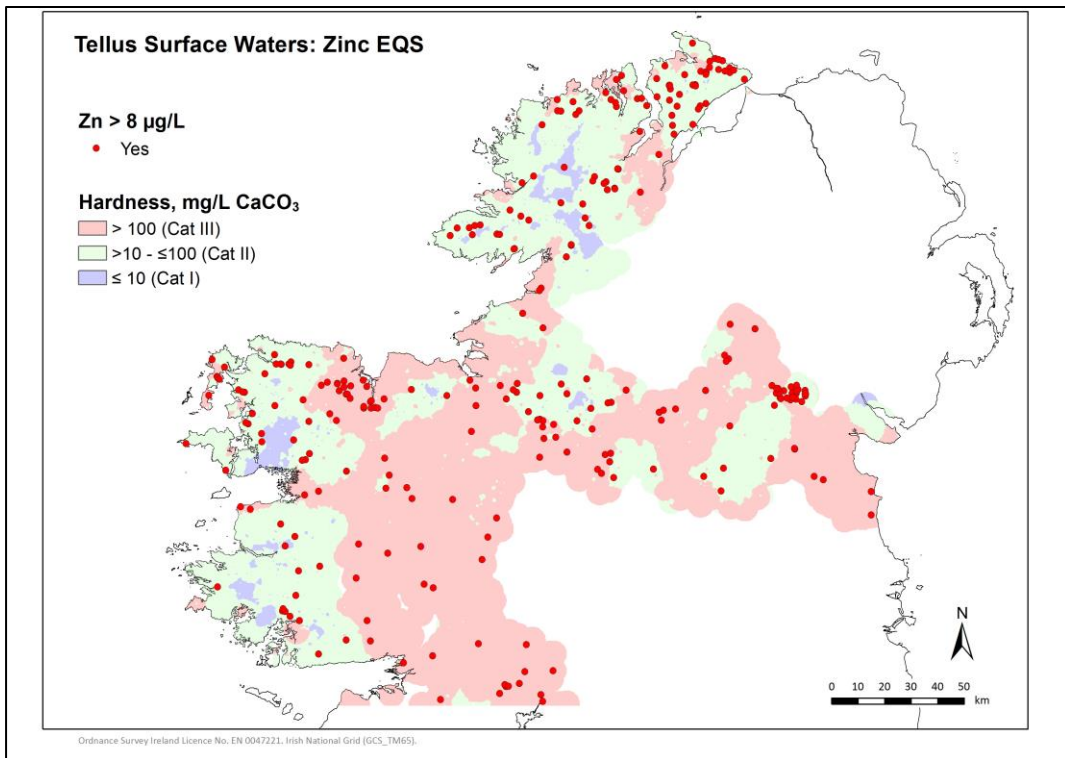


Figure 3.17 Distribution of sites for which the measured Zn concentration in Tellus stream water samples exceeds 8 µg/L, the minimum EQS value.

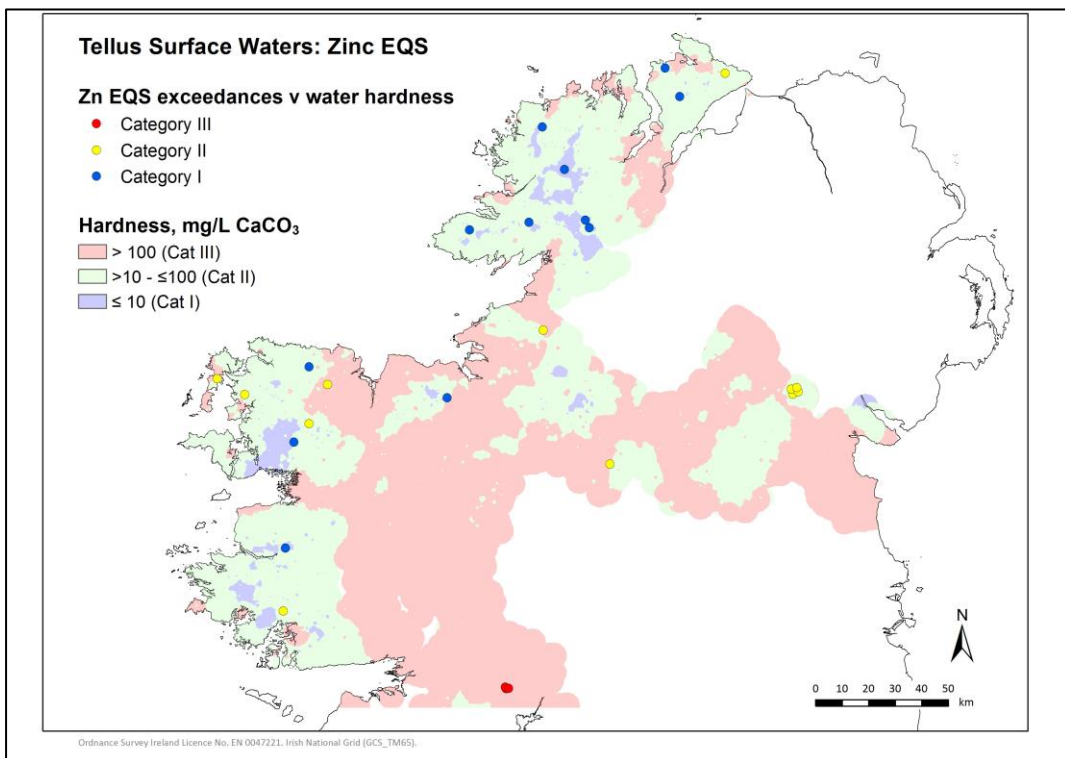


Figure 3.18 Distribution of sites for which the measured Zn concentration in Tellus stream water samples exceeds the EQS value after correction for water hardness.

3.3.2.2 Cd EQS and water hardness



Figure 3.19 shows a map of stream water hardness in the study area, classified according to the EQS for Cd: < 40 mg/L (Category I); > 40 mg/L and ≤ 50 mg/L (Category II); > 50 mg/L and ≤ 100 mg/L (Category III); > 100 mg/L and ≤ 200 mg/L (Category IV); > 200 mg/L CaCO₃ eq. (Category V). Also on Figure 3.19 are sites where the measured Tellus stream water concentration exceeds the lowest Cd EQS, 0.08 µg/L. These exceedances include several clusters related to known Zn mineralization (in County Monaghan and at Tynagh, County Galway) and to Namurian bedrock around Lough Allen and east of Westport in County Mayo.

The total number of Tellus sites for which Cd exceeds 0.08 µg/L is 130, or 1.9 % of the total. When allowance is made for hardness (Figure 3.20), 79 (1.2 %) exceed the EQS: 31 exceed the ≤ 0.08 µg/L limit for hardness (Category I); 6 exceed the 0.08 µg/L limit for hardness (Category II); 32 exceed the 0.09 µg/L limit for hardness (Category III); seven exceed the 0.15 µg/L limit for hardness (Category IV); three exceed the 0.25 µg/L limit for hardness (Category V).

In the case of Cd, application of hardness data reduces the number of Cd exceedances observed by just under 40 %. Unlike Zn, Cd is not widely dispersed in stream water at elevated concentrations and relatively high concentrations are typically related to specific non-carbonate bedrock sources. Hence, higher EQS values, based on increased water hardness that is intrinsically related to the presence of carbonate bedrock, do not affect the observed rate of EQS exceedance as strongly as is the case for Zn. Nevertheless, the estimated reduction in the rate of EQS exceedance is still significant.

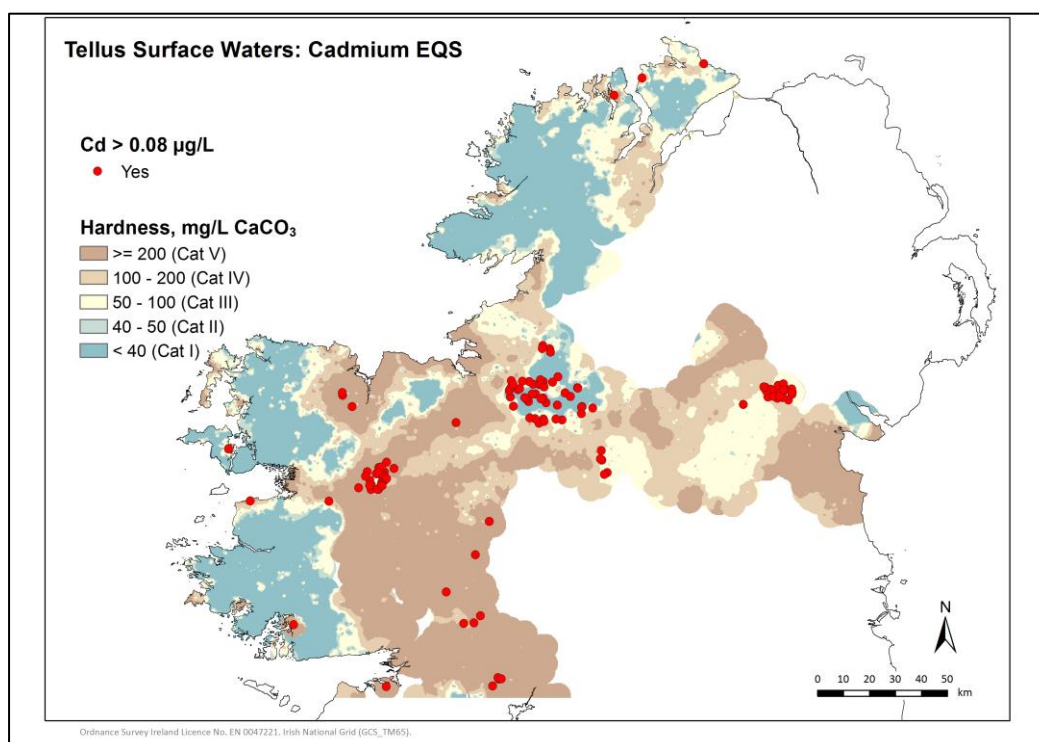


Figure 3.19 Distribution of sites for which the measured Cd concentration in Tellus stream water samples exceeds 0.08 µg/L, the minimum EQS value.



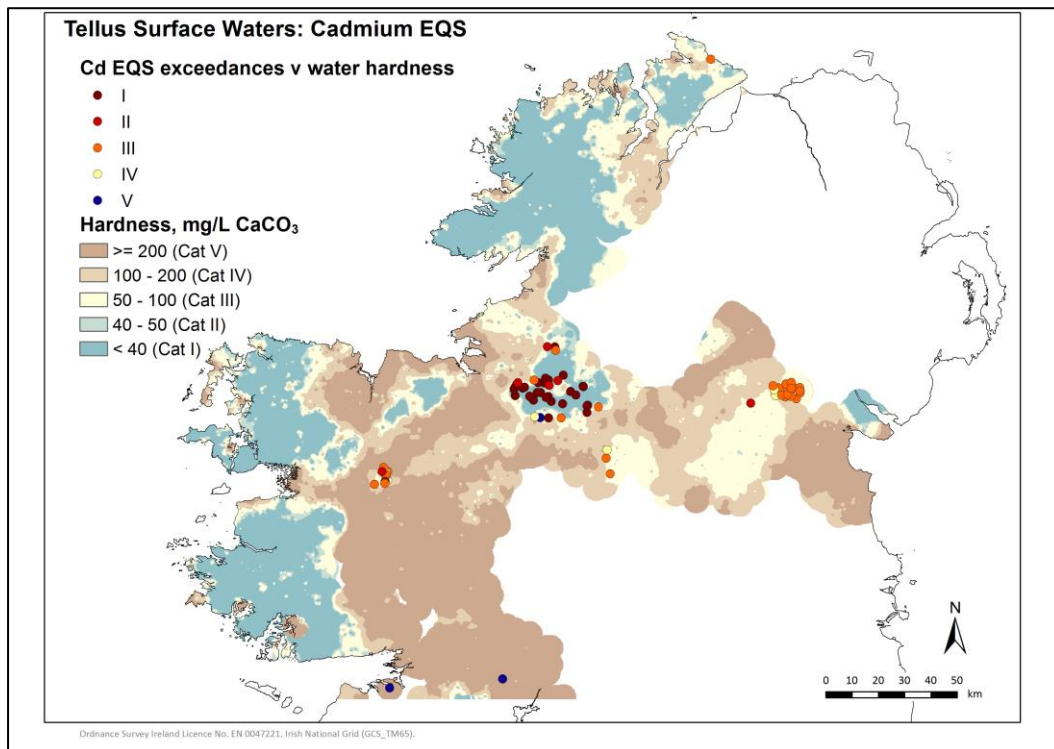


Figure 3.20 Distribution of sites for which the measured Cd concentration in Tellus stream water samples exceeds the EQS value after correction for water hardness.

3.3.2.3 Cu EQS and water hardness

Copper is the third metal for which the EQS varies according to water hardness. Figure 3.21 shows a map of stream water hardness in the study area, classified according to the EQS for Cu: ≤ 100 mg/L CaCO₃ eq. (Category I) or > 100 mg/L CaCO₃ eq. (Category II). Also on Figure 3.21 are sites where the measured Tellus stream water concentration exceeds the lowest Cu EQS, 5 μ g/L. There are no clear bedrock-related clusters of Cu exceedances, albeit the relatively high concentrations observed for north Donegal could point to a possible influence of Dalradian bedrock.

The total number of sites for which the measured concentration of Cu exceeds 5 μ g/L is 103, or 1.5 % of the total. When allowance is made for hardness (Figure 3.22), 77 (1.1 %) exceed the EQS: three exceed the 30 μ g/L limit for hardness > 100 mg/L CaCO₃ eq. (Category II) and 74 exceed the 5 μ g/L limit for hardness ≤ 100 mg/L CaCO₃. Overall, application of water hardness data has only a very limited effect on the rate of exceedance of the Cu EQS. Most of the sites in north Donegal that exceed the lower EQS are also in the lower water hardness category so that application of the hardness categories has little or no effect.



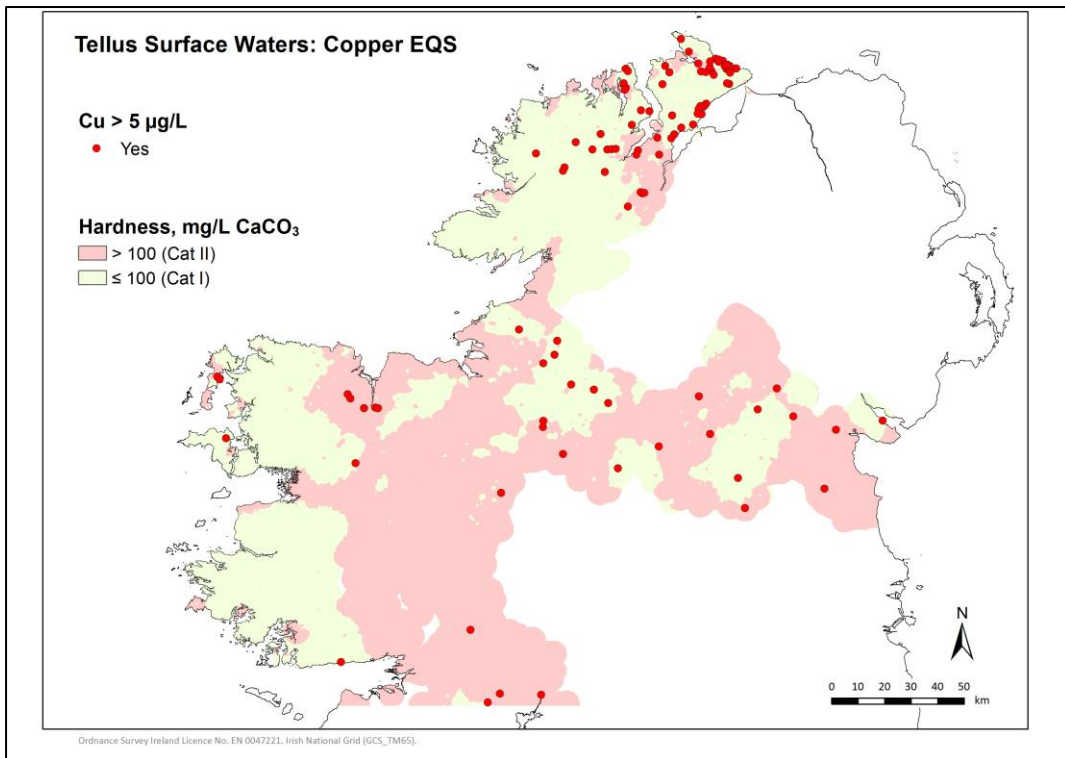


Figure 3.21 Distribution of sites for which the measured Cu concentration in Tellus stream water samples exceeds 5 µg/L, the minimum EQS value.

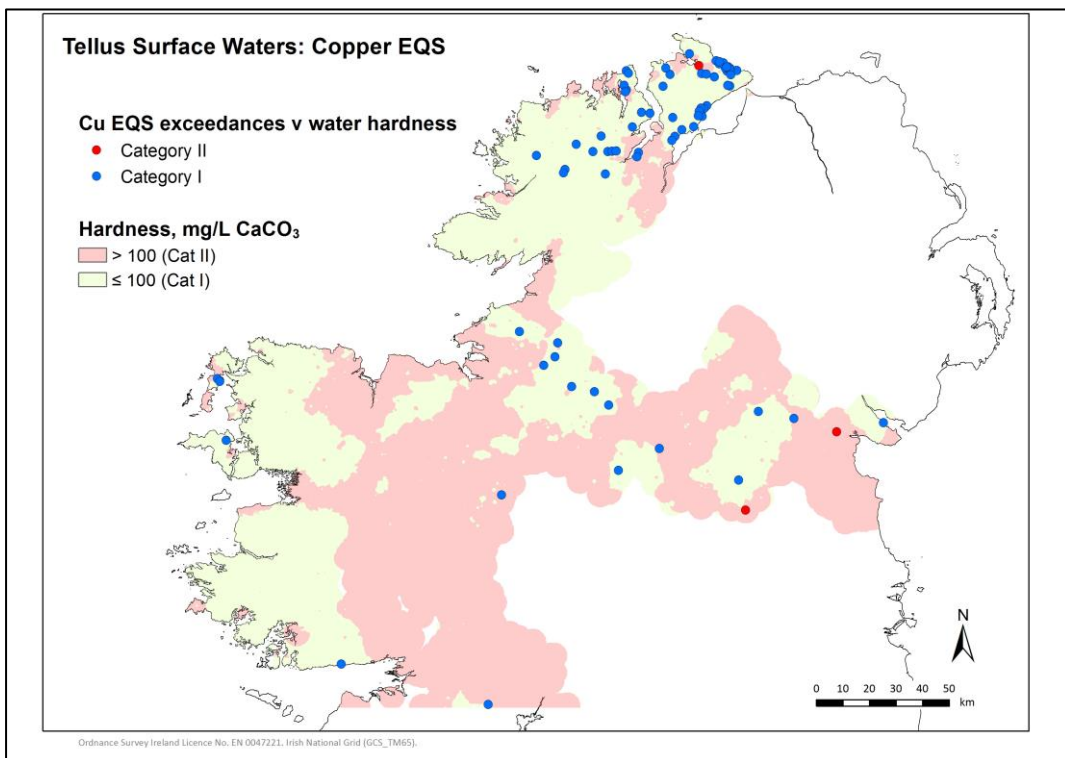


Figure 3.22 Distribution of sites for which the measured Cu concentration in Tellus stream water samples exceeds the EQS value after correction for water hardness.



3.3.2.4 Water hardness and EQS value: summary

Based on a review of Tellus stream water data, an estimate of the water hardness at any given sampling site appears to be of high importance in assessing exceedances of Zn EQS values. Without hardness data it is likely that the degree of Zn exceedance of the EQS will be significantly overstated where the lowest EQS value is used as part of a conservative approach. Tellus high-resolution baseline stream water data allow reliable mapping of water hardness in areas where water monitoring stations are sampled. This can help reduce the number of sites that are falsely flagged for Zn exceedance.

The review of Tellus data for Cd and Cu suggest that for these elements application of water hardness data would have a more limited impact on EQS assessment, although still quite significant for Cd. This exercise was carried out using Tellus data from samples taken in upper catchments – samples from monitoring sites may yield different results in respect of Cd and Cu.

3.4 Stream Water Geochemistry and Mineralization

3.4.1 Review of mineralization in the region

There are numerous occurrences of base metal (Zn, Pb, Cu) mineralization in the region covered by Tellus stream water geochemistry and several of these have been exploited in the past, mostly for Zn and Pb (see section 3.4.2). Other commodities for which deposits have been discovered if not exploited include gold (Au), chromium (Cr) and tungsten (W). Section 4 provides a multivariate examination of chalcophile elements that provides some insight into areas of potential mineralization.

Known base metal occurrences (Fig. 3.23) include the former mines of Tynagh, (commodities produced: Zn, Pb, Cu, Ba, Ag) (Clifford *et al.* 1986), Glengowla (Pb, Ag) (Cole 1922) and Clements (Pb, Ag) (Cole 1922, Reynolds *et al.* 1986) in County Galway; Abbeystown (Zn, Pb) (Hitzman 1986) in County Sligo; Twigspark (Pb) in County Leitrim (Cole 1922); Keeldrum (Pb) (Cole 1922, Stanley *et al.* 2009), Glenaboghill (Pb), Ballyshannon (Pb) and Glentogher (Pb, Ag) (Cole 1922, McArdle *et al.* 1986) in County Donegal; Tassan, Annaglogh, Coolartragh and Hope mines in County Monaghan (Pb, Ag) (Morris 1984).

Gold mineralization occurs in the Dalradian metasediments of north Donegal (Inishowen) (Arkle Resources 2021), the Lower Palaeozoic sediments of south Mayo (Lecanvey, Cregganbaun) (Aherne *et al.* 1992; Thompson *et al.* 1992), Inishturk island and in the Lower Palaeozoic rocks of the Longford-Down Inlier in Monaghan (Clontibret) (Conroy Gold and Natural Resources 2021).

Small occurrences of tungsten are widespread throughout the western part of the Connemara Dalradian succession where scheelite is a common component of calc-silicate skarns. Chromium is enriched in mafic rocks of the Connemara Metagabbro and



Gneiss Complex, notably in the layered Dawros peridotite (Hunt *et al.* 2011). It is also sporadically enriched in serpentinite bodies and clastic sequences within both the Dalradian and overlying Lower Palaeozoic sequences of Galway and Mayo.

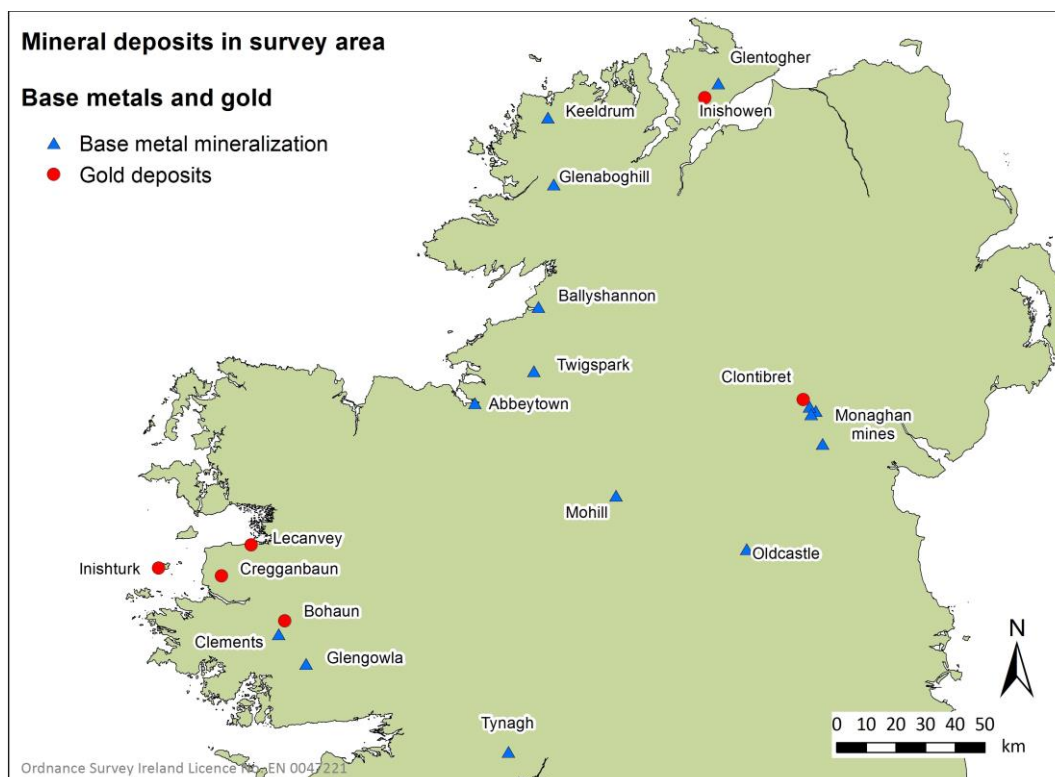


Figure 3.23. Location of known base metal mineralization in the study area.

3.4.2 Base metal mineralization and surface water geochemistry

Stream water Zn (\pm Pb \pm Cd) anomalies (Figures 3.24, 3.25 and 3.26) can be observed near Tynagh, the Monaghan mines, Glengowla, Clements, Abbeytown, Ballyshannon, Glenaboghill, Keeldrum and Glentogher. Not all of these observed anomalies occur downstream of the mines and thus may be reflective of the presence of bedrock mineralization in the general area rather than representing contamination by mining. However, at Tynagh there is direct evidence from previous studies (e.g. Stanley *et al.* 2009) that downstream Zn concentrations in stream water can, at least in part, be related to mine waste or mine water discharges.

Elsewhere in the region, base metal anomalies in stream water can be observed close to known but unworked bedrock occurrences of mineralization, notably near Oldcastle in County Meath and Mohill in County Roscommon. There are numerous occurrences of base metal (Zn, Pb, Cu) mineralization in the region covered by Tellus stream water geochemistry and several of these have been exploited in the past, mostly for Zn and Pb. Other commodities for which deposits have been discovered if not exploited include Au, Cr and W. Section 4 provides a multivariate examination of chalcophile elements that provides some insight into areas of potential mineralization.



Comparison of univariate maps for stream sediments and stream waters (Figure 3.27) indicate that stream water geochemistry may identify known base metal and gold mineralization as readily as stream sediment geochemistry.

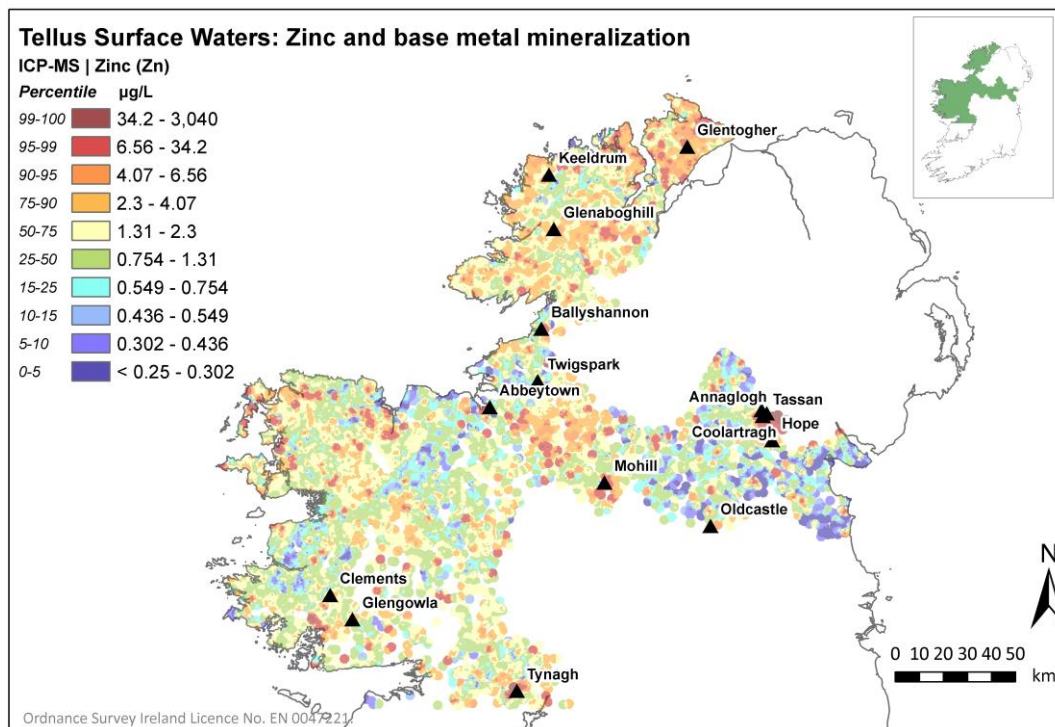


Figure 3.24. Location of known base metal mineralization shown on stream water Zn distribution.

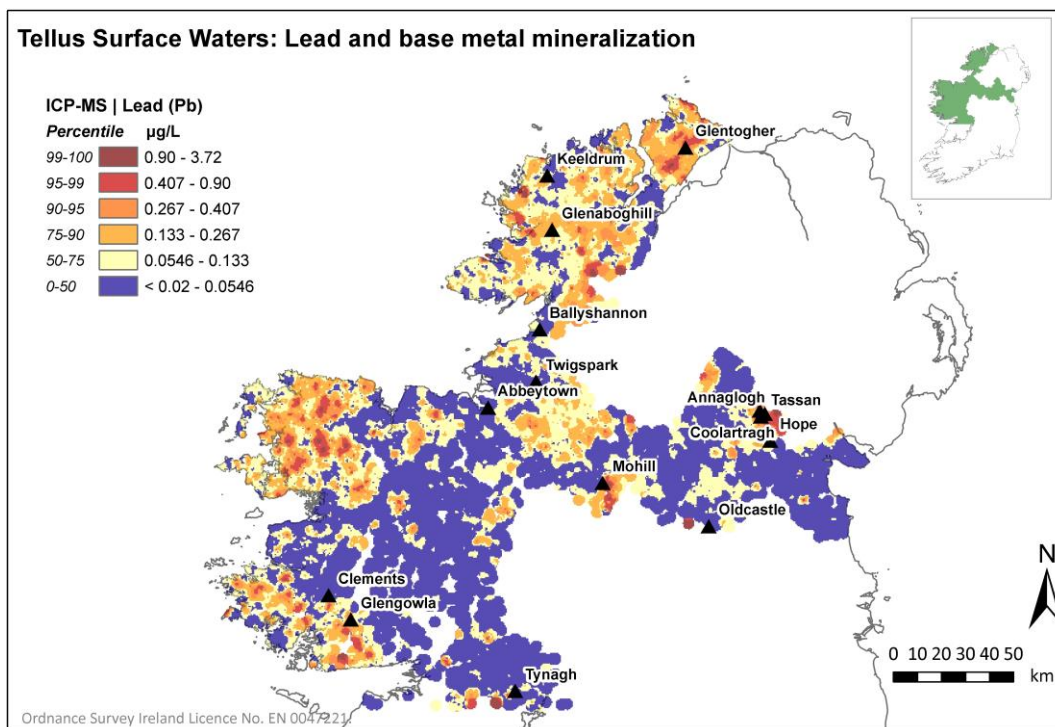


Figure 3.25. Location of known base metal mineralization shown on the stream water Pb distribution.



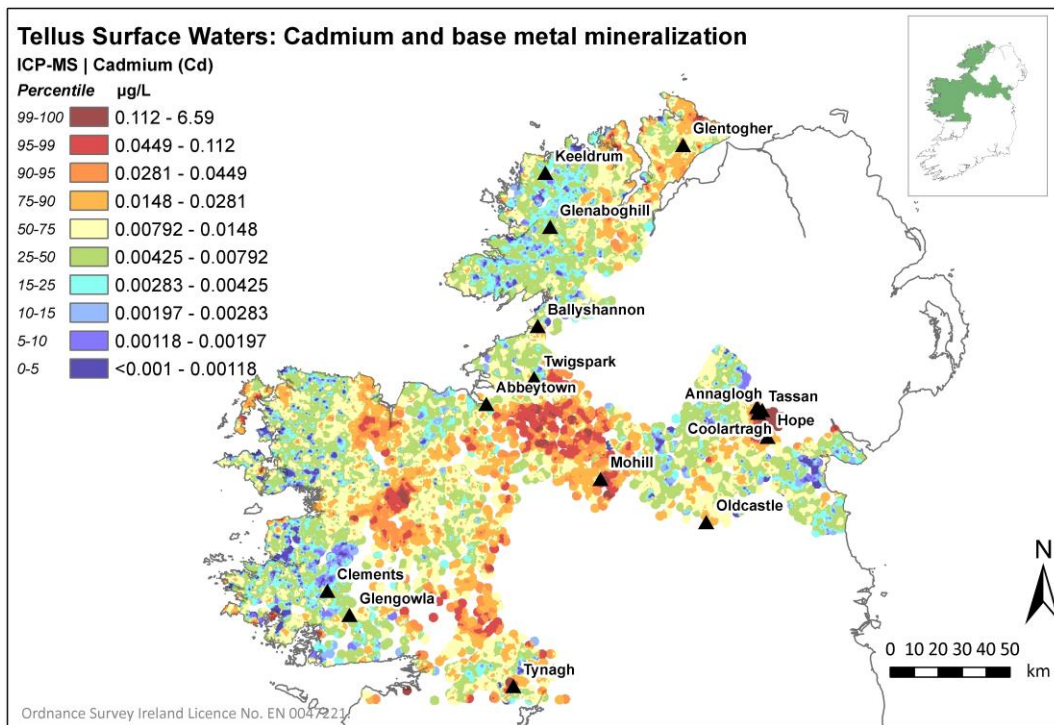


Figure 3.26. Location of known base metal mineralization shown on stream water Cd distribution.



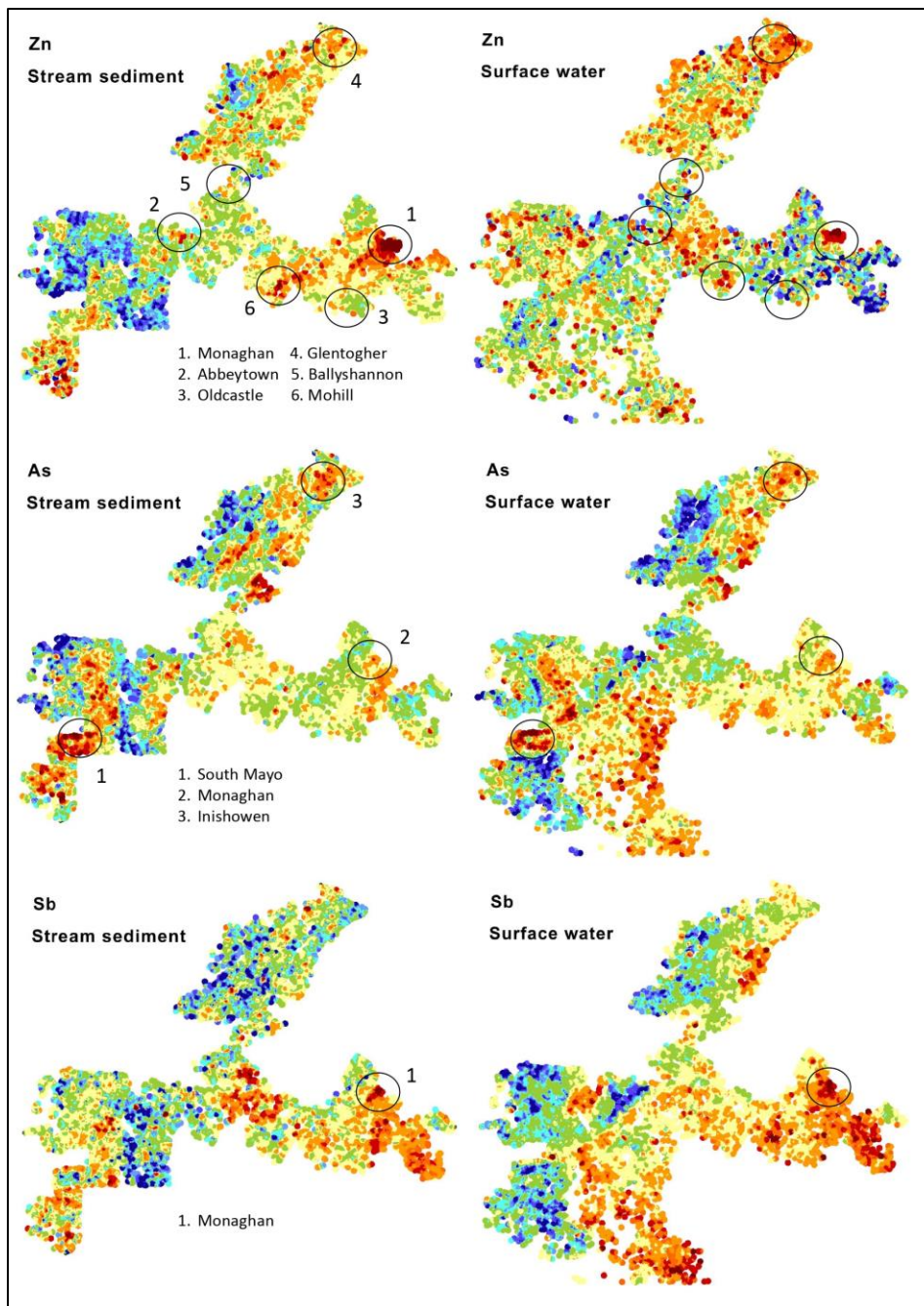


Figure 3.27 Comparison of As, Sb and Zn distributions in Tellus stream sediment and stream water data, with locations of known base metal and gold mineralization highlighted. Colours for element classes as in Figure 3.21.

While these univariate maps present clear evidence of spatial association between Zn, Pb and Cd stream water geochemical anomalies and known mineralization, there are clearly numerous stream water samples with “anomalous” concentrations that cannot be readily associated with any known mineral occurrence. Geostatistical exploration provides a means of refining this data further and an example follows for Zn and Cd.

Cluster analysis (Section 4.3) shows that Zn and Cd are closely associated in surface water samples that drain Lower Carboniferous bedrock and greywacke of the Longford-



Down inlier, the two bedrock units that host the most significant base metal mineralization in the survey area. These elements have similar atomic radii and form a solid-solution series in sphalerite. Cadmium is a notable trace element in numerous Zn-Pb deposits in Ireland (e.g. Slowey 1986; Wilkinson *et al.* 2005; Stanley *et al.* 2009, Torremans *et al.* 2018). NPOC is part of a larger cluster with both Zn and Cd and can be interpreted to reflect complexation of metals by organic-rich material (Section 4.3). Thus, apparent anomalies of Zn and Cd may reflect base-metal mineralization or simply enrichment following complexation within organic-rich soils and sediments.

In order to explore the data further, it is necessary to define what an anomalous concentration of Zn or Cd is. The use of inflection points on the Q-Q plot was discussed above (Section 3.2). Samples with Zn concentration above the inflection point of 34 ug/L (Table 3.2) are effectively all related to known mineralization. To widen the search somewhat for this exercise, values around the 98th percentile of Zn and Cd (20 and 0.08 ug/L, respectively) were selected as the threshold of anomalous concentrations. Figure 3.28 shows a scatterplot of Zn v Cd (here multiplied by 100 for plotting convenience). Points for which both Zn and Cd are equal to or exceed their respective 98th percentile value are magenta-coloured. Figure 3.29 plots Zn and Cd together with NPOC and again the “anomalous” points are highlighted. This plot suggests that “anomalous” Zn and Cd values generally have relatively low-NPOC concentrations. By excluding those few points with higher NPOC concentrations it is possible to refine this further, improving the likelihood of avoiding “anomalous” Zn and Cd values that owe their relatively high concentrations to organic complexation rather than mineralization. Figure 3.30 shows the same data on a map – the distribution of anomalous points clearly coincides with that of known mineralization. Other single “anomalies” can be assessed by reference to Figure 3.30 to determine if there is a likelihood that they reflect an organic influence. This approach is explored further in Section 4 and Appendix D where a Principal Component Analysis of the stream water data is shown to enhance the possibility of recognizing processes related to base metal mineralization.



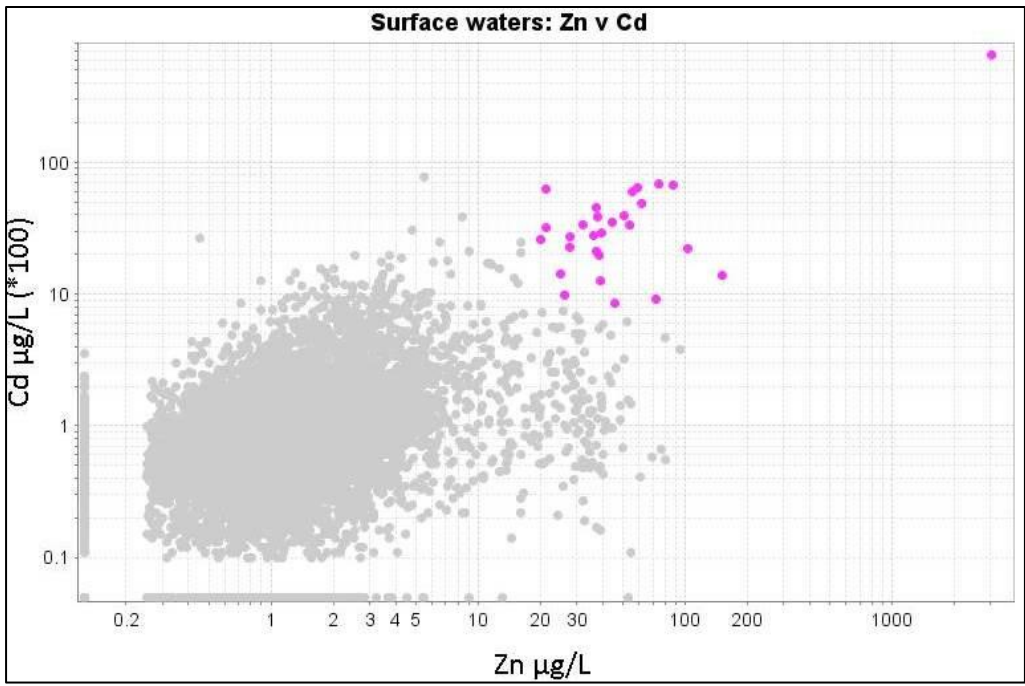


Figure 3.28 Zn v Cd in Tellus stream water: magenta colours are points for which both Zn and Cd equal or exceed their respective 98th percentile value.

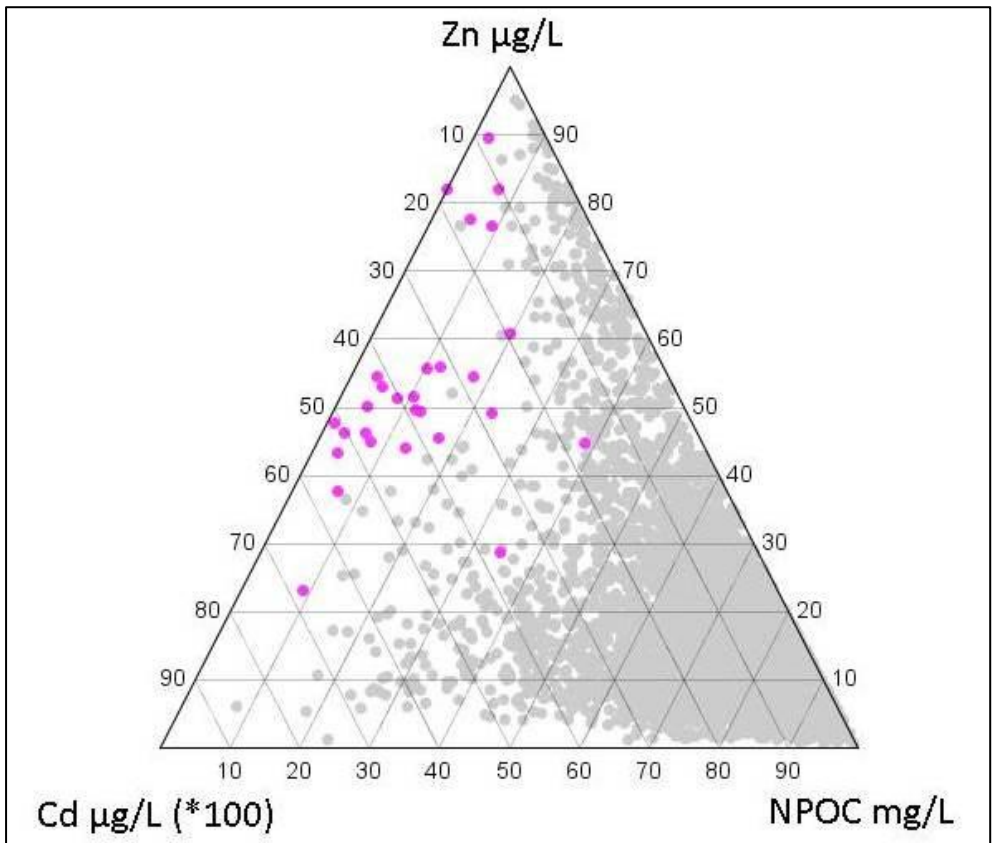


Figure 3.29 Ternary diagram plotting Zn and Cd with NPOC.



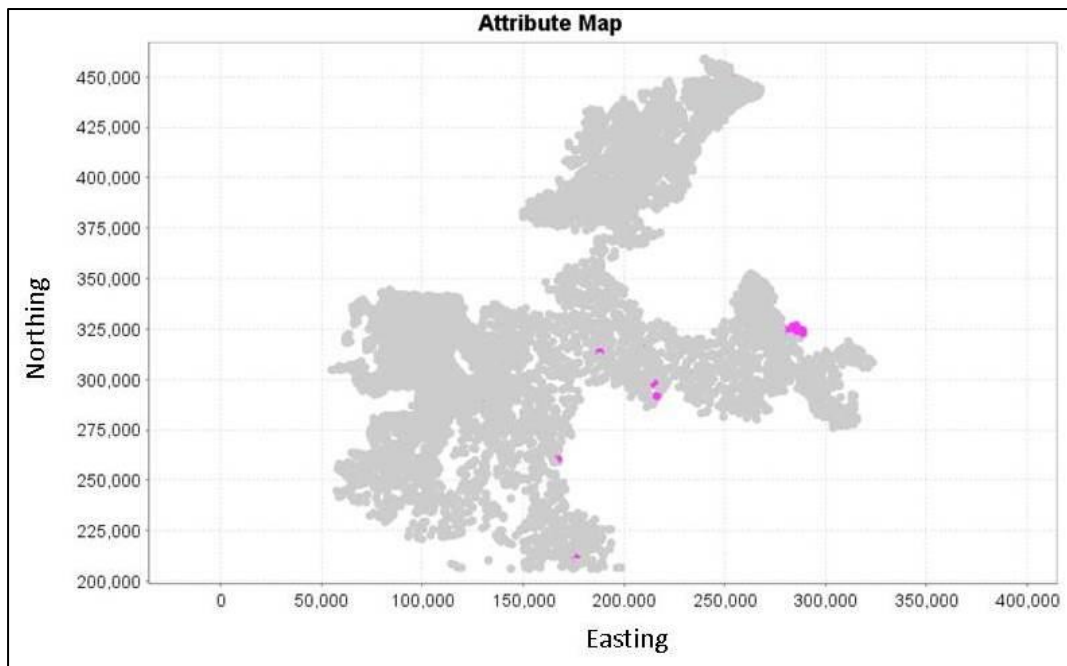


Figure 3.30 Map of “anomalous” Zn and Cd points.

3.4.3 Gold mineralization and stream water geochemistry

Several gold deposits have been discovered in recent decades, notably in counties Mayo (Lecanvey, Cregganbaun, Inishturk), Donegal (Inishowen) and Monaghan (Clontibret) (Figure 3.31). Arsenic is a typical pathfinder element for Au and most of these deposits have an associated stream water As anomaly (Fig. 3.31). At Clontibret, where stibnite (Sb_2S_3) is part of the mineral assemblage, a strong Sb anomaly is apparent in the surface water data, as is the case for both stream sediments and topsoils in the area (Figure 3.27). A similar spatial association between Sb and As in stream water can be observed in Inishowen where bedrock gold has been discovered in recent years, following publication of Tellus stream sediment data. However, more precise statistical correlations have not been defined and the value of stream water data in gold prospectivity needs further assessment.



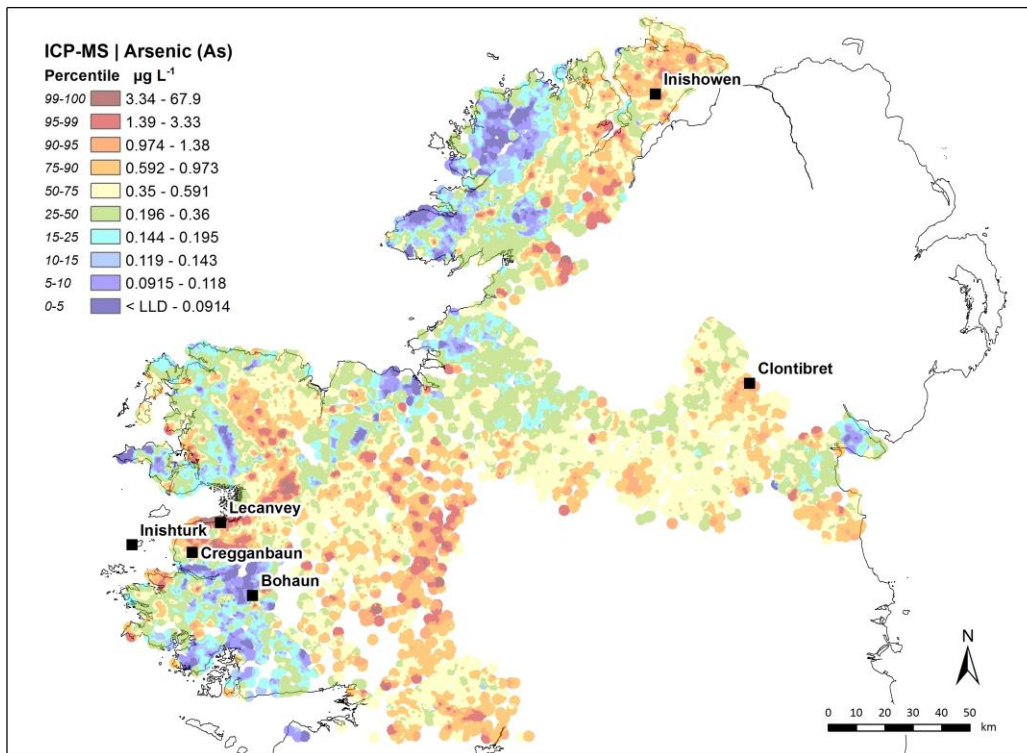


Fig. 3.31 Location of known gold mineralization shown on stream water As distribution.

3.5. Anthropogenic impacts on stream water: nitrate and phosphorus

As stated in the latest EPA water quality report (Trodd and O’Boyle 2020), “the main problem damaging our waters is the presence of too much nutrients such as phosphorus and nitrogen which come primarily from agriculture and waste water”. Nitrate was found to be increasing in almost 50 % of river sites sampled while phosphate levels were also rising in around 25 % of river sites (Figures 1.1 and 1.2). In the case of nitrate, the highest concentrations are observed in the south, southeast and east of the country where more intensive farming is coupled with freely draining soils and relatively low rainfall (Trodd and O’Boyle 2020). For phosphate, relatively high concentrations are found in catchments in the east (Liffey and Dublin Bay, Nanny-Devlin), northeast (Erne catchment) and south (Shannon Estuary South catchment).

Absolute concentrations of NO_3^- observed in the Tellus survey are lower than those observed in the EPA monitoring programme, with 4% of Tellus samples falling into the category considered ‘unsatisfactory’ quality by the EPA, compared to 47% of samples in the EPA monitoring network. This observation is not unexpected considering that Tellus samples are located up-catchment in smaller streams with fewer anthropogenic pressures than rivers. However, it does indicate that the influence of agriculture is pervasive across catchments, as 96% of the ‘unsatisfactory’ observations in the Tellus dataset occur in areas of agricultural land use, including pasture and arable types. The effect of land use is further explored through spatial and statistical analysis here.



Nitrate and phosphorus in Tellus stream water data have broadly similar distributions to those of EPA's monitoring data, with higher concentrations occurring over the more productive agricultural land, both arable land and pasture (Figures 3.32 – 3.37). County Louth and the Foyle valley in east County Donegal are particularly notable for high nitrate concentrations that coincide quite closely with the distribution of arable land. More broadly there is a general association in the midlands between nitrate and pasture land that is predominantly underlain by Carboniferous limestone bedrock and Lower Palaeozoic greywacke of the Longford-Down inlier. A similar distribution can be observed for phosphate¹.

Boxplots of nitrate (Figure 3.34) and phosphorus (Figure 3.37) data classified by land cover (Corine) and statistics in respect of the same (Tables 3.3 and 3.4) emphasize the relationship between both nutrients and agricultural land and, by extension, agricultural practices.

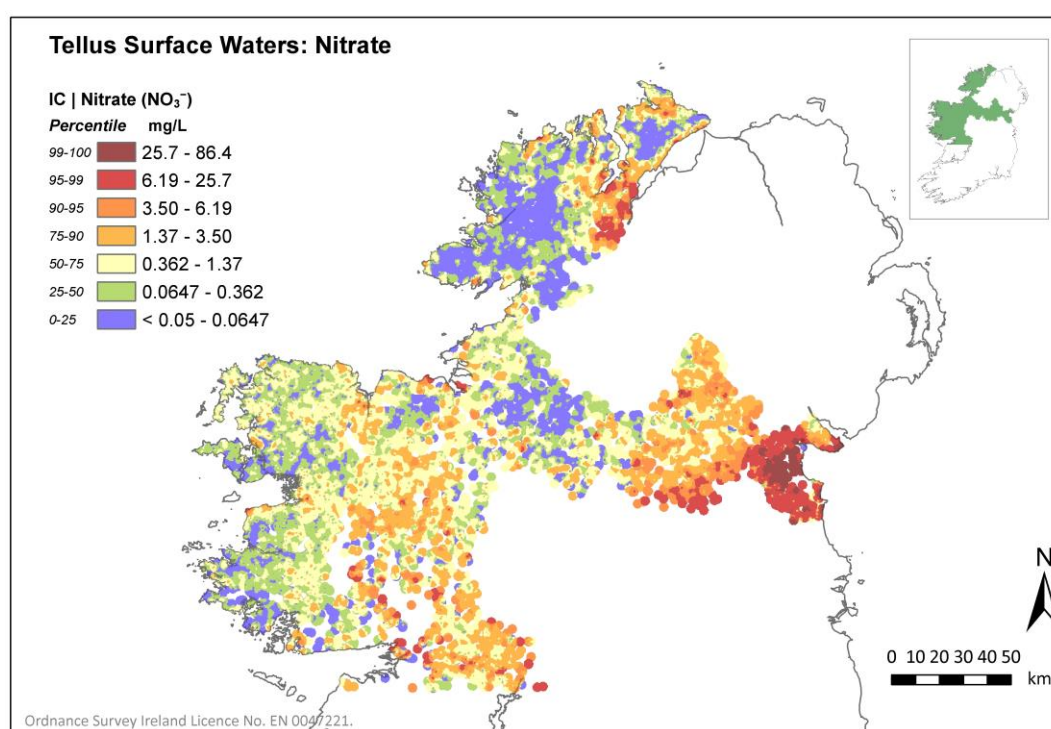


Figure 3.32 Distribution of nitrate in Tellus stream water samples.

¹ In the case of phosphorus, the regulations refer to molybdate reactive phosphorus (MRP), usually considered to be equivalent to orthophosphate. Orthophosphate was measured for Tellus samples using ion chromatography but only a small proportion of samples yielded results above the detection limit of 0.05 mg/L. Total dissolved phosphorus was measured by ICP-MS and is used here instead. Total dissolved phosphorus will exceed MRP by an unknown amount but nevertheless provides an indication of the distribution of phosphorus in stream waters and points to geographic areas where exceedances of EQS are most likely to occur.



Land Cover	Count	Min, NO ₃ ⁻ mg/L	Max, NO ₃ ⁻ mg/L	Median, NO ₃ ⁻ mg/L
All	6354	< 0.05	86.4	0.38
Arable land	60	< 0.05	86.4	21.2
Pasture	2732	< 0.05	53.3	1.19
Natural grassland	60	< 0.05	3.51	0.07
Moor / heathland	81	< 0.05	1.77	< 0.05
Coniferous forest	260	< 0.05	3.81	0.08
Agriculture / natural vegetation	1051	< 0.05	14.2	0.27
Peat bogs	2110	< 0.05	7.03	0.08

Table 3.3 Stream water nitrate (NO₃⁻) statistics for some Corine land Cover classes.

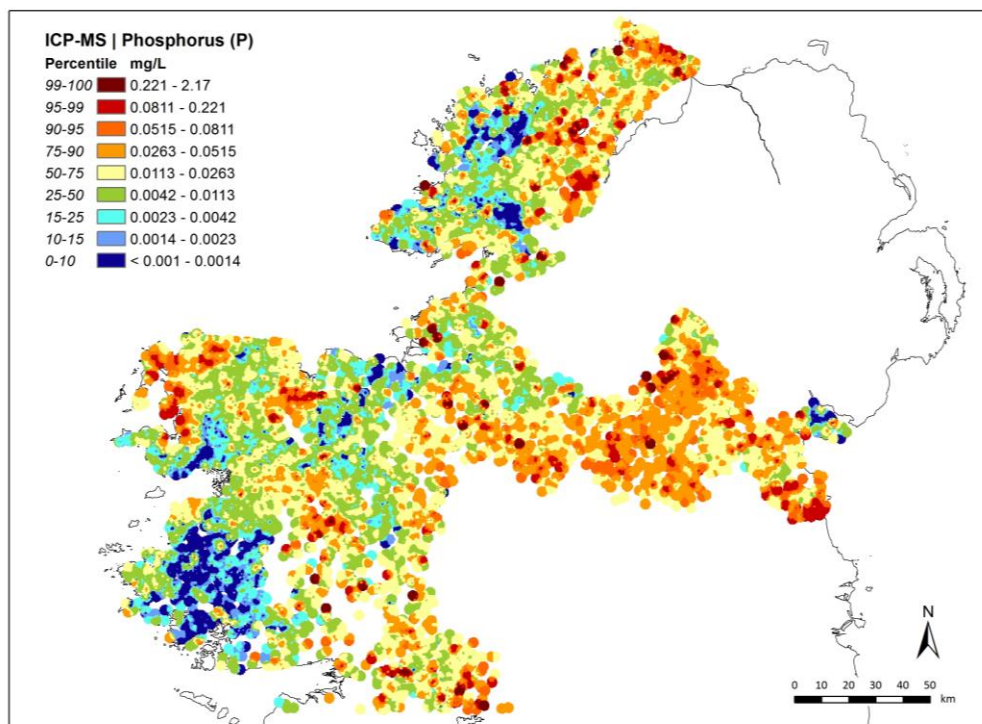


Figure 3.35 Distribution of phosphorus (total, by ICP-MS) in Tellus stream water samples.



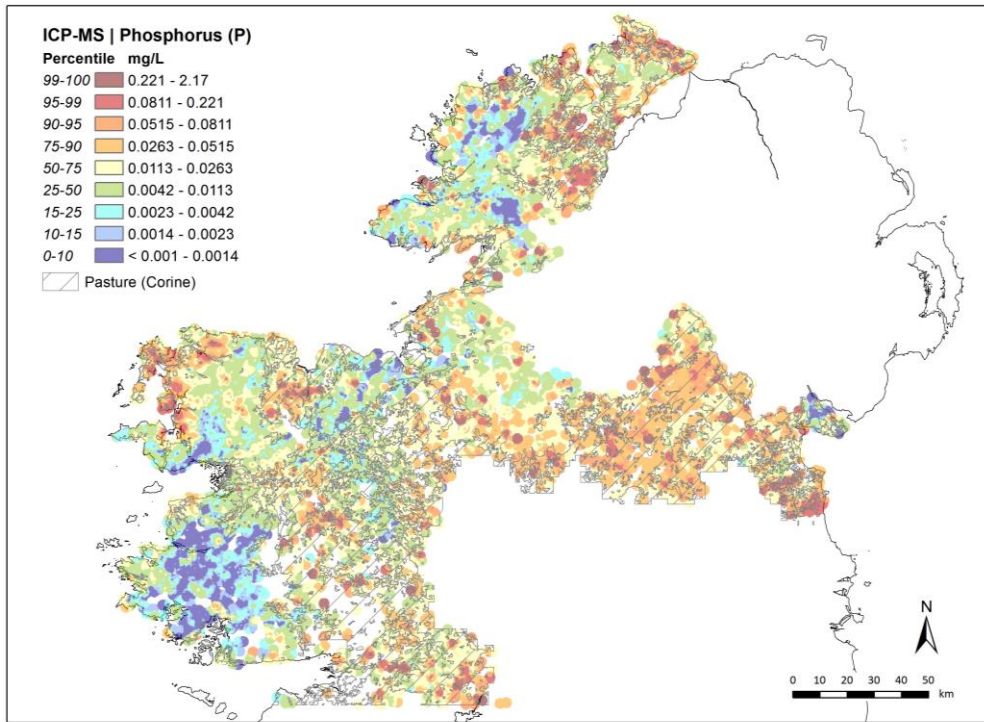


Figure 3.36 Distribution of phosphorus in Tellus stream water samples and areas of pasture.

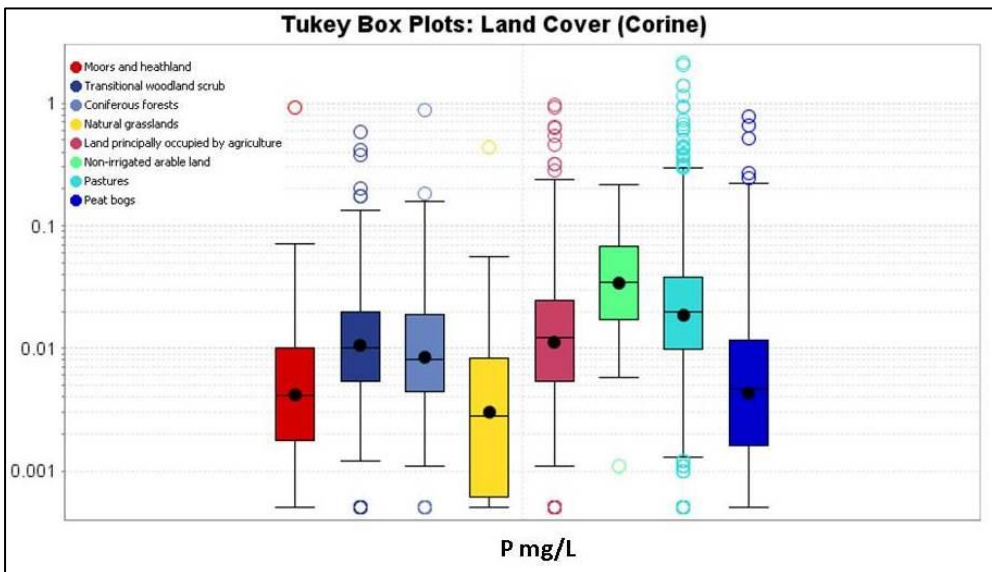


Figure 3.37 Tukey boxplot (log₁₀) of stream water phosphorus data classified by major land Cover (Corine) classes.



Land Cover	Count	Min, P mg/L	Max, P mg/L	Median, P mg/L
All	6354	< 0.001	2.17	0.0114
Arable land	60	0.0011	0.214	0.0345
Pasture	2732	< 0.001	2.17	0.0198
Natural grassland	60	< 0.001	0.435	0.0028
Moor / heathland	81	< 0.001	0.913	0.0041
Coniferous forest	260	< 0.001	0.0181	0.0081
Agriculture / natural vegetation	1051	< 0.001	0.956	0.0121
Peat bogs	2110	< 0.001	0.787	0.0046

Table 3.4 Stream water phosphorus (P) statistics for Corine Land Cover classes

In County Louth univariate mapping suggests that high concentrations of Ca, Mg, Ba, HCO_3^- and U in stream water are also associated with the high nitrate concentrations. Multivariate statistical analysis (Section 4) confirms these observations, with nitrate associated with HCO_3^- , Ca, U, Sr, F, Mg, SO_4^{2-} and Ba in PC biplots and on cluster dendrograms. In part this reflects an association with limestone bedrock across the region but in Louth the bedrock is Lower Palaeozoic greywacke. There, the source of Ca and Mg in stream waters is more likely to be agricultural activity, including liming and fertilizer application. The associated high bicarbonate concentrations may account for the elevated U concentrations since U is commonly associated with HCO_3^- owing to the stability in solution of U carbonates and bicarbonates (De Vivo *et al.* 2006). However, there is the possibility that some of the observed high U in stream waters may reflect leaching of fertilizer applied to topsoils in the area (e.g. Molina *et al.* 2009, Khater 2006).

The Tellus stream water data are comparable to EPA monitoring data (Trodd and O’Boyle 2020), with both indicating that higher concentrations of nitrates and phosphorus occur in stream waters draining the more productive agricultural land, both arable land and pasture. However, Tellus data provide a more detailed picture of the impact of agriculture on water quality and, as the samples were collected from first- and second-order streams, they indicate that these impacts are pervasive, occurring in the upper parts of catchments, with few areas of improved agricultural land in the survey area unaffected by nitrate or phosphorus inputs.

Another potential factor for understanding nitrate distribution in stream water is the permeability or drainage characteristics of the surrounding soils. “Well-drained soils” are mentioned by Trodd and O’Boyle (2020) as a factor in the occurrence of relatively high nitrate concentrations in stream water in the southeast of the country. The Teagasc-EPA Irish National Soils Map is the most up-to-date map of soil classes in Ireland and includes a drainage classification (Simo *et al.* 2014). When combined with the Tellus stream water data it suggests a clear link between drainage characteristics and nitrate concentrations in stream water (Figure 3.38, Table 3.5). A similar, if less well-defined, relationship appears to exist for total phosphorus measured by ICP-MS (Figure 3.39, Table 3.6).



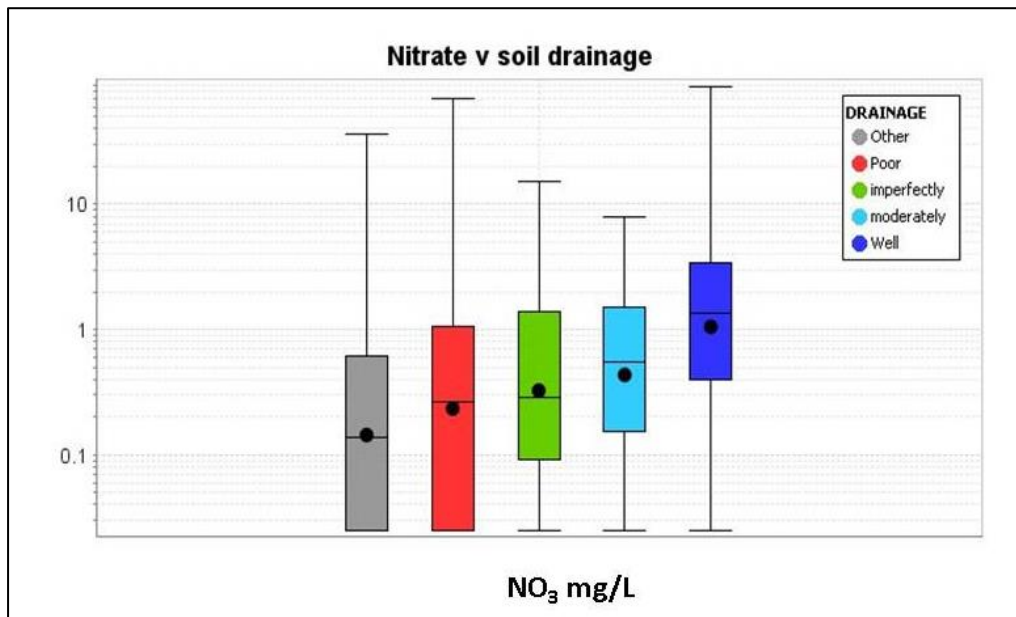


Figure 3.38 Nitrate concentrations (log 10) in stream water v Irish National Soils Map (INSM) soil drainage classes.

INSM drainage class	Count	Min, NO ₃ ⁻ mg/L	Max, NO ₃ ⁻ mg/L	Median, NO ₃ ⁻ mg/L
All	6819	< 0.05	86.4	0.365
Well drained	1075	< 0.05	86.4	1.34
Moderately drained	95	< 0.05	8.03	0.547
Imperfectly drained	210	< 0.05	15.1	0.291
Poorly drained	5285	< 0.05	70.72	0.264
Other (rock, made ground, etc.)	154	< 0.05	36.2	0.137

Table 3.5 Stream water nitrate (NO₃⁻) statistics for INSM drainage classes.



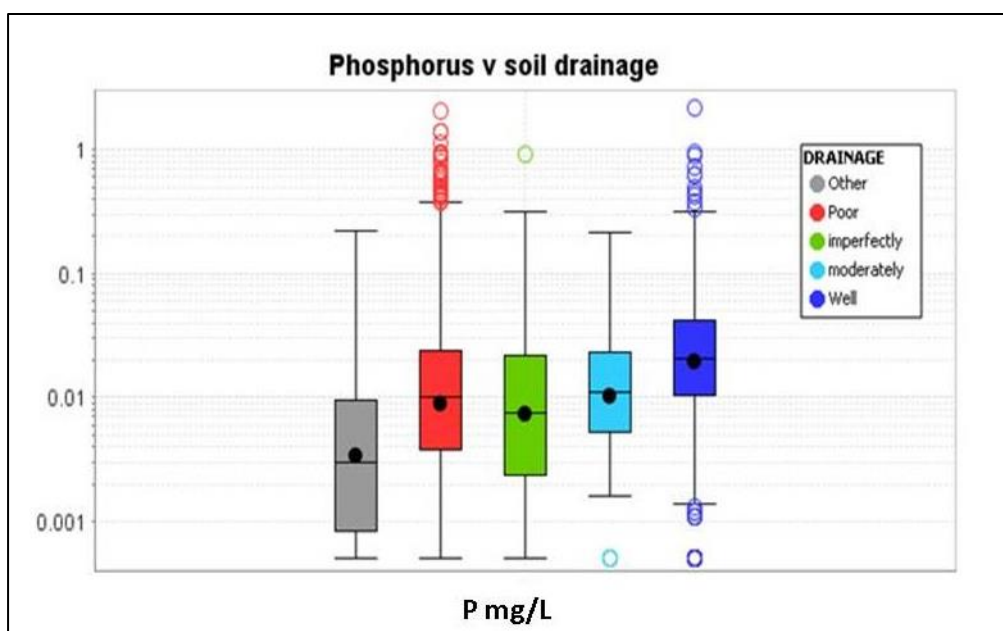


Figure 3.39 Phosphorus (P) concentrations (log 10) in stream water v Irish National Soils Map (INSM) soil drainage classes.

INSM drainage class	Count	Min, P mg/L	Max, P mg/L	Median, P mg/L
All	6819	< 0.001	2.17	0.0114
Well drained	1075	< 0.001	2.17	0.0204
Moderately drained	95	< 0.001	0.213	0.0112
Imperfectly drained	210	< 0.001	0.913	0.008
Poorly drained	5285	< 0.001	2.04	0.010
Other (rock, made ground, etc.)	154	< 0.001	0.219	0.003

Table 3.6 Stream water phosphorus (P) statistics for INSM drainage classes.



4. Multivariate statistical analysis

Multivariate statistical analyses, including Principal Component Analysis, Random Forests analysis and cluster analysis, were carried out on the stream water data to explore further the controls on stream water chemistry suggested by univariate analysis (Section 3). Multivariate analyses were considered primarily in the context of bedrock geology, subsoil geology and land cover, and were used to explore the influence on stream water chemistry of processes such as mineralization and anthropogenic activities.

4.1 Data preparation for multivariate statistical analysis

Grunsky (2010) provides details on a systematic methodology for the screening and adjustments that should be made prior to statistical evaluation of geochemical survey data. The Tellus dataset include data for 6,835 sites. For each element, values that were reported at less than the lower limit of detection (LLD) were reported with a value equal to half the detection limit. Values that exceed the upper limit of detection were set to the upper limit of detection. All data were converted to $\mu\text{g/L}$, i.e. values reported at mg/L were multiplied by 1000 and values reported at % were multiplied by 100000. Values reported at less than the lower limit of detection are termed “censored” and can influence statistical measures such as the mean and variance and subsequent interactions between elements (Grunsky 2010). Consequently, censored values were adjusted to minimize this effect by a method of imputation that creates a range of values randomly generated between a minimum value (> 0) and the lower limit of detection.

The R package zCompositions was used to generate replacement values with the function IrEM, (Palarea-Albaladejo *et al.* 2014). This method uses the Expectation-Maximum Likelihood algorithm for estimating replacement values (imputation) for data that are compositional (geochemistry).

Quantile-Quantile (Q-Q) plots were generated to assist in defining outliers and range of values for further processing. Evaluation of the Q-Q plots indicated that the following elements be dropped owing to too many values $< \text{LLD}$: Ag, Bi, Ga, Hf, Tm, Lu, B, Tb, Ta, W, Tl, HPO_4 , NO_2 . For this study the threshold for element removal occurred when the 90th percentile was equal to or less than the detection limit. This left 53 elements as follows: HCO_3^- , NPOC, SO_4^{2-} , NO_3^- , Br, Ca, Cl, F, K, Mg, Na, P, S, Al, As, Ba, Be, Cd, Ce, Co, Cr, Cs, Cu, Dy, Er, Eu, Fe, Gd, Ho, La, Li, Mn, Mo, Nb, Nd, Ni, Pb, Pr, Rb, Sb, Se, Si, Sm, Sn, Sr, Th, Ti, U, V, Y, Yb, Zn, Zr.

The data were joined with several thematic maps in order to assess possible influences on the stream water chemistry, including bedrock geology, subsoil type and land use.

From these the following elements were evaluated within the context of the research objectives, including the assembly of 53 of the elements and sub-compositions that



reflect **metals/metalloids** (As, Cr, Cu, Zn), nutrients (NO_3^- , P) and base metal mineralization (Cu, Pb, Zn, Cd, As, Sb).

4.2 Principal Component Analysis

The results of Principal Component Analysis (PCA) are summarized below. A fuller account is presented in Appendix A.

Following the transformation of the imputed geochemical data using a log-centred transform, the data were treated with a PCA. When geochemical surveys are comprised of several thousand samples and analysed for more than 20 elements, it is difficult to observe and relate correlations between elements and their corresponding combined signatures in the geographic sense. One very effective method for evaluating large multi-element geochemical datasets is through the application of PCA and its use in geochemical survey investigations is documented in Grunsky (2010). The objective of PCA is to reduce the number of variables necessary to describe the observed variation within a dataset. This is achieved by forming linear combinations of the variables (components) that describe the distribution of the data. These linear combinations are derived from some measure of association (i.e. correlation or covariance matrix).

Figure 4.1 shows an ordered screeplot of the PCA, where it can be observed that the first principal component accounts for 50 % of the geochemical variability and the second for > 8 % of the variability. Altogether, the first eight components account for a large proportion of the variability of the data, estimated to be more than 80 %.

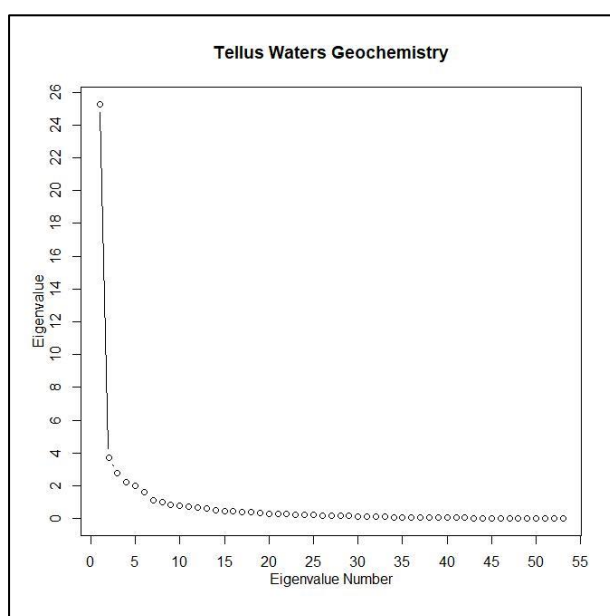


Figure 4.1 Ordered screeplot of PCA. The steep decay of eigenvalues indicates “structure” in the data. The first two components describe the dominant processes in the data. The remaining components are under-sampled processes or random events.



Distinct elemental associations observed in PCA may represent mineralogical relationships that are governed by mineral stoichiometry, adsorption, weathering, stream water effects due to Eh and pH conditions and non-linear gravitational effects.

A graphical way of describing the inter-element relationships within and between the principal components is through the use of a principal component biplot (Grunsky 2010).

4.2.1 Principal Components Associated with Rock Type

Figure 4.2 shows a principal component biplot for PC1 vs. PC2 for all water analyses, based on underlying bedrock. PC1 and PC2 are main components and typically reflect major processes such as geogenic influence. Other PCs reflect subsidiary processes. Biplots for other principal components are displayed in Appendix A.

Each point symbol in Figure 4.2 is classified according to rock type based on GSI's 1:1,000,000 bedrock geology map (Figure 3.1). The element symbols are coloured according to their Goldschmidt, i.e. lithophile, siderophile or chalcophile, classification (Levinson 1974, p.62). Anion symbols are also coded with a unique colour. Figure 4.3 shows the distribution of points for some individual rock types on the PC1 v PC2 plot. For sites underlain by granitic rocks there is relative enrichment in lithophile (Ce, Nd, La, Al, Ti, Sm, Gd, Eu, Yb, Ho, Er, Y, Th), siderophile (Fe) and chalcophile (Pb) elements along the positive portion of the PC1 axis, implying that these elements are strongly associated with this rock type. On the PC1 v PC2 plot for sites underlain by limestones, the biplot shows a relative increase in NO_3^- , HCO_3^- , Ca, U, Sr, F, Mg, SO_4^{2-} , Ba, Mo along the negative portion of the PC1 axis. The association of U with HCO_3^- likely reflects the stability of hexavalent U carbonates and bicarbonates in solution (De Vivo *et al.* 2006). The relative enrichment of Ca, Sr, F, Mg and Ba reflect the underlying Carboniferous limestone-dominated lithologies. These lithologies underlie large areas of pasture and the observed relative enrichment of NO_3^- and SO_4^{2-} likely reflects the addition of fertilizer and other agricultural activities. The greywacke plot suggests mixing between the different components, reflecting the diverse range of source material that contributes to clastic sedimentary rocks. In contrast, the orthogneiss plot strongly resembles the granite plot, consistent with the origin of these rocks as metamorphosed granites.

The degree of overlap between the plots limits the conclusions that can be inferred from them but it is clear that the Principal Component Analysis does generally discriminate between the main rock types, implying that the water geochemistry at least partly reflects bedrock composition.



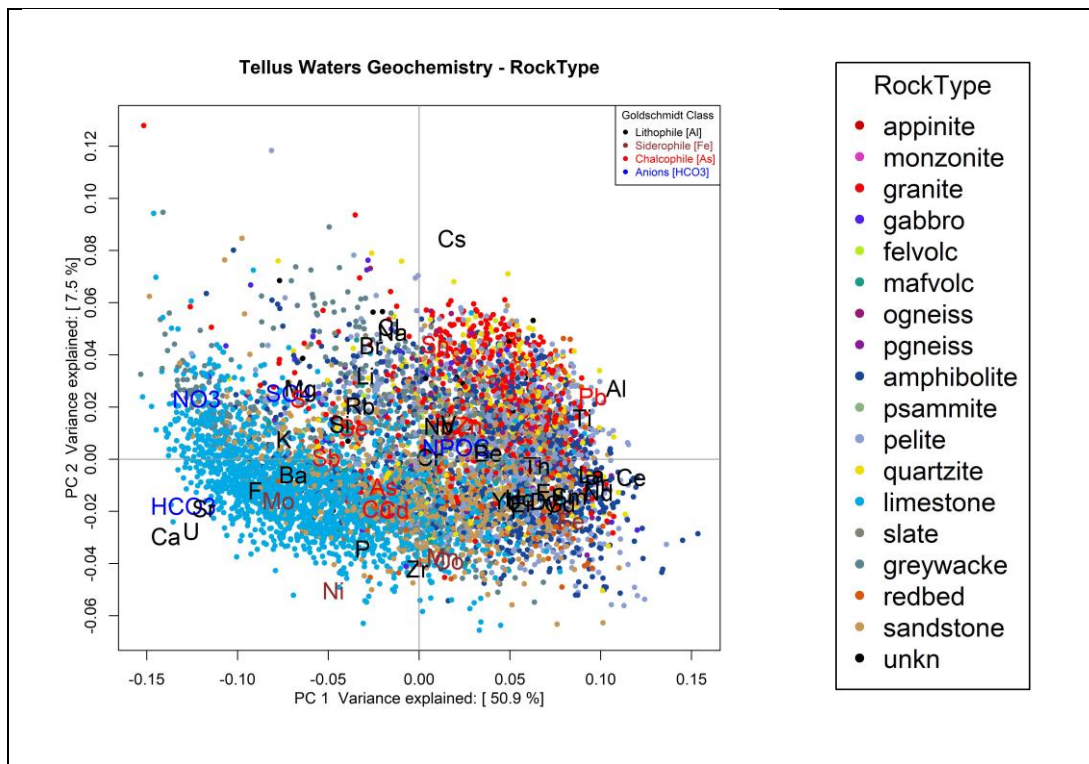


Figure 4.2 PC1 vs. PC2 biplot for all water analyses. Colours/symbols represent the underlying bedrock at each sample site.



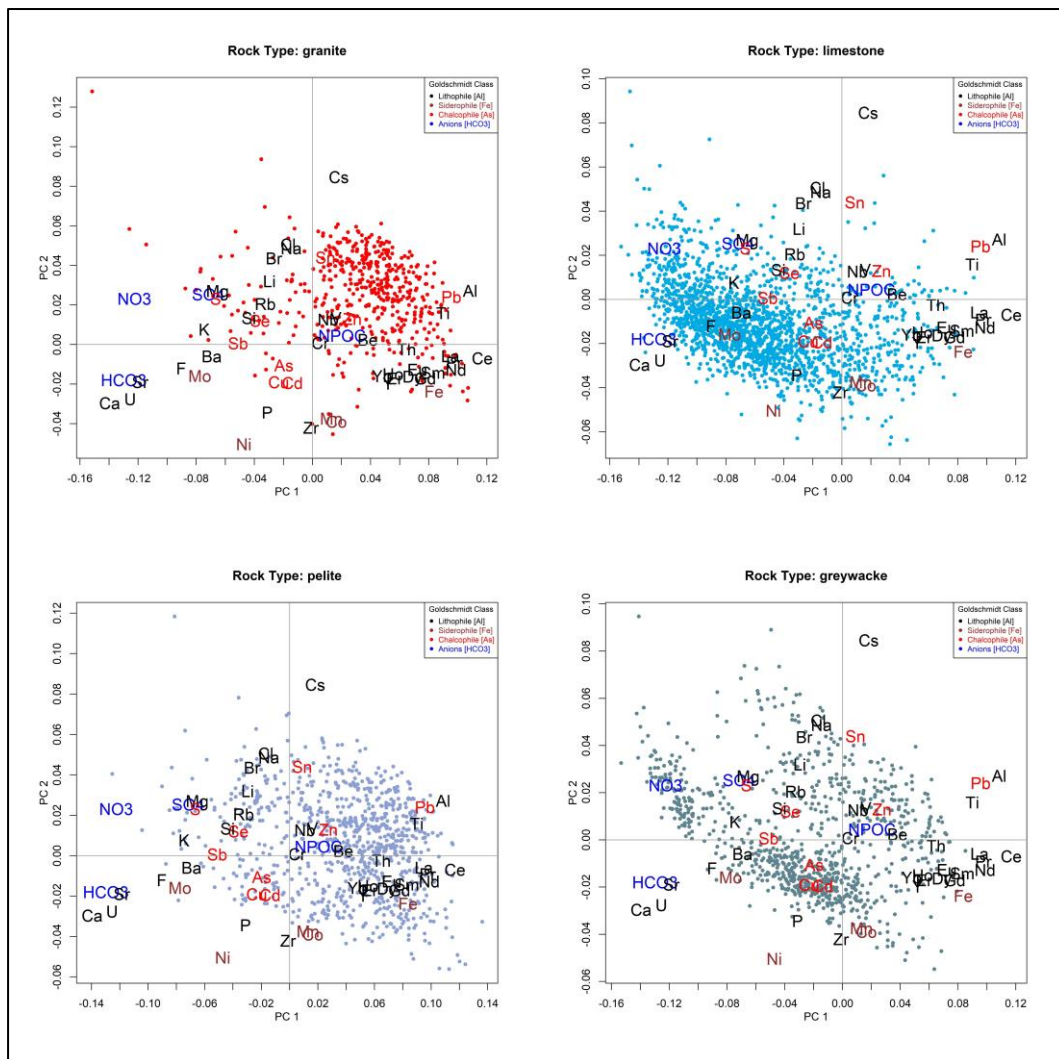


Figure 4.3 PC1 vs. PC2 biplots for all water analyses for four individual bedrock classes.

4.2.2 Principal Components Associated with Subsoil type

Figure 4.4 shows a principal component biplot for PC1 v PC2 for all water analyses, based on underlying subsoil. Each point symbol is classified according to subsoil type based on the Teagasc subsoil map (Figure 3.2). The element symbols are coloured according to the Goldschmidt classification and anion symbols are also coded with a unique colour. The plot demonstrates some distinct clusters of analyses based on subsoil type, albeit with considerable overlap among the various types. Biplots of PCs 1–8 tagged with Teagasc subsoil classes and biplots of PC1 v PC2 for each of the Teagasc subsoil classes are shown in Appendix A.



Ireland (Glennon *et al.* 2020). The individual SRF geochemical domains comprise areas where bedrock and subsoil have broadly similar geochemical characteristics and are in effect a simplification and combination of the bedrock and subsoil maps. Figure 4.6 shows principal component biplots for PC1 vs. PC2 for stream waters based on six of the seven domains. The plots largely resemble those of their corresponding rock types, i.e. D1 (Namurian shale and sandstone), D2 (limestone), D3 (ORS sandstone), D5 (Lower Palaeozoic sandstone and shale), D6 (granitic rock) and D7 (metamorphic rock). Appendix A shows biplots for PCs 1-8 tagged with the SRF geochemical domain classes and biplots of PC1 v PC2 are shown for each of the SRF geochemical domain classes.

The SRF plots show that regardless of whether the stream water data are classified according to bedrock or subsoil, or some combination of the two, their geochemistry has a strong geogenic signature. This is consistent with observed geogenic control of both stream sediment and topsoil geochemistry in the region (Gallagher *et al.* 2016a, 2016b).



4.2.4 Principal Components Associated with Land Cover classes

Figure 4.7 shows the principal component biplot for PC1 v PC2 for all water analyses, based on Land Cover (Corine) classes (Lydon and Smith 2014). Figure 4.8 shows principal component biplots for PC1 v PC2 for the main land cover classes, namely pasture, arable land, forestry, transitional woodland, moorland / heathland and peat bog. Biplots of PCs 1–8 tagged with land cover classes and biplots of PC1 v PC2 for each of the land cover classes are shown in Appendix A.

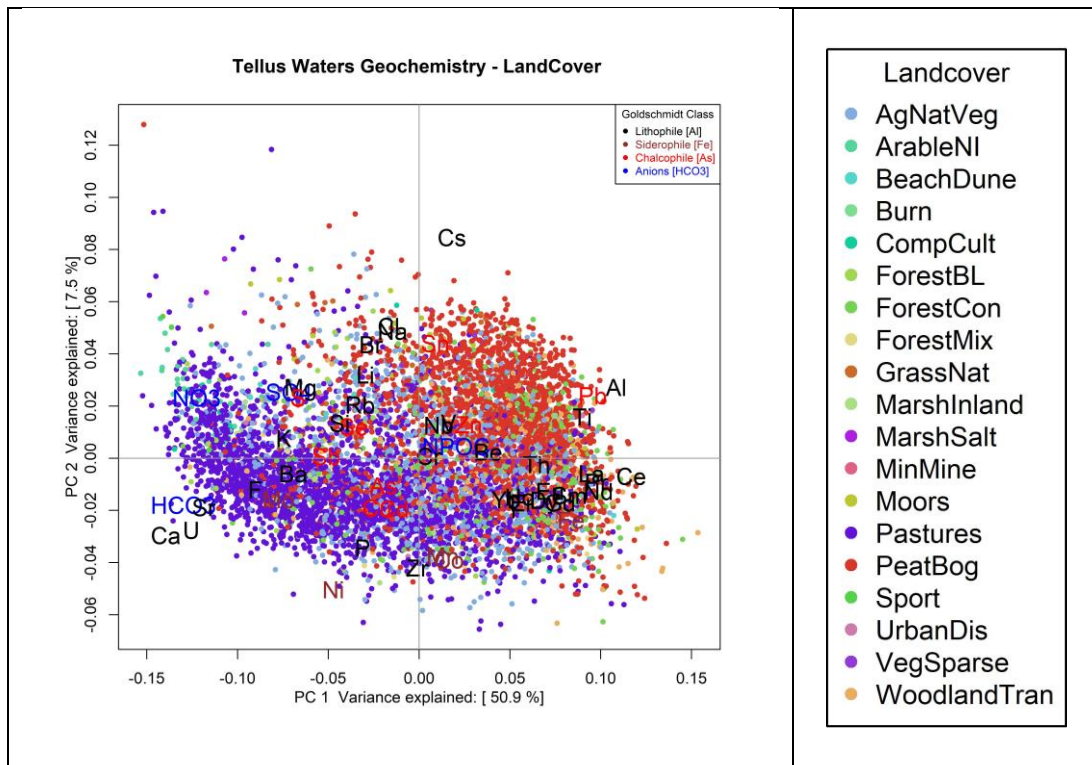


Figure 4.7 PC1 vs. PC2 biplot for all water analyses, based on land cover classes.

The land cover classes observed in Figure 4.7 are dominated by a distinction between stream water draining pasture and stream water draining peat bog. The biplot for pasture (Figure 4.8) strongly resembles that for limestone bedrock and SRF Geochemical Domain 2 (Figure 4.3 and 4.6), which is unsurprising as those parts of the area underlain by limestone are predominantly used for pasture. Similarly, the biplot for peat bog resembles that for blanket peat (Figure 4.5) but also that for granite and metamorphic rock (Figure 4.3), the bedrock commonly found below the areas of blanket bog in the study area. The biplot for stream water draining arable land (Figure 4.8) illustrates the association between nitrate in stream water and cultivation, as previously inferred from univariate analysis (Section 3.5).



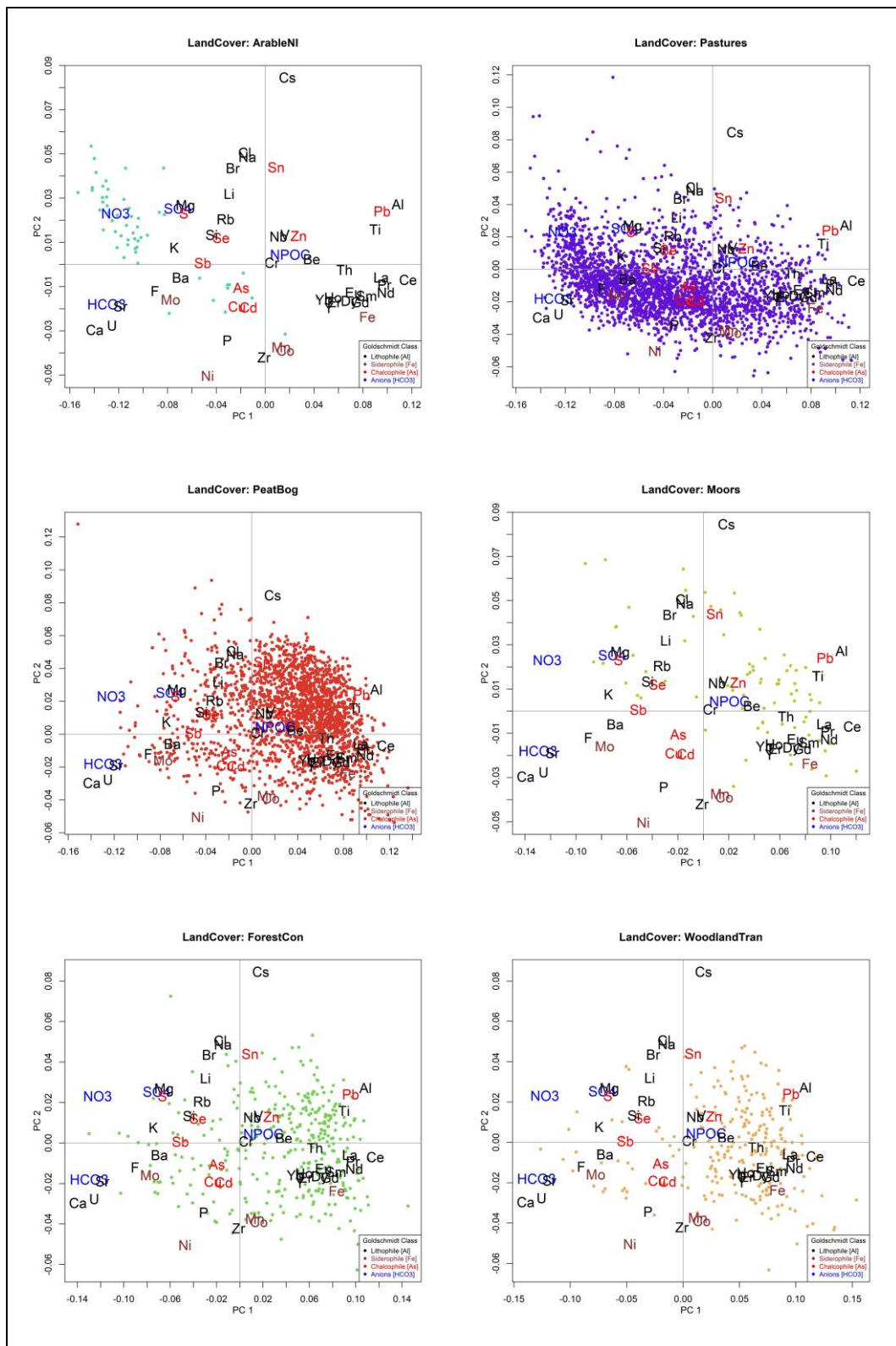


Figure 4.8 PC1 vs. PC2 biplots for all water analyses for the main land cover classes.

On the PC2 v PC3 biplots (Figure 4.9, 4.10) stream water samples classified by the Corine Land cCover peat bog class and by Teagasc blanket peat subsoil class display a distinct absence (negative PC2 and/or PC3) of components typically associated with carbonate



rocks and agricultural activities, such as Ca, HCO_3^- , NO_3^- and P. Conversely, these stream water samples exhibit a relative enrichment trend (positive PC2 and/or PC3) in chalcophile elements, including Zn and Pb, that may be ascribed to element adsorption in the organic-rich peat. The biplots of PC3 v PC4 (Figures 4.11, 4.12) also highlight a relative enrichment trend in chalcophile elements that is interpreted to represent element adsorption in the organic-rich peat (BkPt and Cut). The maps of PC3 and PC4 (Figures 4.10, 4.12) show that the positive scores of PC3 and PC4 principal components that have chalcophile enrichment without corresponding NPOC enrichment may be useful for targeting exploration strategies (see also Section 3.4).

Positive scores for PC4 are dominated by stream water samples draining tills (TNSSs, TLs, TLPSs) and alluvium (A) or where bedrock is close to the surface (Rck, KaRck). The ubiquitous distribution of NPOC and chalcophile elements is likely due to the influence of stream water draining subsoils with high organic material content. As shown in the map of Figure 4.10, the PC3 signature of NPOC-As-Zn-Pb is highest in the western part of the area, where there are dominant peat deposits, and diminishes eastward.

PC4 also shows a strong NPOC- SO_4^{2-} signature with an increase of chalcophile elements Cd-Sb-C-Se-Pb-Zn-Mo in areas dominated by peat but also in some areas that are not dominated by peat (Figure 4.12). This signature is also likely to be mainly a consequence of the influence of organic material in the soils drained by stream waters.

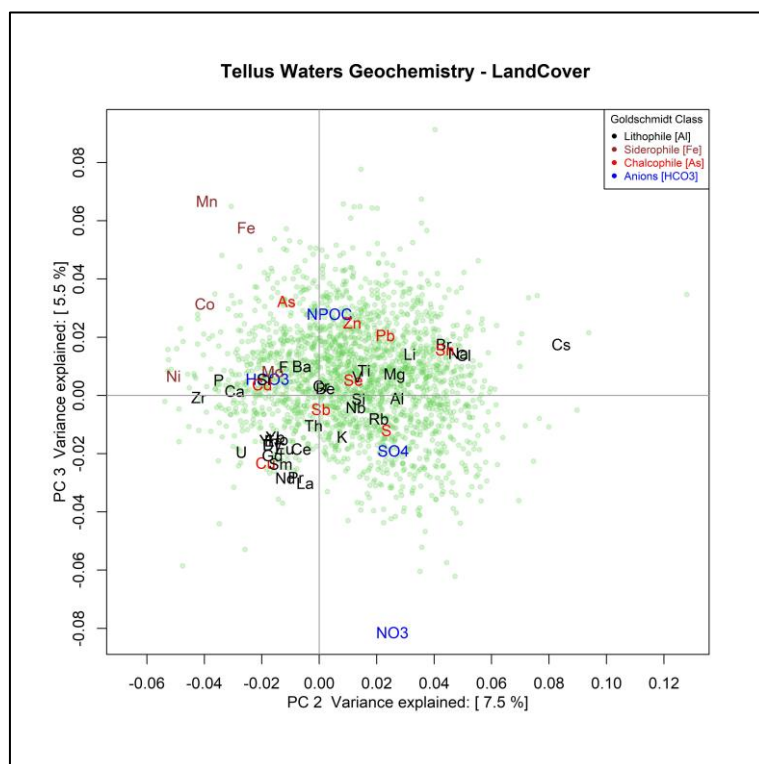


Figure 4.9 PC2 v PC3 biplot for all water analyses, based on underlying bedrock. Legend for the principal component scores is shown in Figure 4.7.



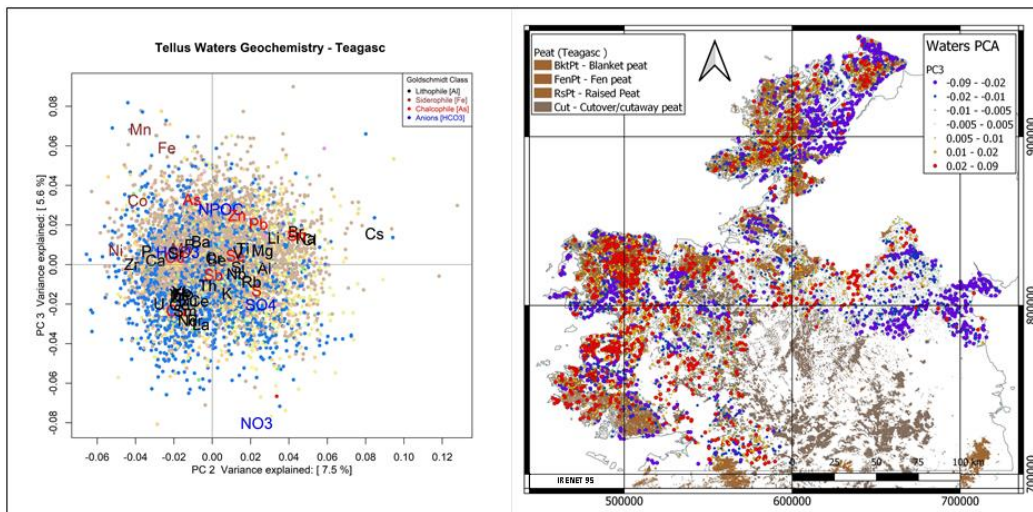


Figure 4.10 PC2vPC3 for stream waters draining Blanket Peat.

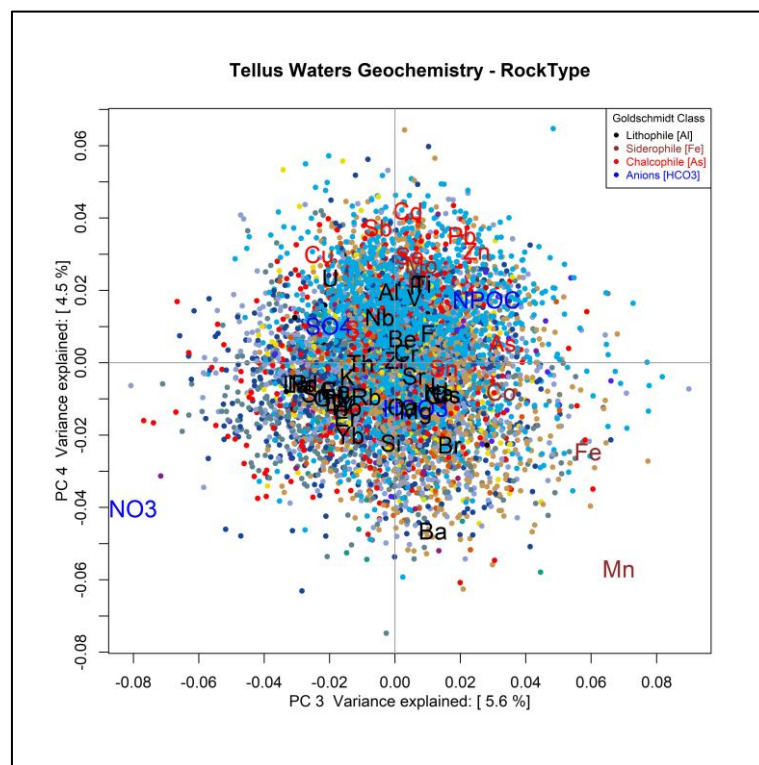


Figure 4.11 PC3 v PC4 biplot for all water analyses, based on underlying bedrock. Legend for the principal component scores is shown in Figure 4.7.



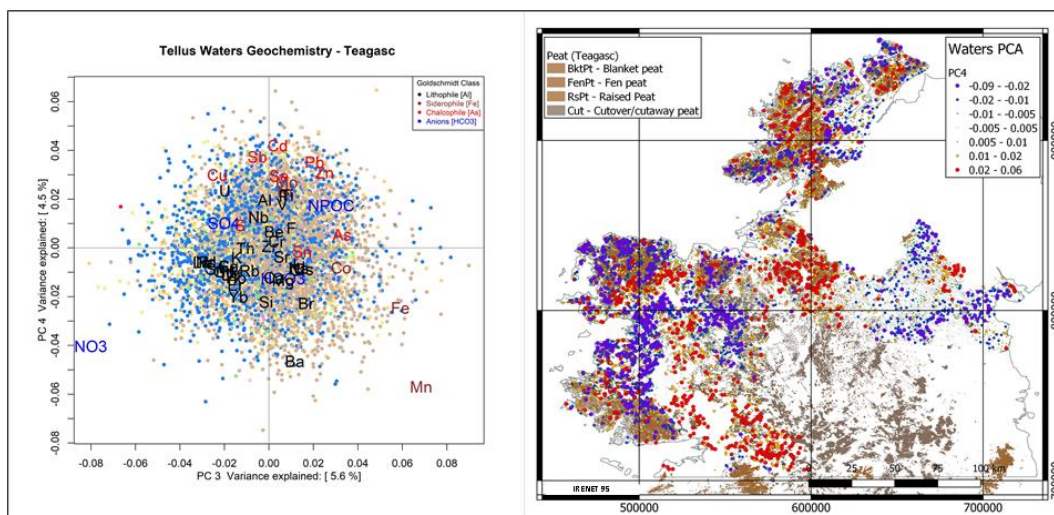


Figure 4.12 PC3vPC4 biplot for stream water draining Blanket Peat. The waters show relative chalcophile enrichment along the positive PC4 axis corresponding with a relative increase in NPOC and SO_4^{2-} .

4.2.5 Principal Components: Mineralization

4.2.5.1 Base metal signatures based on a PCA of the complete suite of elements.

As discussed above, base metal element enrichment/depletion can be observed in PC analyses of the entire suite of elements. The relative and absolute contributions of the first eight principal components (Tables A3 and A4) along with corresponding Principal Component Analysis biplots show that most of the variability of Zn is accounted for in PCs 3, 4, 11 and 16 (not shown). Most of the variability of Pb is accounted for in PCs 1, 4 and 6.

The presence of peat and organic matter in soils and their ability to adsorb chalcophile elements complicates the detection of base metal deposits using simple geochemical methods. As suggested by Figures 4.5 and 4.7 there are groups of elements in stream waters for which relative enrichment and relative depletion may be associated with the occurrence of peat. The association between chalcophile elements in stream water and geology is explored further in Appendix D, where the stream water data are examined in the context of existing base and precious metal occurrences, prospects and deposits.

4.2.5.2 Base metal signatures based on a PCA of chalcophile elements only

A Principal Component Analysis of the stream waters data enhances the possibility of recognizing processes related to base metal mineralization. A separate PCA was carried out on nine chalcophile elements: Cu, Zn, Pb, Cd, S, As, Sb, Se and Sn. Biplots were prepared over the first eight principal components with the principal component scores coded by rock type and, initially, Teagasc subsoils. However, the PC biplots coded by the Teagasc subsoil classification proved difficult to interpret, primarily owing to the very



large number of subsoil classes and the overwhelming number of sites that drain blanket peat and cut peat. An alternative approach was adopted, utilizing the SRF Geochemical Domains for classification since these domains are derived mainly from the Teagasc subsoil classes through their amalgamation, with some input from bedrock geology where the subsoil is not classified, e.g. where bedrock is within 1 m of the surface. Peat or peaty subsoil is not accounted for in this classification. Symbol sizes were created based on values of $Zn \geq 20 \mu\text{g/L}$ and $100 * Cd \geq 10 \mu\text{g/L}$ (see sections 3.5) and a distance measure of a stream water sample site to the closest mineral occurrence obtained from the GSI Mineral Localities database. Figures 4.13 and 4.14 show the Zn and $100 * Cd$ values that exceed the 98th percentile for both Zn and $100 * Cd$ ($20 \mu\text{g/L}$ and $10 \mu\text{g/L}$ respectively), which occur as distinct outliers in the PC1 v PC2 biplots for both rock type and Teagasc subsoils. The corresponding distance to mineral location biplot shows the Zn and Cd outliers as having a closer proximity ($< 2000 \text{ m}$) to mineral occurrence locations.

Appendix D provides a complete gallery of PC biplots for the first seven principal components along with corresponding maps of the components.

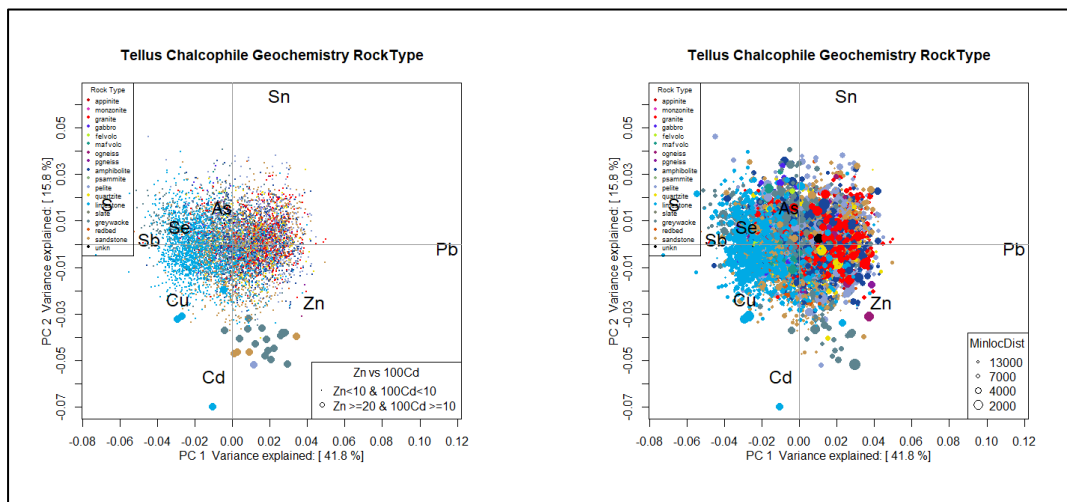


Figure 4.13. PCA biplot of PC1 v PC2. Colours and symbols tagged with rock type. Symbol size is based on the Zn and $100 * Cd$ enrichment measure and a measure of distance (km) to the closest mineral location. Lithologies with higher abundances of Cd, Zn and Cu include Carboniferous limestone, Lower Palaeozoic sediments and Namurian sediments. The shortest distances to mineral localities with high Zn and Cd are for stream waters draining Lower Palaeozoic greywacke and other sediments in the area of Pb–Zn mineralization in County Monaghan but limestone-related mineralization is also highlighted.



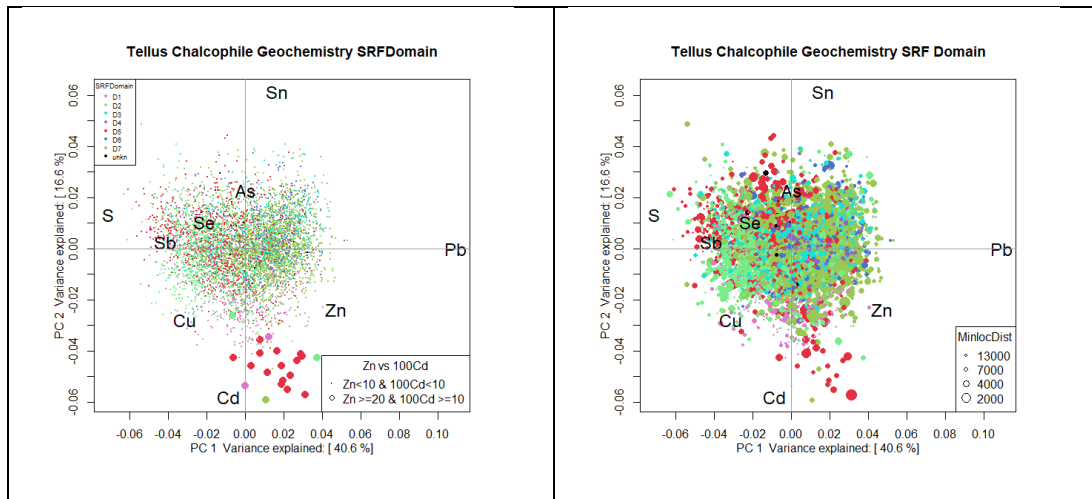


Figure 4.14 PCA biplot of PC1vPC2. Colours and symbols tagged with SRF Geochemical Domain. Symbol size is based on values of Zn ≥ 20 $\mu\text{g/L}$ and $100 \times \text{Cd} > 10$ $\mu\text{g/L}$ and a measure of distance (km) to the closest mineral locality. Zn and Cd enrichment and proximity to mineralization are strongly associated with Domain 5 (Lower Palaeozoic sediments), Domain 2 (Carboniferous limestone) and Domain 1 (Namurian rocks). The association with Domain 5 reflects the large area of Zn and Cd geochemical anomalies in County Monaghan, in the historic lead mining district, while that related to Domain 2 is primarily a reflection of anomalies around Tynagh mine in County Galway.

Table 4.1 shows the loadings (R-Scores, Relative and Absolute Contribution) for the chalcophile suite of element. The signs of the R-Scores indicate that there are positive and negative associations with the base metals (Cu, Pb, Zn) that highlight different processes associated with bedrock, surficial processes and ore deposits. These associations are illustrated in Figures 4.15 and 4.16.



Tellus Waters - Chalcophile Geochemistry								
Eigenvalues	PC1	PC2	PC3	PC4	PC5	PC6	PC7	PC8
λ	2.39	0.91	0.62	0.55	0.46	0.39	0.25	0.15
$\lambda\%$	41.7832	15.9091	10.8392	9.6154	8.042	6.8182	4.3706	2.6224
$\Sigma\lambda\%$	41.7832	57.6923	68.5315	78.1469	86.1888	93.007	97.3776	100
R-Scores	PC1	PC2	PC3	PC4	PC5	PC6	PC7	PC8
Cu	-0.2882	-0.2345	-0.0676	-0.4646	-0.2324	0.3091	-0.014	-0.0743
Zn	0.4368	-0.2482	0.3462	-0.1745	0.4724	0.024	-0.0319	0.0299
As	-0.0523	0.1591	-0.4907	0.205	0.2862	0.2282	0.1413	-0.0286
Se	-0.2829	0.0773	-0.0306	0.1251	0.0392	-0.1804	-0.2932	-0.2378
S	-0.6686	0.1708	0.1602	-0.1134	-0.0024	-0.2907	0.307	-0.0371
Cd	-0.0982	-0.5665	0.162	0.4555	-0.1948	0.0659	0.0603	0.0315
Sn	0.2509	0.6382	0.3371	0.1295	-0.1555	0.2224	-0.0376	0.0483
Sb	-0.4442	0.0218	-0.1955	-0.07	-0.0093	-0.1445	-0.1924	0.2794
Pb	1.1467	-0.0182	-0.221	-0.0927	-0.2033	-0.2341	0.0606	-0.0113
Relative Contributions	PC1	PC2	PC3	PC4	PC5	PC6	PC7	PC8
Cu	16.1712	10.7059	0.8892	42.0104	10.513	18.5971	0.0383	1.0749
Zn	30.3641	9.8004	19.0715	4.8451	35.5227	0.092	0.1621	0.1421
As	0.5864	5.4356	51.7154	9.024	17.5907	11.1826	4.2892	0.176
Se	28.6702	2.142	0.3355	5.6076	0.5494	11.6536	30.7866	20.2552
S	64.3324	4.2001	3.6947	1.8499	8.00E-04	12.164	13.5598	0.1984
Cd	1.5779	52.506	4.2932	33.9458	6.2101	0.71	0.5943	0.1628
Sn	9.2846	60.0716	16.7531	2.4741	3.5668	7.2966	0.2089	0.3442
Sb	52.3463	0.1263	10.1398	1.3003	0.0231	5.5363	9.8164	20.7115
Pb	89.2924	0.0225	3.3157	0.5831	2.8078	3.7207	0.2492	0.0087
Absolute Contributions	PC1	PC2	PC3	PC4	PC5	PC6	PC7	PC8
Cu	3.4781	6.0701	0.7383	38.9212	11.6337	24.2037	0.0796	3.7643
Zn	7.9877	6.7963	19.3678	5.4903	48.0795	0.1465	0.4122	0.6086
As	0.1143	2.7936	38.9224	7.5784	17.6451	13.1924	8.0838	0.5588
Se	3.351	0.66	0.1514	2.8233	0.3304	8.2421	34.7851	38.5457
S	18.7147	3.2209	4.1492	2.318	0.0013	21.4124	38.1326	0.9398
Cd	0.4037	35.4127	4.2402	37.4107	8.1747	1.0992	1.4698	0.678
Sn	2.6359	44.9573	18.3607	3.0255	5.21	12.5349	0.5734	1.5912
Sb	8.2624	0.0526	6.1785	0.8841	0.0188	5.2878	14.9782	53.2266
Pb	55.0523	0.0365	7.8916	1.5485	8.9067	13.881	1.4852	0.087

Table 4.1 Principal component eigenvalues, loadings, relative and absolute contributions for chalcophile suite of elements.

Figures 4.15 and 4.16 show maps of the scores for PC1 and PC2 with mineral occurrences identified according to the MinLocs mineral commodity. The two maps highlight distinct differences in chalcophile element enrichment and depletion. Positive PC1 scores, indicating a relative enrichment in Pb, Zn and Sn, are highest in the western region while negative scores, indicating a relative increase in S, Sb and Cu, predominate in the eastern and southern regions of the sampling area. Negative scores on the map of PC2 display relative Cd-Zn-Cu enrichment in areas where there are known mineral occurrences and mine sites.



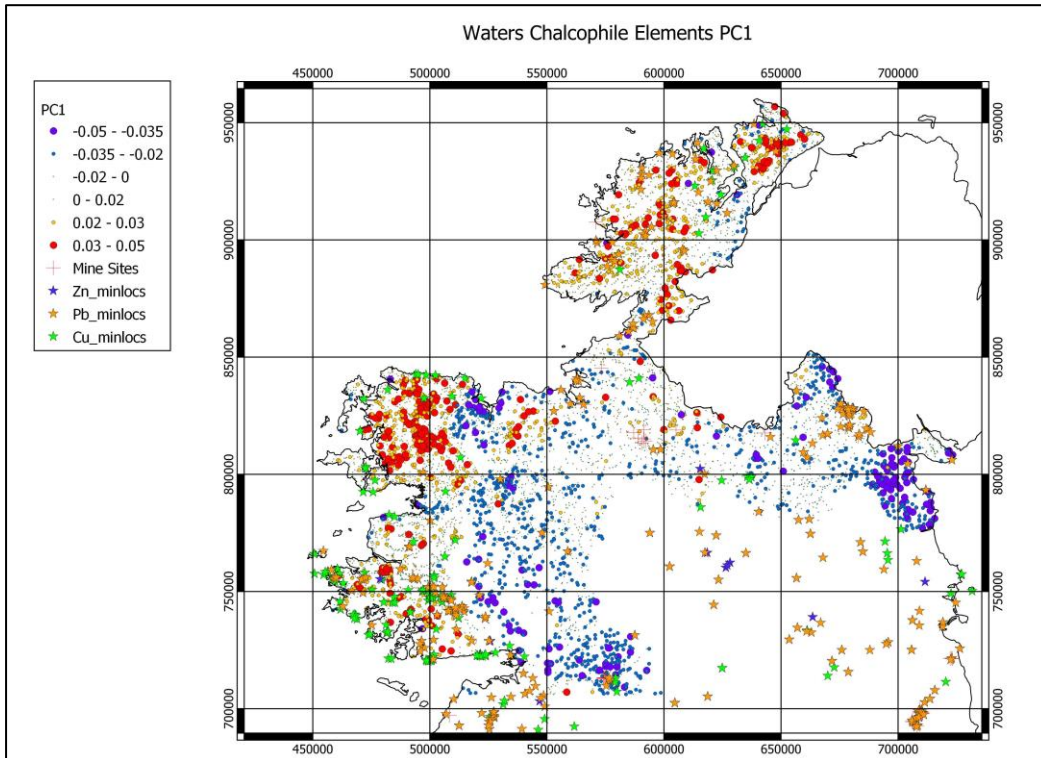


Figure 4.15. Map of PC1 scores. Relative enrichment of Zn, Pb and Sn in stream water samples coincide with positive PC1 scores. Relative enrichment of S, Sb, Cu, Se coincide with negative PC1 scores.

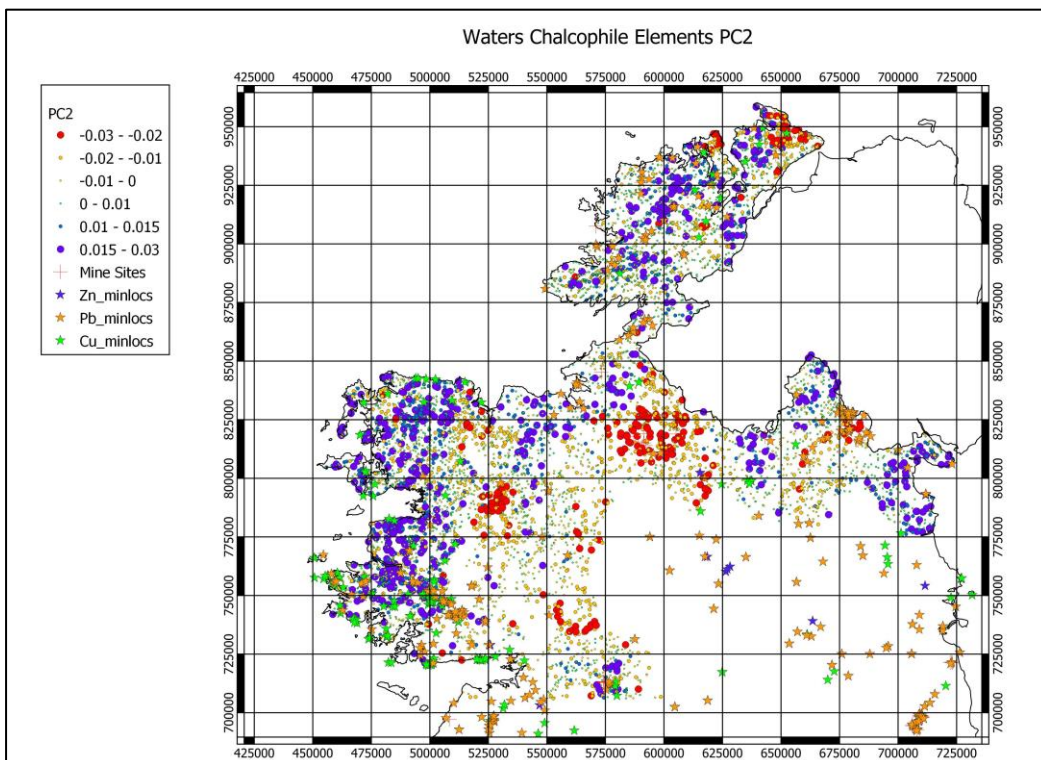


Figure 4.16 Map of PC2 scores. Negative scores indicate relative enrichment in Cd, Cu and Zn.



Appendix D contains maps of the other principal components, which highlight regional features including the presence of peat and signatures associated with base metal mineralization.

4.2.6 Multivariate assessment of selected elements/anions associated with anthropogenic activity

Anions analysed as part of the Tellus stream water dataset appear to be dominantly associated with anthropogenic activities, notably agriculture (Section 3.5). A Principal Component Analysis was carried out on the anions F^- , Cl^- , HCO_3^- , SO_4^{2-} and NO_3^- , along with NPOC and P. Table 4.2 shows the eigenvalues and loadings of anions across the three principal components. Blue cells indicate a negative loading value. Red cells indicate a positive loading value. The magnitude of each loading indicates the amount of variability each element has over the suite of four elements.

Tellus Waters Geochemistry - Anions/Nutrients								
Eigenvalues	PC1	PC2	PC3	PC4	PC5	PC6	PC7	PC8
λ	25.29	3.73	2.77	2.24	2	1.61	1.13	1.02
$\lambda\%$	50.8853	7.505	5.5734	4.507	4.0241	3.2394	2.2736	2.0523
$\Sigma\lambda\%$	50.8853	58.3903	63.9638	68.4708	72.495	75.7344	78.008	80.0604
R-Scores								
	PC1	PC2	PC3	PC4	PC5	PC6	PC7	PC8
F	-0.9034	-0.1204	0.1004	0.0814	0.2555	-0.1115	0.0118	0.0144
Cl	-0.1673	0.5061	0.1264	-0.0898	0.0654	0.0924	0.0275	-0.0594
HCO3	-1.2985	-0.1796	0.0624	-0.1252	0.2067	-0.1476	0.0873	-0.0319
SO4	-0.716	0.2537	-0.2024	0.1017	-0.0197	0.3931	-0.1206	-0.0977
NO3	-1.2259	0.2314	-0.8014	-0.4029	-0.6942	-0.4854	-0.0417	0.3731
NPOC	0.2045	0.0448	0.2802	0.1742	0.0435	-0.2667	0.0247	-0.0161
P	-0.312	-0.3433	0.0673	0.2125	-0.5124	-0.072	0.5046	-0.3511
Relative Contributions								
	PC1	PC2	PC3	PC4	PC5	PC6	PC7	PC8
F	67.4985	1.1986	0.8339	0.5483	5.399	1.0287	0.0115	0.0171
Cl	6.6735	61.0455	3.8102	1.9217	1.0196	2.0352	0.1802	0.8418
HCO3	79.8065	1.5265	0.1845	0.7419	2.0229	1.0309	0.3608	0.0483
SO4	50.9997	6.4032	4.0756	1.0294	0.0385	15.3697	1.4461	0.9491
NO3	46.1403	1.6435	19.7176	4.984	14.7953	7.2348	0.0535	4.2735
NPOC	11.929	0.5725	22.3937	8.6565	0.5403	20.2893	0.1741	0.074
P	8.6114	10.427	0.4008	3.996	23.2314	0.4587	22.5276	10.9046
Absolute Contributions								
	PC1	PC2	PC3	PC4	PC5	PC6	PC7	PC8
F	3.2274	0.3889	0.3636	0.2961	3.2561	0.7749	0.0123	0.0202
Cl	0.1107	6.8713	0.5764	0.3601	0.2133	0.5319	0.0668	0.3446
HCO3	6.6671	0.8652	0.1406	0.7001	2.1315	1.3568	0.6729	0.0996
SO4	2.0271	1.7269	1.4773	0.4622	0.0193	9.6247	1.2833	0.9309
NO3	5.9427	1.4362	23.1593	7.2508	24.0352	14.6803	0.1539	13.5825
NPOC	0.1654	0.0539	2.831	1.3555	0.0945	4.4311	0.0539	0.0253
P	0.3848	3.1618	0.1634	2.0172	13.0951	0.323	22.4776	12.026

Table 4.2 Eigenvalues and loadings of the selected anions/elements.



Figure 4.17 shows the principal component biplot for PC1vPC2, coded by rock type. The biplot shows that there is a relationship between certain rock types and the presence/absence of bicarbonate (HCO_3^-). As expected, limestone is associated with relative enrichment of HCO_3^- while clastic and crystalline rocks (granites, greywackes, etc.) are associated with a relative depletion of HCO_3^- . Figure 4.20 shows a map of PC2 for stream water samples overlaid on areas of limestone bedrock. The negative PC2 scores align closely with the limestone bedrock.

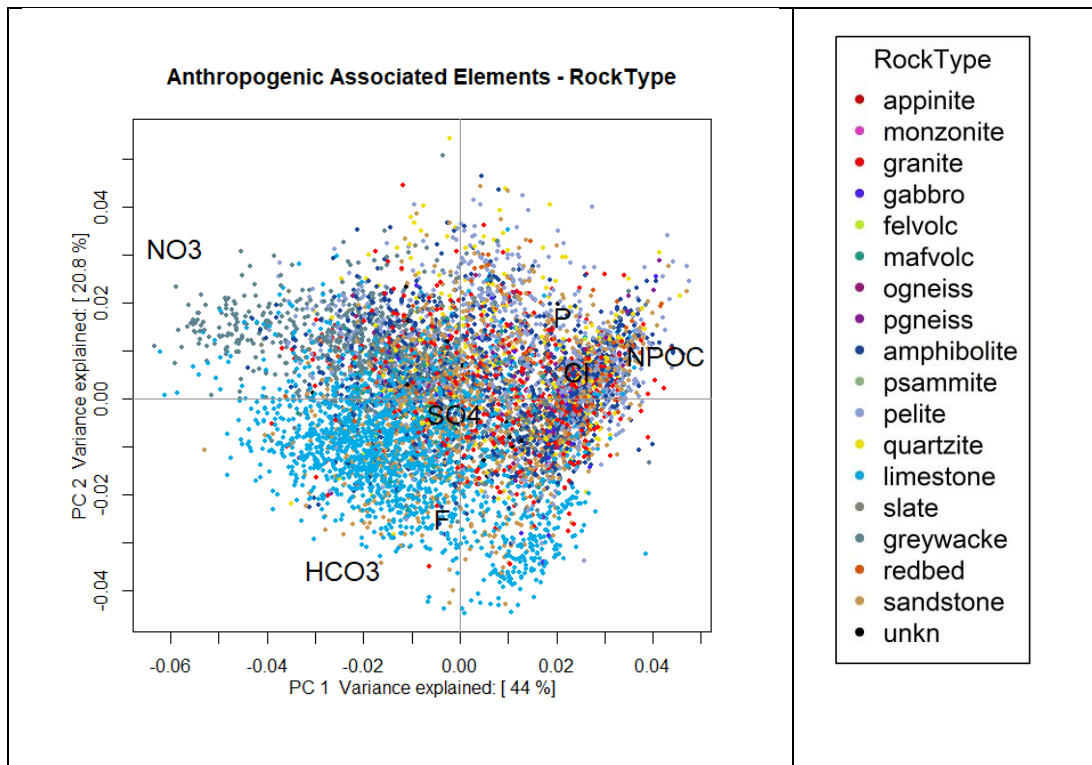


Figure 4.17 Principal component biplot (PC1vPC2) for anions / elements associated with anthropogenic activity classified by rock type.



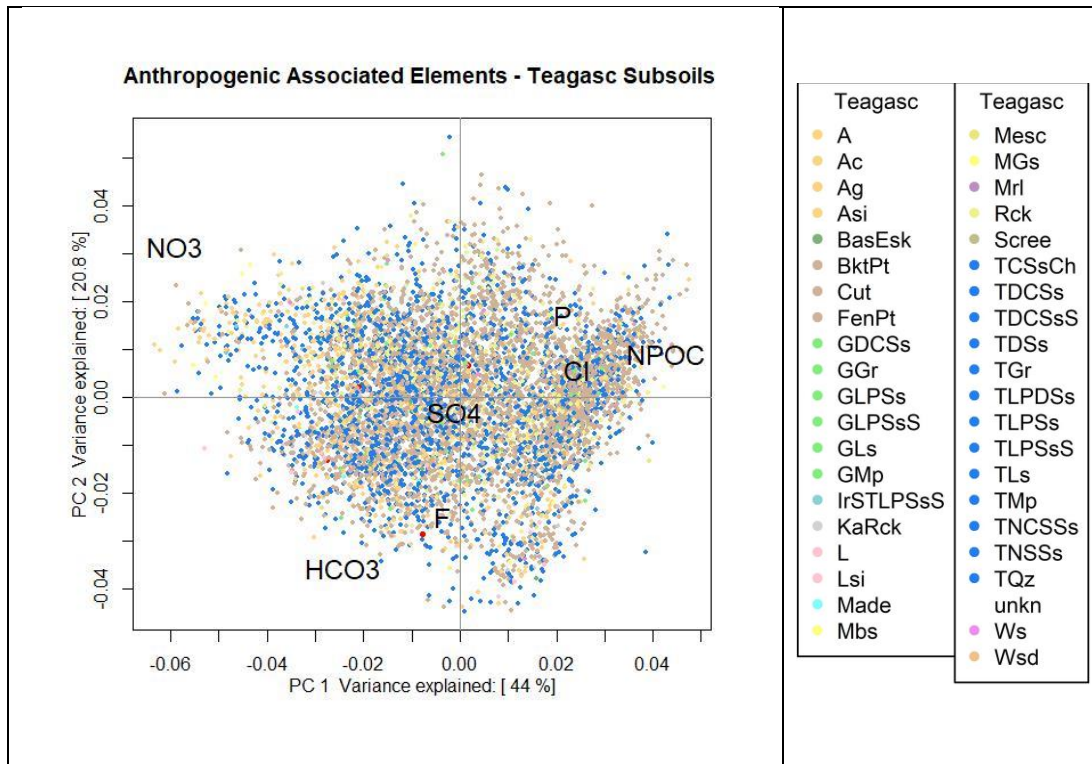


Figure 4.18 Principal component biplot (PC1vPC2) for anions / elements associated with anthropogenic activity classified by Teagasc subsoils.

Figure 4.18 shows a PC1 v PC2 biplot for stream water data classified by Teagasc subsoils. Relative enrichment of NPOC is associated with peat, which is shown on the map in Figure 4.19. Areas with relative enrichment in NPOC are associated with both peat and till subsoil. Areas with relative enrichment in NO_3^- and F^- (negative PC1) occur in the central part of the map (Figure 4.19) where land use is dominated by agriculture, chiefly pasture.



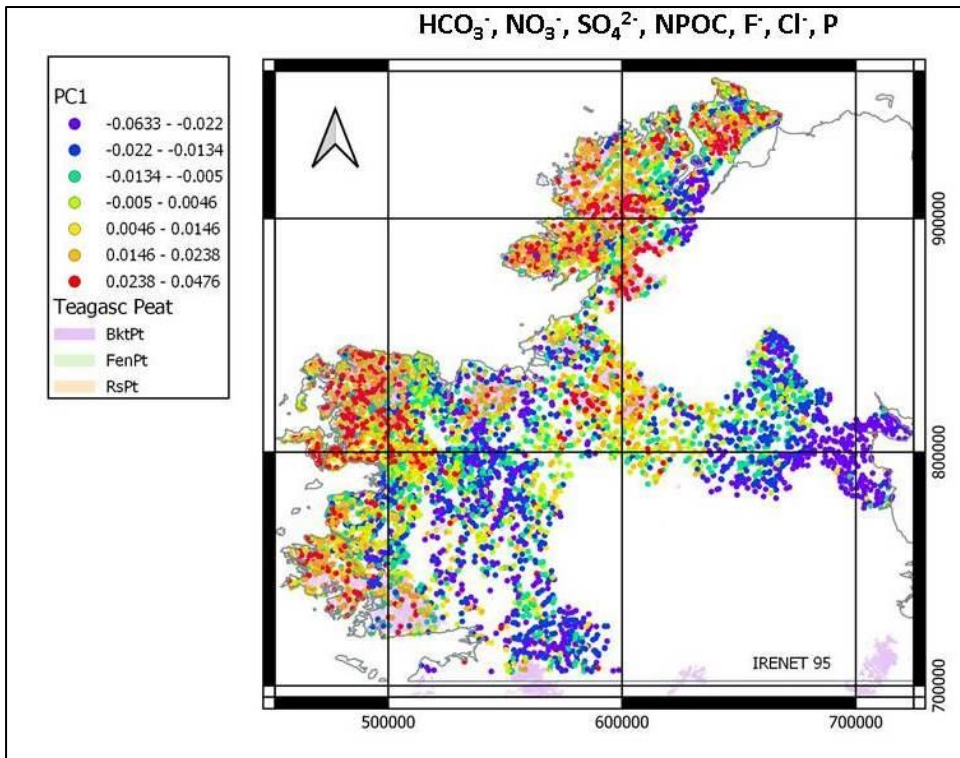


Figure 4.19 Map of PC1 showing the relative enrichment of NPOC along the positive PC1 axis, associated with peat.

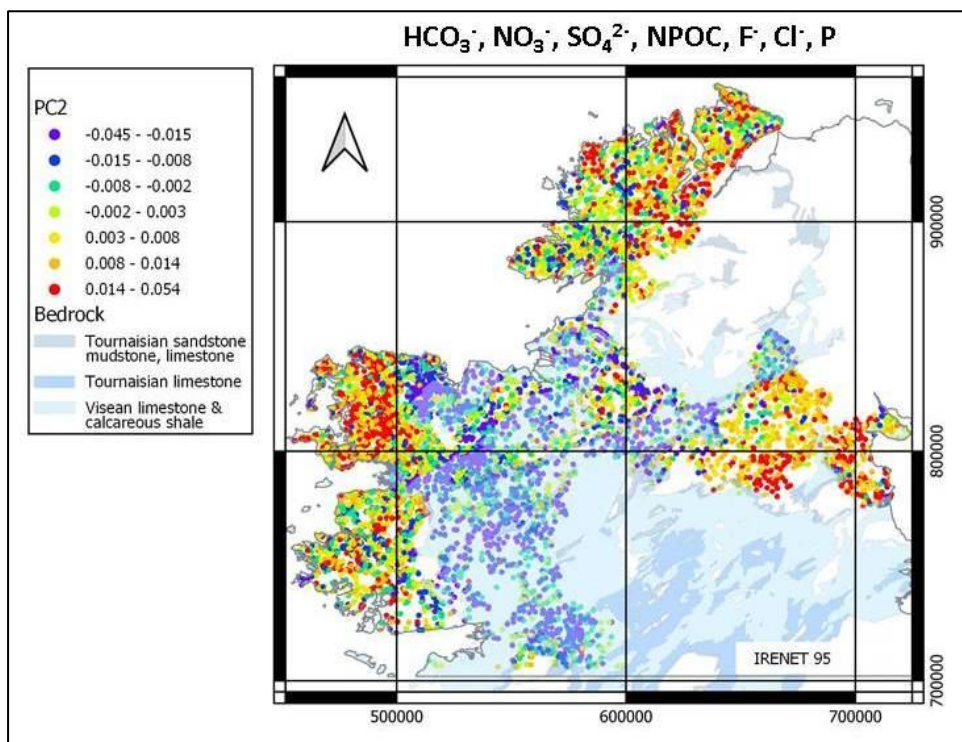


Figure 4.20 Map of PC2 showing the relative enrichment of HCO_3^- and F^- along the negative PC2 axis and the association with limestone.



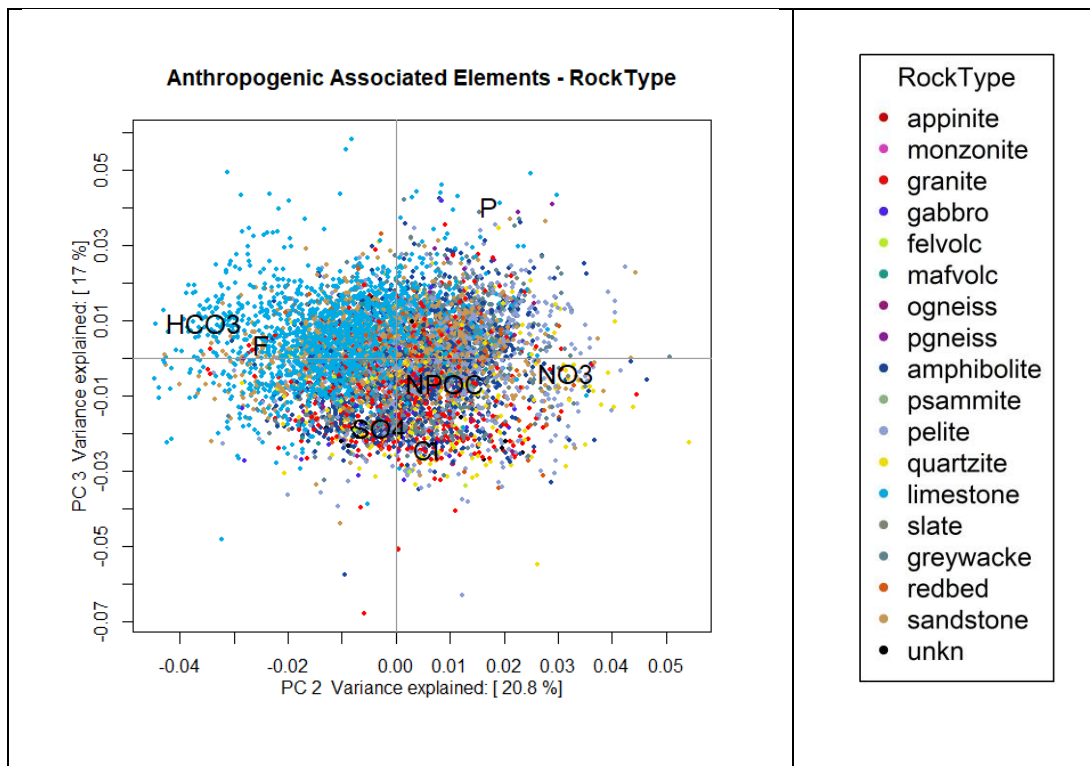


Figure 4.21 Biplot of PC2 v PC3 for anions / elements associated with anthropogenic activity classified by rock type.

Figure 4.21 displays a biplot for PC2 v PC3 where positive PC2 and PC3 scores indicate relative enrichment in P. This is displayed in Figure 4.22 where positive PC3 scores coincide with areas with a relative enrichment in P. Negative PC3 scores reflect a relative depletion of P in stream waters and are associated with peat and non-agricultural land cover classes.



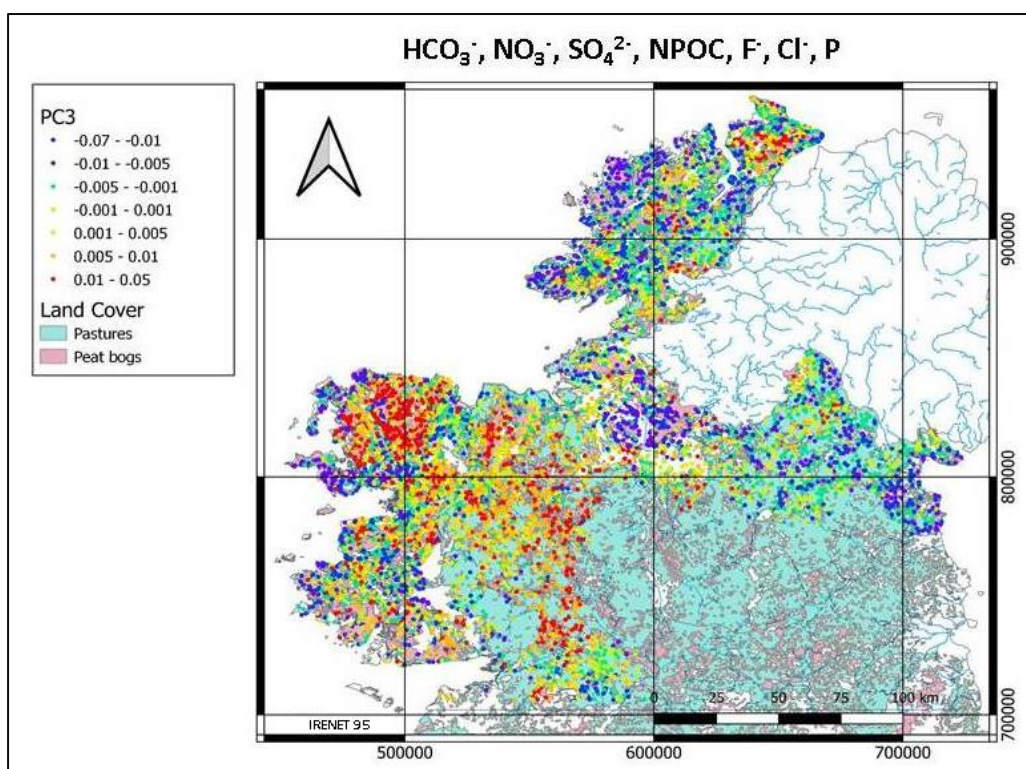


Figure 4.22 Map of PC3 showing the association of P enrichment in both pasture land and peat.

The patterns observed in the dominant principal component biplots and the associated maps indicate that anthropogenic effects are present as geospatially coherent areas.

4.3 Cluster Analysis

4.3.1 Hierarchical Cluster Analysis

Cluster analysis methods are useful as an exploratory tool for detecting groups of multi-element data that may not be readily observable in simple scatter plots or through the use of methods such as PCA. The main objective of clustering algorithms is to identify distinct natural groupings within multi-dimensional data. Clustering methods can be broadly classified as hierarchical or non-hierarchical. A detailed discussion of cluster analysis is provided in Appendix B where further outputs of the cluster analysis are displayed.

Hierarchical cluster analysis was applied to the waters geochemical data, using seven different hierarchical clustering methods to create dendrograms for rock types (1:1,000,000 bedrock geology map) and subsoils (Teagasc subsoils map). Only the results from the application of Ward's method (Ward 1963) are presented here. The dendrograms have potential use in identifying specific processes but do not provide any geospatial association, which makes it difficult to tie the observed correlations within and between clusters with known or speculative processes.



The interpretation of the dendrograms requires some prior knowledge about how the elements may be linked through processes such as mineralogy, weathering, streamwater modification, mass transport and organic complexation/adsorption. Ward's method (Ward 1963) was chosen as it is based on concepts related to analysis of variance, which is consistent with the methods employed to evaluate multi-element geochemical data in this study.

Figure 4.23 shows an example of a dendrogram of the elements, in this case for the rock type limestone. Dendrograms for other rock types are shown in Appendix B. Figure 4.23 displays a cluster of NO_3^- -U- HCO_3^- -Ca- F^- -Sr-Mo-Sb-Se- SO_4^{2-} -S-K-Br-Mg. Many of these elements are also part of a cluster in dendrograms for other rock types. The cluster appears to reflect the composition of dominant limestone bedrock (Ca, Mg, Sr, HCO_3^-) and the tills with dominant limestone clasts that form the subsoils, as well as agricultural activities such as nutrient inputs to overlying pasture (NO_3^-). Elements such as Mo, Se and U may reflect the presence of shales interbedded with limestone but U is also commonly associated with HCO_3^- owing to the stability in solution of U carbonates and bicarbonates (De Vivo *et al.* 2006).

There is also a cluster of Al-Fe-Ti and several rare earth elements that probably reflects a contribution from silicates found in non-limestone bedrock and in subsoil comprised of till with dominant silicate rock clasts. This is something that is replicated in dendrograms for other rock types. NPOC (organic carbon) is typically in a cluster with Zn, Cd and others elements such as V and Mn, consistent with the role of organic matter in complexation of metals, as previously inferred from Principal Component Analysis (Section 4.2).



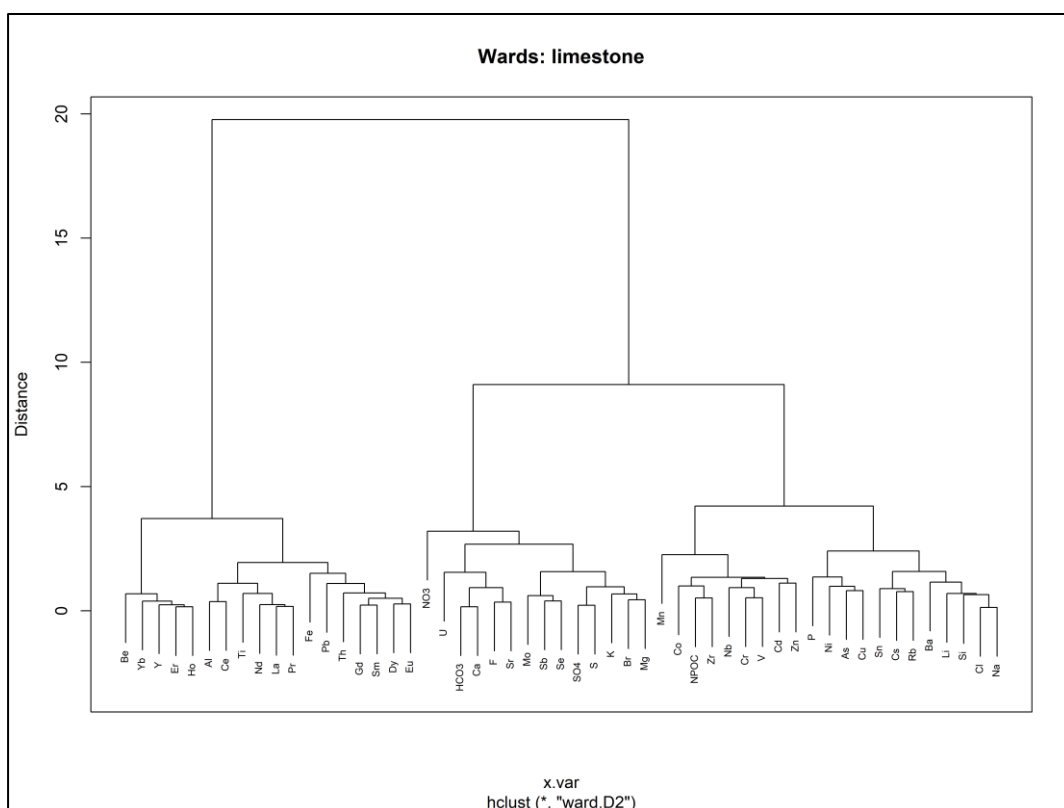


Figure 4.23 Dendrogram of Tellus surface waters data (clr transform) overlying limestone bedrock, based on Wards clustering algorithm.

The dendrogram of Figure 4.24 shows a cluster analysis of all of the waters data, i.e. irrespective of bedrock, subsoil type, etc. The groupings of the elements highlight some general patterns that are interpreted as follows:

- 1) A multi-element signature related to bedrock is located on the left side of the dendrogram. This grouping contains several lithophile and rare earth elements that are associated with granitoid and metamorphic rock types along with mixtures of Phanerozoic sediments (greywacke, shale, sandstone).
- 2) A multi-element group that shows associations of anions/nutrients associated with anthropogenic (agricultural) activities overlying limestone bedrock.
- 3) The right side of the dendrogram shows at least three groups that likely represent variations on peat and the underlying bedrock. A unique group that shows a Br-Na-Cl association likely reflects a marine influence.



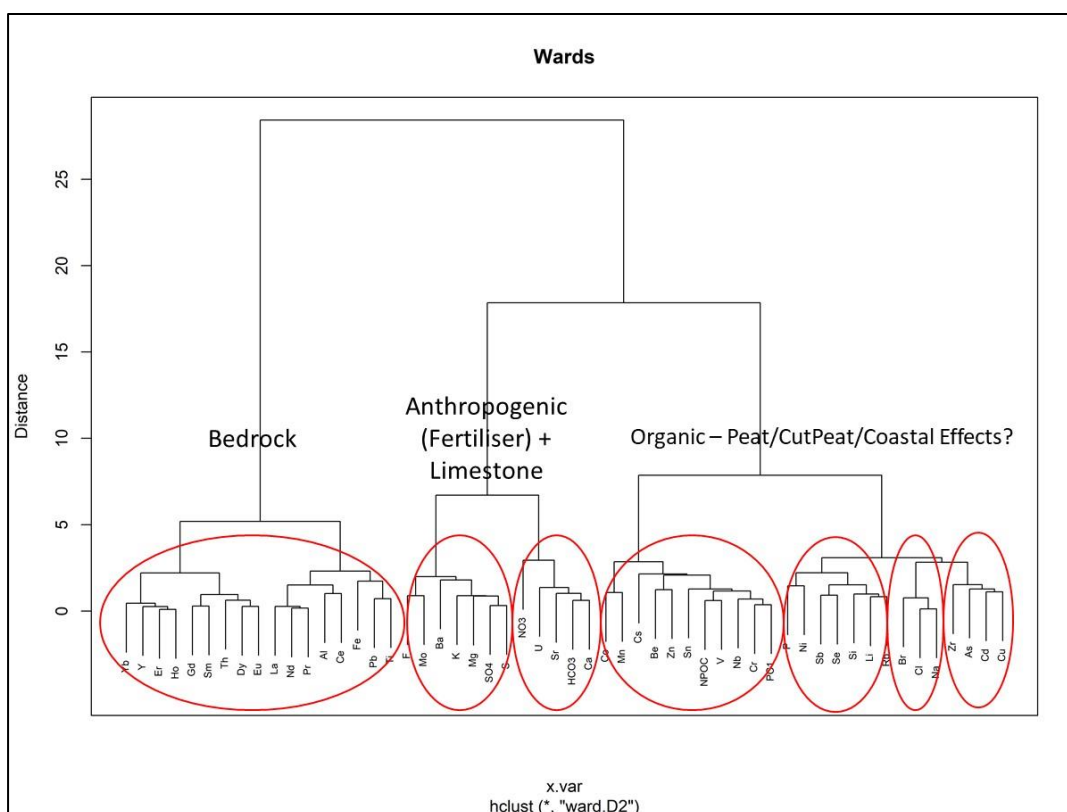


Figure 4.24 Dendrogram of all Tellus stream waters data (clr transform) based on Ward's clustering algorithm. The three levels of multi-element association are possibly linked to features related to bedrock composition, anthropogenic effects from agricultural activities and chalcophile enrichment associated with peat formation. The marine signature (Na-Cl-Br) is associated with peat that is located near coastal areas.

In summary, the dendrograms derived from hierarchical cluster analysis have the potential to identify specific processes but do not provide any geospatial association. The order of analyses can be identified based on the distance matrix determined from all of the analyses and this can be visualized geospatially but it is difficult to tie the observed correlations within and between clusters with known or speculative processes. However, creating geospatial maps of the q-mode order is technically challenging. It is more informative to use other methods of clustering to render geospatial associations.

4.3.2 Other Methods of Clustering Tellus Waters Geochemistry

Appendix B provides a detailed description of both hierarchical and non-hierarchical clustering methods that have been applied to the Tellus waters geochemistry. The application of these clustering methods consistently highlights that the chemistry of the Tellus waters reflect bedrock composition, soil composition / modification and the presence of peat.



4.4 Random Forests Classification

Random Forests (RF) (Breiman 2001; Harris and Grunsky 2015) is an ensemble, multiple decision-tree classifier. RF classification was applied to each of the four themes (rock type, subsoil, SRF Geochemical Domains, land cover) with the function "randomForest" from the R package "RandomForest", using the parameters listed in Table 4.3.

Parameter	Comment
ntree = 5	Default number of t grown for each sample site
type = "classification"	Type of prediction for each class for each theme: "regression", "classification" or "unsupervised".
proximity = TRUE	Proximity (distance) between observations are measured as part of clustering process
classwt = prior probabilities	Prior probabilities that are measured for each class for each theme
importance = TRUE	Relative importance of predictors
norm votes = TRUE	The final results of votes are expressed as fractions

Table 4.3 Random Forest Parameters.

Because of the imbalance of classes in the themes for rock type, Teagasc subsoil and Land Cover, prior probabilities were included in the RF classification. Imbalance refers to unequal numbers of observations for each class. Classes with large numbers of observations can "mask" and "swamp" classes with a small number of observations. Some of these classes may be compositionally similar or are "weak" classifiers (Schapire 1990), where the classification rate is nearly the same as a random guess. This is particularly the case for the Teagasc subsoil classes, where numerous classes with very limited geographical extent are intersected by relatively few stream water sites. Grunsky *et al.* (2018) provide a detailed examination of the use of RF classification based on multi-element soil geochemistry to predict surface lithology, soil ombrotype, thermoclimatic region and terrestrial ecosystems over the continental United States.

A measure of variable significance is provided by the Gini index, which calculates the amount of probability of a specific class that is classified incorrectly when selected randomly. Increasing Gini index values indicates that the variable is better at discriminating between the classes. Variables with low Gini index values are less significant for discriminating between the classes.

A full description of the RF analysis with accompanying illustrations is contained in Appendix C.

4.4.1 Random Forests – Rock Type

Figure 4.25 shows the variable significance obtained from the application of rock type based on the principal components. The figure shows the mean decrease measure of the Gini index. A higher Gini index indicates that the variable is better at discriminating



between the classes. For rock type, PCs 1, 5, 2, 7, 6 are the main variables for classifying the rock types from the waters chemistry, with PC1 by far the single-most important one (Figure 4.25).

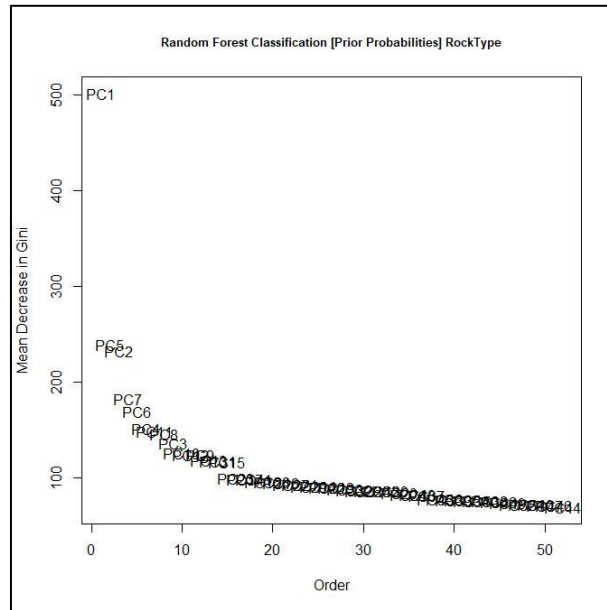


Figure 4.25 Mean decrease of Gini index (Rock Type).

The overall accuracy of the RF predictions for rock type is 69.7 %, which is the average predictive accuracy over all of the classes. The precision of the predicted rock types indicates that amphibolite (57 %), greywacke (84 %), limestone (93 %), sandstone (53 %), pelite (57 %) and granite (67 %) are well predicted (Tables C.1 and C2 Appendix C). Classes including appinite, felsic volcanics, gabbro, mafic volcanics and orthogneiss are not well predicted because (i) they have very low counts in the initial dataset and (ii) they overlap with other classes, despite the correction applied by the prior probabilities. This is also reflected in the measure of recall. Recall values indicate the success of capturing the positive results. High recall values (see Appendix C, section C.1, Table C.3) are noted for limestone, greywacke and amphibolite. Comparison of the precision and recall indicates that the two measures do not correlate well for most of the classes. This indicates significant confusion in the prediction. Sources of error or uncertainty in the predictions may include compositional overlap of the chemistry of the waters between the rock types, misclassification of the original site and the variability created by the range of influences on stream water chemical composition.

Figures 4.26 and 4.27 show two maps, one classifying the stream water data according to underlying rock types and the other showing the predicted classes (rock types) based on RF analysis. From the scale of the maps as presented in Figure 4.26 the predictions of the rock types are reasonably close to the mapped rock types.



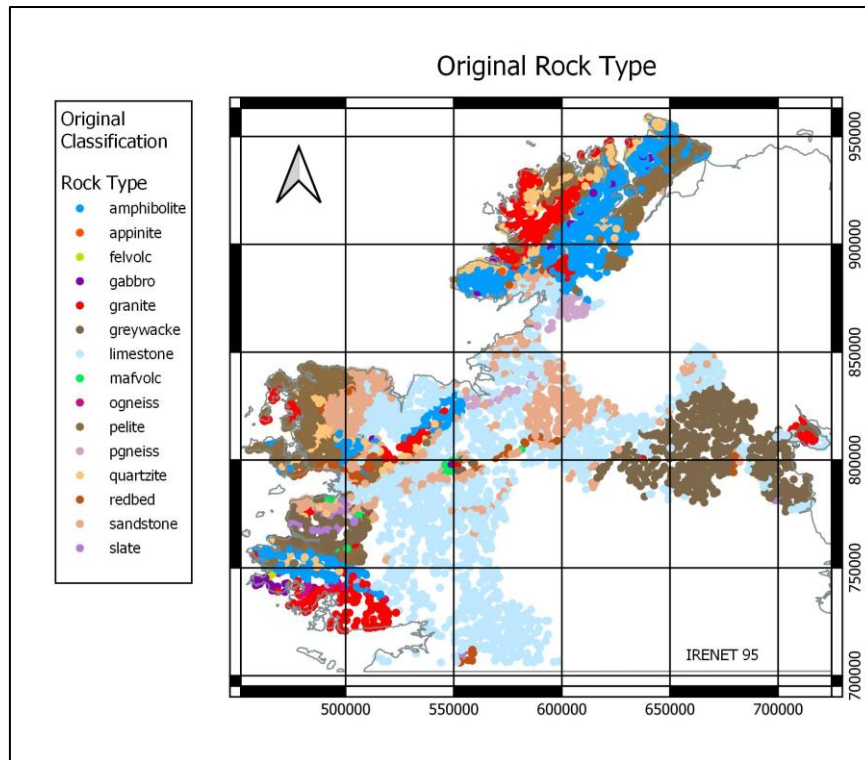


Figure 4.26 Stream water sites classified by mapped rock type.

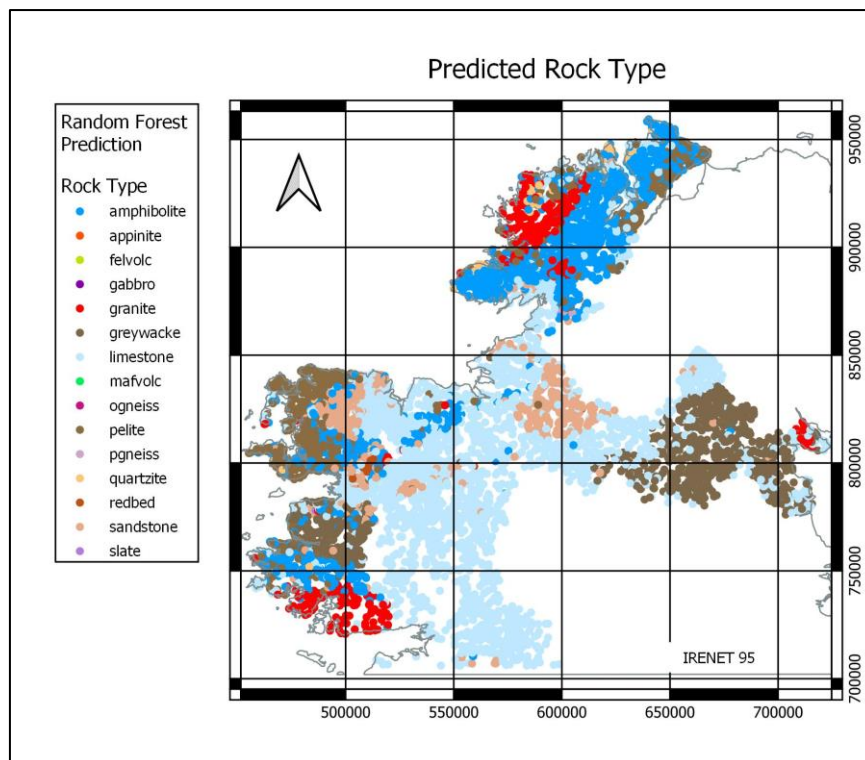


Figure 4.27 Stream water sites classified by RF prediction.



4.4.2 Random Forests – Teagasc Subsoil

Figures 4.28, 4.29 and 4.30 show the variable significance (Gini index) and the original and predicted maps for the Teagasc subsoil classes. There are 40 subsoil classes mapped within the survey area and inevitably there are some among them that intersect only a few stream water sites. The under-representation of these classes within any classification scheme can yield uncertain results. Figure 4.28 shows that PC2 is the dominant principal component for discriminating between the subsoil classes. Additionally, in descending order, PC13, PC1, PC7, PC4, PC8 and PC5 can help discriminate between the subsoil classes. For the 40 classes of subsoil, the only classes that show any form of classification accuracy are alluvium (20 %), blanket peat (97 %), cutover peat (73 %), rock (3 %) and several classes of till with dominant clasts derived from the Phanerozoic sedimentary assemblages including Lower Palaeozoic sandstone (8 %), Lower Palaeozoic sandstone and shale (5 %), Carboniferous limestone (11 %), metamorphic rock (25 %) and Namurian shale and sandstone (29 %) (Table C.4, Appendix C). Measures of precision and recall (not shown) are low and/or inconsistent. Although there is significant uncertainty in the class prediction, nevertheless the method of RF predicts the classes in a consistent manner as shown in Figures 4.29 and 4.30 where the distribution of the broad subsoil classes of the original sites is very similar to that of the predicted subsoil sites. Despite the low prediction accuracies for individual classes, the overall accuracy is 49.4 %, which suggests that the dominant classes are reasonably well predicted.

Further refinement in the use of Teagasc subsoil through the reduction of the number of classes by increased generalization of the class features is warranted. The SRF Geochemical Domains represent just such a reduction.

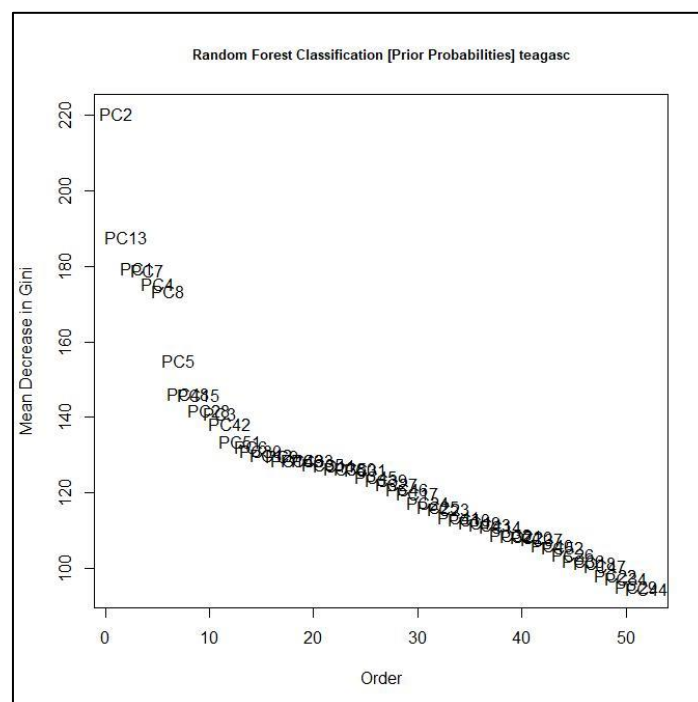


Figure 4.28 Mean decrease of Gini index (Teagasc subsoil classes).



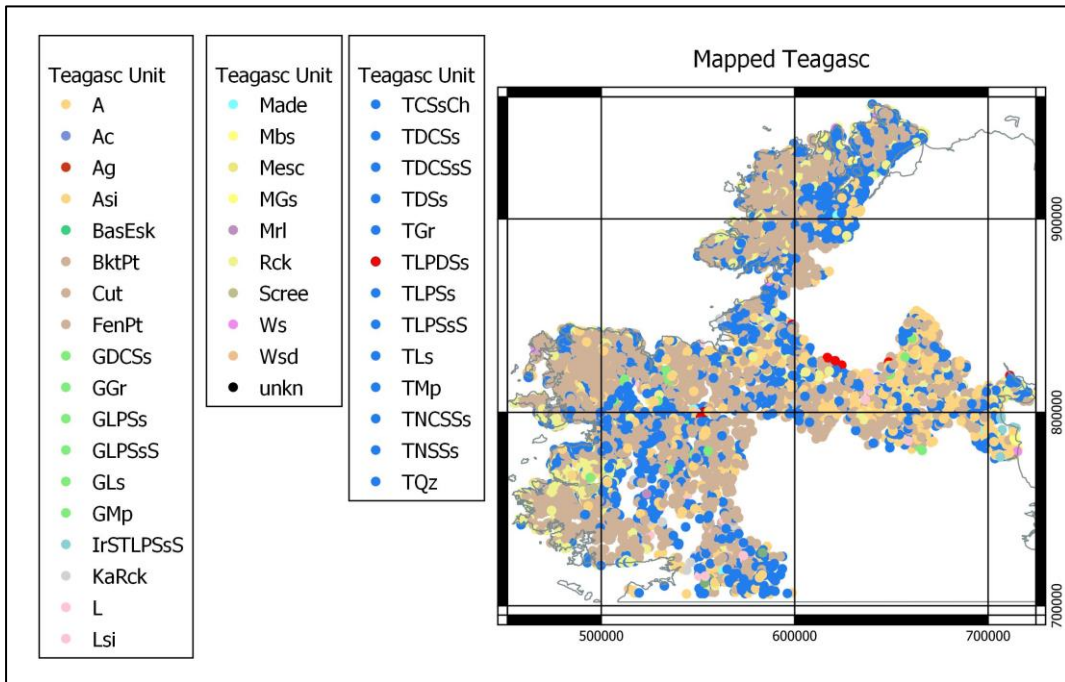


Figure 4.29 Stream water sites classified by mapped subsoil class.

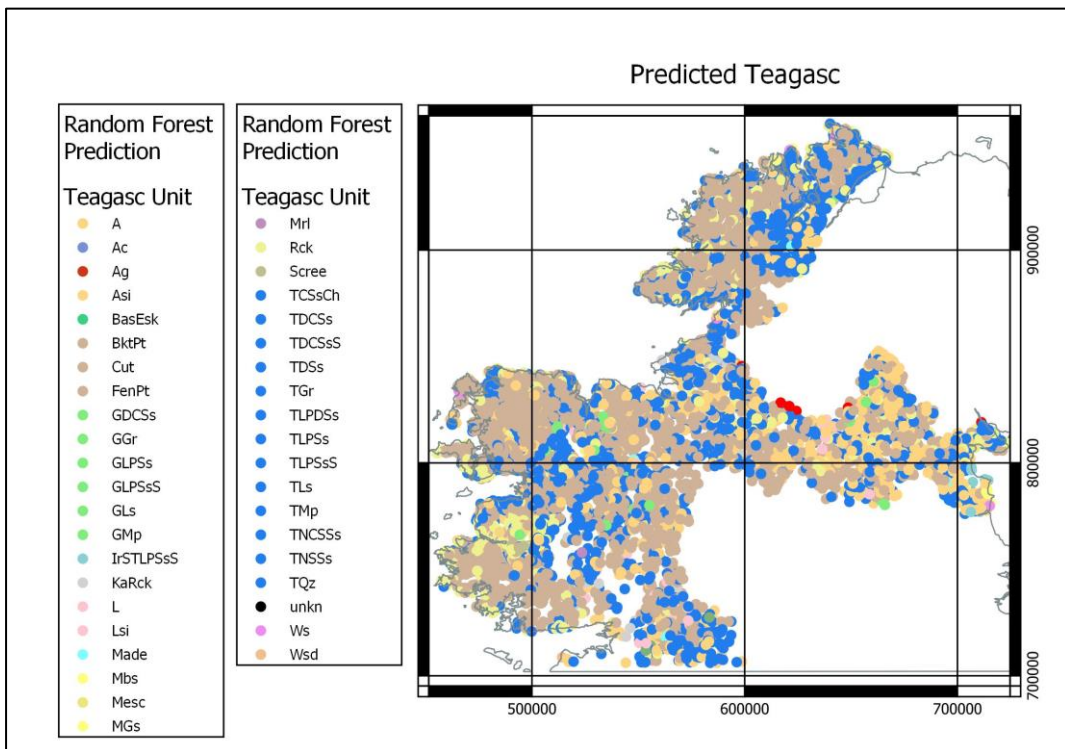


Figure 4.30 Stream water sites classified by subsoil types as predicted by Random Forests.



4.4.3 Random Forests – SRF Geochemical Domains

For the SRF Geochemical Domains, several principal components contribute to the discrimination of the seven domains (Figure 4.31). The main components in descending order of importance are PC2, PC1, PC7, PC5, PC6, PC13, PC4 and PC8. The overall prediction accuracy is 76.8 % (Appendix C, Section C.3). The accuracies of the predicted domains are 59 % (Domain 1), 84 % (Domain 2), 23 % (Domain 3), 11 % (Domain 4), 71 % (Domain 5), 46 % (Domain 6) and 97 % (Domain 7) (Table C.5, Appendix C). The measures of precision and recall (not shown) are better than those reported for the prediction of rock type and subsoils. Figures 4.32 and 4.33 show that the geospatial extent of each of the domains in the predicted map is similar to that in the original map. Some prediction overlap is observed for Domain 1 and Domain 2 and for Domain 6 and Domain 7, while Domain 4 displays a very low prediction accuracy and significant confusion with Domains 2 and 7. The generally strong agreement between the original domain map and the map predicted from RF analysis both validates the geochemical domain map itself and provides further support for the observation that the stream water data carry a strong geogenic signal.

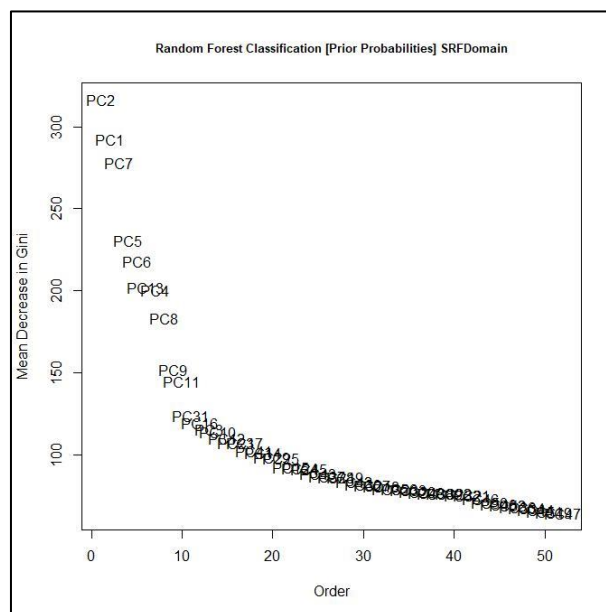


Figure 4.31 Mean decrease of Gini index (SRF Geochemical Domain).



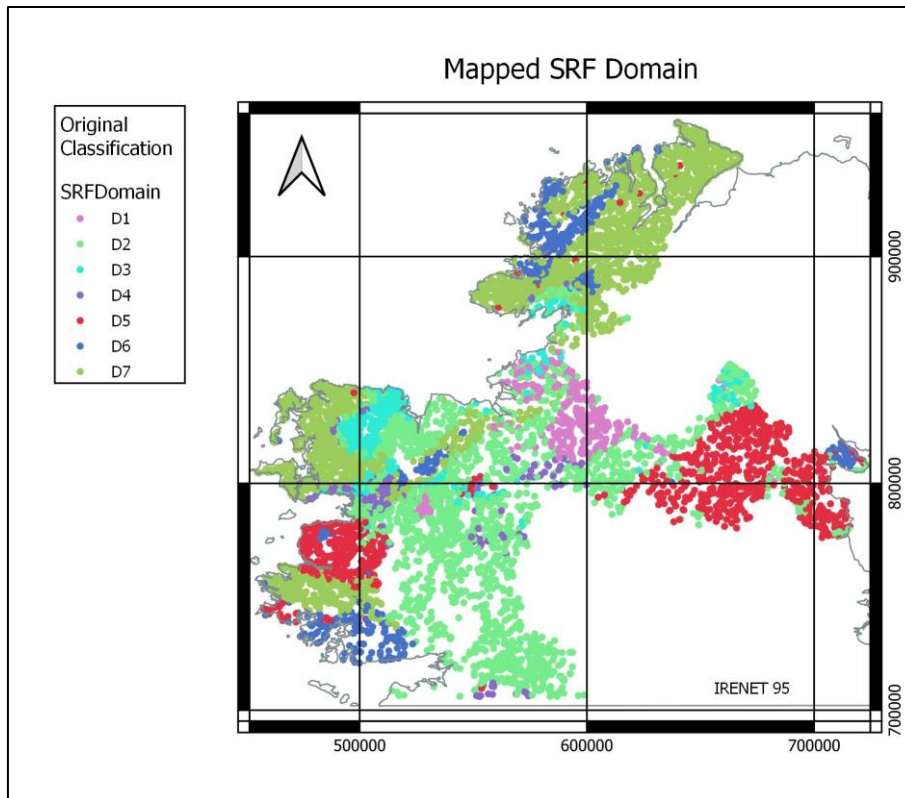


Figure 4.32 Stream water samples classified by mapped SRF Geochemical Domain.

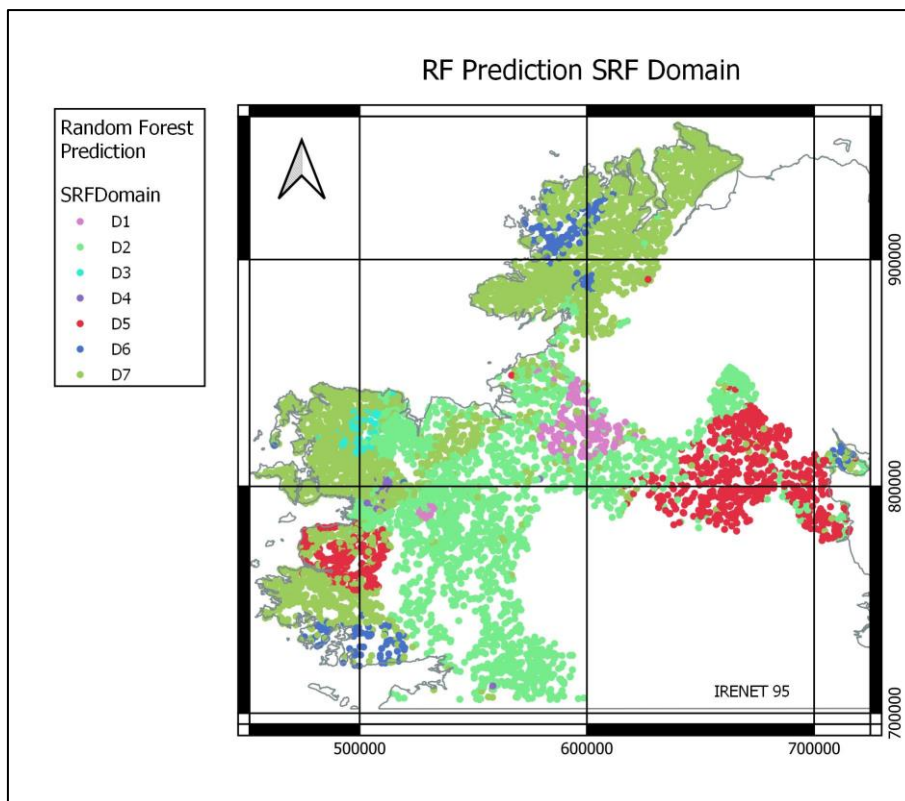


Figure 4.33 Stream water samples classified by SRF Geochemical Domain as predicted by Random Forests.



4.4.4 Random Forests – Land Cover

The geospatial distributions of many of the Land Cover classes have very limited geospatial extent. The geographically most extensive Land Cover classes in the area covered by Tellus stream water data are pasture and peat bog. This is reflected in the prediction accuracies where these two classes dominate (Table C.6, Appendix C). The variability of the waters compositions for pasture and peat bog classes overlap with all of the other classes, resulting in a sub-optimal classification. Figure 4.34 shows that PC1, PC2, and PC8 are the most significant principal components for discriminating the classes. Figures 4.35 and 4.36 indicate that the broad geospatial patterns of the original and predicted data are similar. The degree of confusion/misclassification is difficult to see at the scale of the figures. Nonetheless, the overall prediction accuracy of 64.5 % indicates that there is useful prediction capacity for peat bog and pasture Land Cover classes.

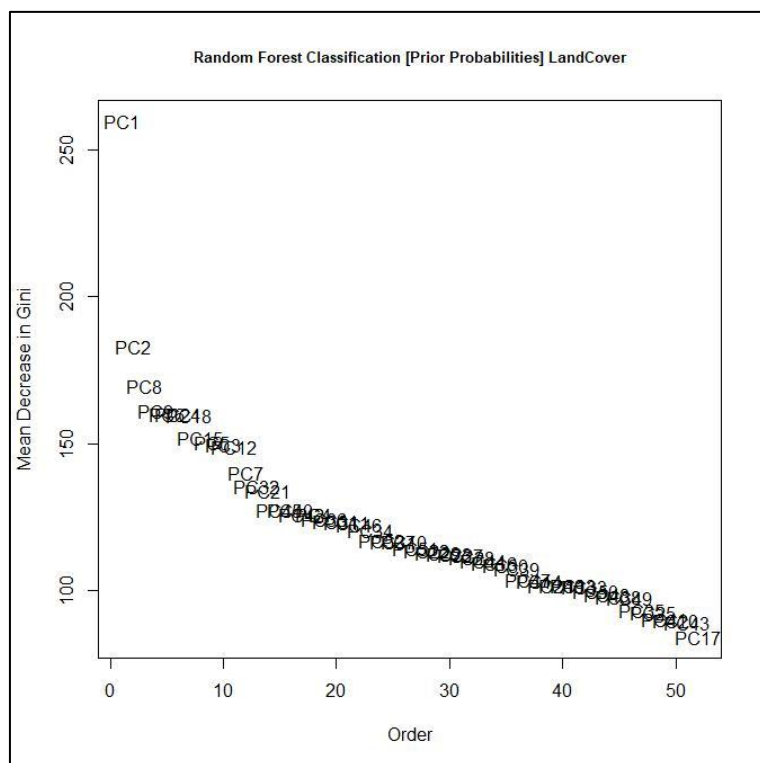


Figure 4.34 Mean decrease of Gini index (Land Cover).



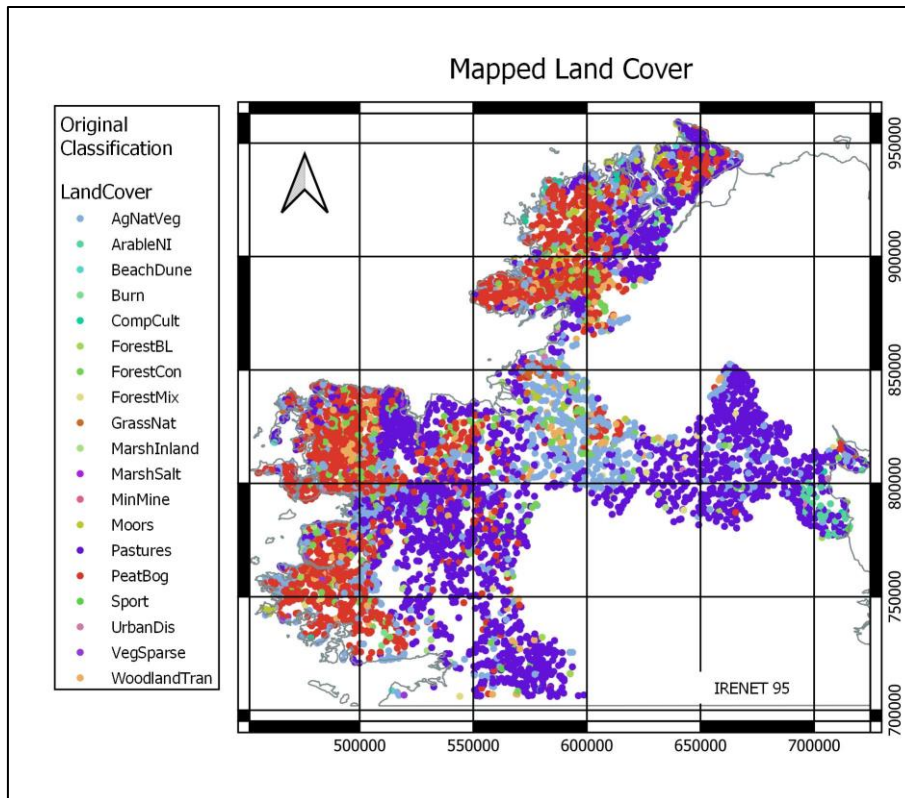


Figure 4.35 Stream water samples classified by mapped Land Cover (Corine).

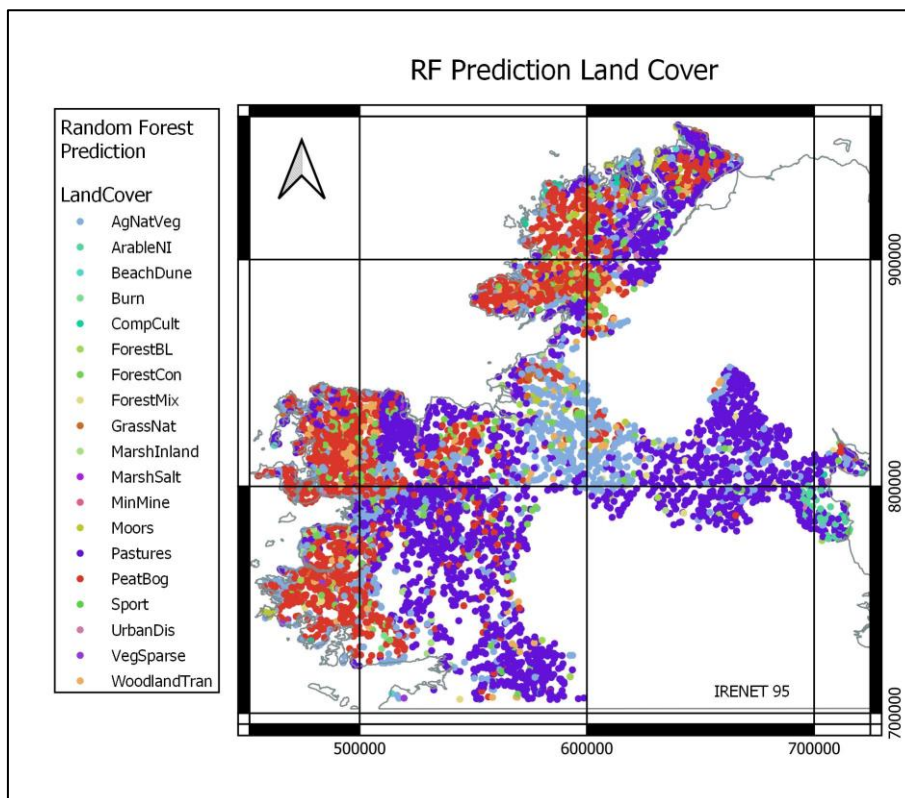


Figure 4.36 Stream water samples classified by random forest prediction.



5. Summary and Conclusions

The Tellus stream water geochemistry dataset has been subject to a range of univariate and multivariate statistical analyses in order to elucidate the factors that influence stream water geochemistry in the survey area. The findings are summarized here with reference to the objectives outlined in Section 1.5: (i) understanding the extent to which the Tellus stream water geochemistry data reflect bedrock geology and other geological influences; (ii) identifying background concentrations for various chemical parameters where possible; (iii) identifying data populations for elements in stream waters in order to identify natural and anthropogenic processes, including inputs of nutrients and potentially harmful substances and (iv) characterizing mineralization signatures in stream water chemistry and identifying potential exploration targets.

5.1 Geogenic control of stream water chemistry

Interpolated univariate maps are at least partly consistent with interpolated maps derived from topsoil and stream sediment geochemistry and indicate that stream water chemistry broadly reflects the composition of bedrock and subsoil. Thus, Ca in stream water strongly reflects the distribution of limestone-dominated Lower Carboniferous rocks in the region while Cr and Ni reflect specific known bedrock sources, including the Longford-Down Inlier greywacke and the rocks of the South Mayo Trough, which include serpentinite and sediments containing Cr-bearing phases such as chromite and fuchsite. Bedrock units with distinctive topsoil and stream sediment geochemical signatures, such as the Namurian shales of the Leitrim Group, find similar expression in stream water geochemistry.

Multivariate statistical analysis provides strong support for geogenic control of stream water geochemistry. Principal Component Analysis and cluster analysis both identify specific element associations that clearly reflect contributions from different bedrock and subsoil compositions such as granitic rocks, limestones and clastic sediments.

PC biplots generated from Principal Component Analysis of stream water data classified by bedrock or subsoil type show that for sites underlain by granitic rocks or subsoil derived from them there is relative enrichment in lithophile (Ce, Nd, La, Al, Ti, Sm, Gd, Eu, Yb, Ho, Er, Y, Th), siderophile (Fe) and chalcophile (Pb) elements along the positive portion of the PC1 axis, implying that these elements are strongly associated with this rock type. For stream water draining Carboniferous limestone or subsoil derived from it there is a clear association with NO_3^- , HCO_3^- , Ca, U, Sr, F^- , Mg, SO_4^{2-} , Ba and Mo. The association of U with HCO_3^- likely reflects the stability of hexavalent U carbonates and bicarbonates in solution (De Vivo *et al.* 2006). The relative enrichment of Ca, Sr, F^- , Mg and Ba reflect the underlying Carboniferous limestone-dominated lithologies. These lithologies underlie large areas of pasture and the observed relative enrichment of NO_3^-



and SO_4^{2-} likely reflects the addition of fertilizer and other agricultural activities. For stream waters draining clastic sediments, such as the greywacke of the Longford-Down Inlier, analysis suggests mixing between the different components, reflecting the diverse range of source material that contributes to clastic sedimentary rocks. There is a significant degree of overlap on the biplots between stream water data classified according to different bedrock / subsoil types but it is clear that the principal component analysis does generally discriminate between the main bedrock / subsoil types, implying that the water geochemistry at least partly reflects geogenic control. The presence of a Fe-Mn association (positive PC3, all elements), suggests the presence of oxyhydroxide coatings on stream sediments clasts.

On the PC biplot, classified by subsoil type, there is a clear distinction between water draining raised bogs and blanket bogs, mirroring that between limestone and granitoid compositions, reflecting the dominant bedrock composition of the areas where these bogs occur.

Cluster analysis of all stream water data, irrespective of bedrock, subsoil type, etc., shows several distinct clusters that can be related to specific bedrock types and geological processes, including limestone, granitic, metamorphic and clastic rocks.

The RF classifications for the four themes (bedrock type, subsoil type, SRF Geochemical Domain and Land Cover) indicate varying success in classification accuracies. For stream waters classified by bedrock type, the RF predictions of the rock types are reasonably close to the mapped rock types. There is a large number (40) of classes represented on the subsoil map and consequently significant uncertainty in the class prediction. Nevertheless, the RF method predicts the classes in a consistent manner and the distribution of the stream water data classified by the main subsoil classes is very similar to that of the predicted subsoil classes. A significant issue in the RF analysis is the under-representation of many classes relative to the dominant classes. In particular, the peat bog classes (subsoil, Land Cover) and pasture (Land Cover) display significant compositional variation, overlapping all of the other less-dominant classes and resulting in “weak” classifications. Further studies of these themes may generalize some of the classes and/or apply methods to improve weak classifications, so that the compositional variance of the newer generalized classes will assist in reducing the influence of the dominant classes.

5.2 Background stream water concentrations

The Tellus stream water data are of sufficient spatial resolution to allow estimation of background or threshold values for elements of interest, not only nationally but at a regional scale, reflecting the geospatial variation in background concentrations that arises owing to variable bedrock and subsoil composition.



Surface water regulations set EQS values for substances that may depend on background concentrations and / or water hardness. Exploratory Data Analysis (EDA) plots were employed for As, Cr, Cu and Zn for the entire Tellus dataset in order to estimate background concentrations in the study area. Quantile-Quantile (Q-Q) plots allow an estimation of threshold or background concentrations for each element by identifying inflection or break point(s) at the upper end of the Q-Q curve. For As, the estimated break point occurs at 10 µg/L, for Cr 1.2 µg/L and for Cu 10 µg/L. In the case of Zn, the curve ramps upwards sharply at c. 6.5 µg/L and flattens out again at c. 34 µg/L, reflecting the multi-modal nature of the Zn data.

These breaks provide estimates of the background concentrations in stream water for each of these elements in the area covered by the Tellus data. Background values for As and Cr are well below the stated EQS limits (25 µg/L for As; 3.4 / 4.7 µg/L for Cr(III) / Cr(VI)). For Cu, the estimated background of 10 µg/L exceeds the stated 5 µg/L EQS for water with a hardness ≤ 100 mg/L CaCO₃ eq but is well below the corresponding 30 µg/L EQS for water with hardness exceeding 100 mg/L CaCO₃ eq. Adding any of these estimated background values to the EQS values to generate “corrected” EQS values would yield higher EQS values. For Zn, the higher estimated background of 34 µg/L exceeds the stated 8 µg/L EQS for water with a hardness < 10 mg/L CaCO₃ eq – adding this value to the stated EQS would eliminate many observed exceedances at the lower end of the scale.

In addition to estimating threshold or background concentrations for each element, Tellus stream water data suggest that consideration of the water hardness at any given sampling site may be of high importance in assessing exceedances of metal EQS values, notably for Zn. Without hardness data it is likely that the degree of Zn exceedance of the EQS will be significantly overstated where the lowest EQS value is used as part of a conservative approach. Tellus high-resolution baseline stream water data allow reliable mapping of water hardness in areas where water monitoring stations are sampled. This can help reduce the number of sites that are flagged for Zn exceedance.

5.3 Natural and anthropogenic processes influencing stream water

The dominant source of anthropogenic impacts on stream water chemistry in the survey area is agricultural activity. This is readily apparent on the map of nitrate distribution, which shows two areas of high nitrate concentrations, in County Louth and east County Donegal, that coincide with the two most intensively cultivated areas of the study region. The median NO₃⁻ concentration for Tellus stream water draining arable land (21.2 mg/L) is over 18 times higher than for pastureland (1.19 mg/L) and almost 80 times higher than for other land uses. Similar, if less stark, distinctions were observed for P. Stream water draining well-drained soil had significantly higher concentration of both NO₃⁻ and P than stream water draining soil in other drainage classes. Stream water draining agricultural



areas had significantly higher concentration of both NO_3^- and P than stream water draining soil in other land use types.

In Louth, univariate mapping also suggests that high concentrations of Ca, Mg, Ba, HCO_3^- and U in stream water are also associated with the high NO_3^- concentrations.

Multivariate statistical analysis confirms these observations, with NO_3^- associated with HCO_3^- , Ca, U, Sr, F^- , Mg, SO_4^{2-} and Ba in PC biplots and on cluster dendrograms. In part this reflects an association with limestone bedrock across the region but in Louth the bedrock is Lower Palaeozoic greywacke and the source of Ca and Mg in stream waters there is more likely to be agricultural activity, including liming and fertilizer application. The high U concentrations may reflect the stability in solution of hexavalent uranium carbonates and bicarbonates that in turn reflect the relatively high HCO_3^- concentrations produced by these agricultural practices. They may also be a direct reflection of the presence of U in fertilizer.

When compared to EPA monitoring data it is clear that Tellus stream water data for nitrate and phosphorus have broadly similar distributions, with higher concentrations occurring over the more productive agricultural land, both arable land and pasture. However, Tellus data provide a more detailed picture of the impact of agriculture on water quality and, as the samples were collected from first- and second-order streams, they indicate that these impacts are pervasive, occurring in the upper parts of catchments, with few areas of agricultural land in the country unaffected by nitrate or phosphorus inputs.

Potentially Harmful Substances are routinely monitored in surface waters for exceedances of EQS values. Tellus data demonstrate that elements such as Cd, Zn and Cr can be present in stream waters in relatively high concentrations, reflecting bedrock composition and unrelated to known anthropogenic activity. However, some of the highest concentrations of Cd, Zn and other metals in the Tellus survey area and elsewhere in Ireland can be directly related to historic mining activity. Current EQS values for several Potentially Harmful Substances vary according to water hardness but lack of water hardness data means that the most conservative threshold values are employed. The high-resolution Tellus data allow generation of interpolated water hardness maps that can be used to assign the correct hardness value to any monitoring site, potentially reducing the number of reported exceedances, especially for Zn.

Apart from anthropogenic processes, the stream water data also display the impacts of natural processes. The map of sodium (Na) distribution shows the impact of seawater and marine aerosols along the western and northern coasts, with enrichment in Na observed where tides and on-shore winds have affected freshwater systems. Similar patterns can be observed for other elements that are present in seawater, such as bromine (Br). A cluster dendrogram highlights the association of Na-Cl-Br that are associated with coastal regions.



The drainage characteristics of soils also contribute to the levels of nutrients in stream water. Combining the drainage classes of the Irish National Soils Map with the Tellus stream water data suggests a clear link between drainage characteristics and nitrate concentrations in stream water. A similar, if less well-defined, relationship appears to exist for total phosphorus.

5.4 Mineralization signatures

Stream water base metal (Zn ± Pb ± Cd) anomalies can be observed near numerous historic mine sites in the Tellus survey area. Not all of these observed anomalies occur downstream of the mines and thus may be reflective of the presence of bedrock mineralization in the general area rather than representing contamination by mining. Base metal anomalies in stream water can also be observed close to known but unworked bedrock occurrences of mineralization. Mineralization signatures in stream water chemistry are not confined to base metals. Gold pathfinder elements As and Sb are enriched in stream waters draining known gold deposits in counties Donegal, Monaghan and Mayo.

On principal component biplots stream water classified by the Corine Land Cover peat bog class displays a distinct absence of components typically associated with carbonate rocks and agricultural activities, such as Ca, HCO_3^- , NO_3^- and P. Conversely, these stream waters exhibit a relative enrichment trend in chalcophile elements, including Zn and Pb, that may be ascribed to element adsorption in the organic-rich peat.

Cluster analysis shows that Zn and Cd are closely associated in stream water samples. Cd is a notable component of sphalerite in many base-metal deposits in Ireland. NPOC is part of a larger cluster with both Zn and Cd and can be interpreted to reflect complexation of metals by organic-rich material such as peat. Thus, apparent anomalies of Zn and Cd may reflect base-metal mineralization or simply enrichment following complexation within organic-rich subsoils and sediments.

Analysis of background threshold values was employed to define anomalous Zn and Cd concentrations. Those anomalous concentrations linked with known mineralization generally have low NPOC concentrations. Principal component analysis reinforces this distinction. Maps of PC3 and PC4 illustrating the positive scores of PC3 and PC4 principal components that have chalcophile enrichment without corresponding NPOC enrichment may be useful for targeting exploration strategies.



6. References

Aherne, S., Reynolds, N.A. & Burke, D.J. (1992). Gold mineralization in the Silurian and Ordovician of south Mayo. In: Bowden, A.A., Earls, G., O'Connor, P.G. & Pyne, J.F. (eds). The Irish Minerals Industry 1980-1990. Irish Association for Economic Geology, Dublin, 39-50.

Arkle Resources (2021). Inishowen Gold Project. <https://arkleresources.com/wp-content/uploads/2021/06/INISHOWEN-GOLD-PROJECT-2021.pdf>

Breiman, L. (2001). Random Forests. *Mach. Learn.* 45, 5–32.

Browne, M.A. and Gallagher, V. (2020). Tellus geochemical survey: shallow topsoil multi-element maps for the northern half of Ireland, Geological Survey Ireland. (<https://www.gsi.ie/en-ie/data-and-maps/Pages/Geochemistry.aspx#>)

Browne, M.A., Szpak, M. and Gallagher, V. (2021). Tellus Geochemical Survey: deeper topsoil multi-element maps for the northern half of Ireland. Geological Survey Ireland. (<https://www.gsi.ie/en-ie/data-and-maps/Pages/Geochemistry.aspx#DeeperTopsoils>)

Bullock, C. and Clinch, J.P. (2001). Cost-Benefit Analysis of a Resource and Environmental Survey of Ireland. Environmental Studies Research Series (ESRS) Working Paper, Department of Environmental Studies, University College Dublin.

Clifford, J.A., Ryan, P. & Kucha, H. (1986). A review of the geological setting of the Tynagh orebody, Co. Galway. In: Andrews, C.J., Crowe, R.W.A., Pennell, W.M. and Pyne, J.F. *Geology and Genesis of mineral deposits in Ireland*. Irish association of Economic Geology, Dublin. 419 – 439

Cole, G. A. J. 1922. Memoir and Map of Localities of Minerals of Economic Importance and Metalliferous Mines in Ireland. Memoirs of the Geological Survey of Ireland.

Conroy Gold and Natural Resources (2021) Clontibret Gold Target. <http://www.conroygoldandnaturalresources.com/projects/clontibret>

Davis, J.C. (2002). Statistics and Data Analysis in Geology. 3rd edn. John Wiley & Sons Inc.

De Vivo, B., Ander, E.L., Bidovec, M., Lima, A., Pirc, S., Reeder, S., Siewers, U. and Smith, B. (2006). Distribution of elements in stream water. In: De Vos, W. and Tarvainen, T. (Eds.) *Foregs Geochemical Atlas of Europe Part 2*. Geological Survey of Finland, Espoo.

European Commission (2009). European Communities environmental objectives (surface waters) regulations 2009. European Commission.

European Commission (2020). Communication from the commission to the European Parliament, the Council, the European Economic and Social Committee and the



Committee of the regions. Critical Raw Materials Resilience: Charting a Path towards greater Security and Sustainability.

Gallagher, V., Knights, K., Carey, S., Glennon, M. and Scanlon, R. (2016a). Atlas of Stream Sediment Geochemistry of the Northern Counties of Ireland: Data from the Tellus and Tellus Border Project. Geological Survey of Ireland.

Gallagher, V., Knights, K., Carey, S., Glennon, M. and Scanlon, R. (2016b). Atlas of Topsoil Geochemistry of the Northern Counties of Ireland: Data from the Tellus and Tellus Border Project. Geological Survey of Ireland.

Gallagher, V., Knights, K., Scanlon, R., Mather, J., Glennon, M. and Hodgson, J. (2018). 'Tellus Survey Ireland: Regional surface water geochemistry as an exploration tool and environmental indicator', *Resources for Future Generations (RFG 2018)*. Premier Conference on Energy Minerals, Water, the Earth. Vancouver, BC, Canada. 16-21 June 2018.

Geological Survey Ireland (2020a). Tellus Stream Waters Geochemical Survey Data - Areas G1, G3 and G4 (2011-2017) [dataset]. Geological Survey Ireland, Ireland. <https://www.gsi.ie/en-ie/data-and-maps/Pages/Geochemistry.aspx#StreamWaterW>.

Geological Survey Ireland (2020b). Tellus Stream Waters Geochemical Survey Data Release Note - Areas G1, G3 and G4 (2011-2017). Geological Survey Ireland, Ireland. https://www.gsi.ie/documents/Tellus_Geochemistry_Survey_Block_G1_G3_G4_Stream_Waters_Data_Release_Notes.pdf.

Geological Survey Ireland (2020c). Tellus Stream Sediment Geochemical Survey Data - Areas G1, G3 and G4 (2011-2017) [dataset]. Geological Survey Ireland, Ireland. <https://www.gsi.ie/en-ie/data-and-maps/Pages/Geochemistry.aspx#StreamSedimentC>.

Geological Survey Ireland (2020d). Tellus Stream Sediment Geochemical Survey Data Release Note- Areas G1, G3 and G4 (2011-2017). Geological Survey Ireland, Ireland. https://www.gsi.ie/documents/Tellus_Geochemistry_Survey_Block_G1_G2_G3_G4_Stream_Sediments_Data_Release_Notes.pdf

Geological Survey Ireland (2020e). Tellus geochemical survey: stream water data from the border and west of Ireland. Geological Survey Ireland, Ireland. Quality report. https://gsi.geodata.gov.ie/downloads/Geochemistry/Reports/Tellus_W_geochemistry_data_report_2020_v1.0.pdf

Glennon, M., Gallagher, V., Meehan, R. and Hodgson, J. (2020). Geochemically Appropriate Levels and Geochemical characterization and geochemically appropriate levels for Soil Recovery Facilities. Geological Survey Ireland report.

Grunsky, E.C. (2010). The interpretation of geochemical survey data. *Geochemistry, Exploration, Environment Analysis*. 10, 27–74.



Grunsky, E.C., Drew, L.J., Smith, D.B. (2018). Analysis of the United States Portion of the North American Soil Geochemical Landscapes Project – A Compositional Framework Approach, in Handbook on Mathematical Geosciences: Fifty Years of IAMG, 313-346, Springer. ISBN 978-3-319-78999-6.

Harris, J.R. and Grunsky, E.C. (2015). Predictive lithological mapping of Canada's north using Random Forest classification applied to geophysical and geochemical data; *Computers & Geosciences*. 80, 9–25.

Hitzman, M.W. (1986). Geology of the Abbeytown Mine, Co. Sligo, Ireland. In: Andrews, C.J., Crowe, R.W.A., Pennell, W.M. and Pyne, J.F. (Eds.) *Geology and Genesis of mineral deposits in Ireland*. Irish association of Economic Geology, Dublin, 341 – 353.

Hunt, E., O'Driscoll, B. and Daly, J.S. (2011). Parental magma composition of the syntectonic Dawros Peridotite chromites, NW Connemara, Ireland. *Geol. Mag.*, 149, 590-605.

Khater, A. (2006). Uranium and heavy metals in Phosphate Fertilizers. In: Merkel, B.J. and Hasche-Berger, A. (Eds), *Uranium, Mining and Hydrogeology*, pp 193-198. Springer (doi: 10.1007/978-3-540-87746-2_26)

Levinson, A.A. (1974). *Introduction to Exploration Geochemistry*, Applied Publishing, Calgary, Canada, 612pp.

Lydon, K. and Smith, G. (2014). CORINE Landcover 2012 Ireland. Final Report. GIO Land Monitoring 2011 – 2013 in the framework of regulation (EU) No 911/2010. EPA / European Environment Agency / Copernicus.

McArdle, P., Reynolds, N., Schaffalitzky, C. and Bell, A.M. (1986). Controls on the mineralization in the Dalradian of Ireland. In: Andrew, C.J., Crowe, R.W.A., Pennell, W.M. and Pyne, J.F. (Eds.) *Geology and Genesis of Mineral Deposits in Ireland*. Irish Association for Economic Geology, Dublin, 31 – 43.

Molina, M., Aburto, F., Calderon, R., Cazanga, M. and Escudey, M. (2009) Trace Element Composition of Selected Fertilizers Used in Chile: Phosphorus Fertilizers as a Source of Long-Term Soil Contamination. *Soil and Sediment Contamination*. 18, 495-511.

Morris, J.H. (1984). The Metallic Mineral Deposits of the Lower Palaeozoic Longford-Down Inlier, in the Republic of Ireland. Geological Survey of Ireland Report Series RS 84/1 (Mineral Resources), pp72.

Nitrates Directive (1991). COUNCIL DIRECTIVE of 12 December 1991 concerning the protection of waters against pollution caused by nitrates from agricultural sources (91/676/EEC). <http://data.europa.eu/eli/dir/1991/676/2008-12-11>.



O'Connor, P.J., Reimann, C. and Kürzl, H. (1988). *A geochemical survey of Inishowen, Co. Donegal*. Geological Survey of Ireland Report Series, RS 88/1.

O'Connor, P.J. and Reimann, C. (1993). Multielement regional geochemical reconnaissance as an aid to target selection in Irish Caledonian terrains. *Journal of Geochemical Exploration*, 47, 63-87.

Palarea-Albaladejo, J., Martín-Fernández, J.A. and Buccianti, A. (2014). Compositional methods for estimating elemental concentrations below the limit of detection in practice using R. *Journal of Geochemical Exploration*. 141, 71–77.

Peters, A., Merrington, G. and Crane, M. (2012). Estimation of background reference concentrations for metals in UK freshwaters. Water Framework Directive – UK Technical Advisory Group (WFD-UKTAG). Sniffer/Environment Agency.

Reynolds, N., McArdle, P., Farrell, L.P.C., Flegg, A.M. (1986). Mineral localities in the Dalradian and associated igneous rocks of Connemara, Co. Galway. Geological Survey of Ireland, Report Series RS 86/3 (Mineral Resources).

Schapire, R. E. (1990). The Strength of Weak Learnability. *Machine Learning*, 5, 197-227.

Simo, I., Creamer, R.E., O'Sullivan, L., Reidy, B., Schulte, R.P.O. and Fealy, R.M. (2014). Irish Soil Information System: Soil property maps (2007-S-CD-1-S1). Final Technical Report 18. Environmental Protection Agency. <http://erc.epa.ie/safer/reports>.

Simpson, P., Edmunds, W., Breward, N., Cook, J., Flight, D., Hall, G. & Lister, T. (1993). Geochemical mapping of stream water for environmental studies and mineral exploration in the UK. *Journal of Geochemical Exploration*, 49, 63-88.

Slowey, E.P. (1986). The zinc-lead and barite deposits at Keel, County Longford. In: C.J. Andrew, R.W.A. Crowe, S. Finlay, W.M. Pennell and J.F. Pyne (eds) *Geology and Genesis of Mineral Deposits in Ireland*. Irish Association for Economic Geology, Dublin, 319–330.

Stanley, G., Gallagher, V., Ní Mhairtín, F., Brogan, J., Lally, P., Doyle, E., and Farrell, L. (2009). *Historic Mine Sites – Inventory and Risk Classification, Volume 1: A joint study carried out by The Environmental Protection Agency and The Geological Survey of Ireland*. Environmental Protection Agency, Wexford, Ireland. Available at: <https://www.epa.ie/publications/monitoring--assessment/assessment/historic-mine-sites---inventory-and-risk-classification-volume-1.php>.

Thompson, S.J., Shine, C.H., Cooper, C., Halls, C. & Zhao, R. (1992). Shear-hosted gold mineralization in Co. Mayo, Ireland. In: Bowden, A.A., Earls, G., O'Connor, P.G. & Pyne, J.F. (eds.) *The Irish Minerals Industry 1980-1990*. Irish Association for Economic Geology, Dublin, 21-38.



Torremans, K., Kyne, R., Doyle, R., Guven, J.F. and Walsh, J.J. (2018). Controls on metal distributions at the Lisheen and Silvermines deposits: insights into fluid flow pathways in Irish-type Zn-Pb deposits. *Economic Geology*, 113, 1455–1477.
<https://pubs.geoscienceworld.org/segweb/economicgeology/article/113/7/1455/566507>

Trodd and O’Boyle (2020). Water quality in 2019: An indicators report. Environmental Protection Agency, Wexford.

Venables, W.N. and Ripley, B.D. (2002). *Modern Applied Statistics with S* (Fourth Edition); Springer, Berlin, 504 p. http://www.bagualu.net/wordpress/wp-content/uploads/2015/10/Modern_Applied_Statistics_With_S.pdf [November 2019].

Wall, B., Cahalane, A. and Derham, J. (eds) (2020). Ireland’s Environment – An Integrated Assessment 2020. Environmental Protection Agency.

Wallace, L., Schroder, I., de Caritat, P., English, P., Boreham, C., Sohn, J., Palatty, P. and Czarnota, K. (2020). Northern Australia Hydrogeochemical Survey, Data Release, Preliminary Interpretation and Atlas — Tennant Creek, McArthur River and Lake Woods Regions. *Geoscience Australia Record 2018/48* (eCat 122089).

Wang, B., Wanty, R. & Vohden, J. (2005). Geochemistry of surface-waters in mineralized and non-mineralized areas of the Yukon-Tanana Uplands. *Impacts of Global Climate Change*.

Ward, J.H.Jr. (1963). Hierarchical grouping to optimize an objective function. *Journal of the American Statistical Association*, 58. 236-244.

Webb, J.S., Nichol, I., Foster, R., Lowenstein, P.I. and Howarth, R.J. (1973). *Provisional Geochemical Atlas of Northern Ireland* (Technical Communication 60). London. Applied Geochemistry Research Group, Imperial College of Science and Technology.
http://www.researchgate.net/publication/265457227_Provisional_Geochemical_Atlas_of_Northern_Ireland.

Wilkinson, J.J., Eyre, S.L. and Boyce, A.J. (2005). Ore-forming processes in Irish-type carbonate-hosted Zn-Pb deposits: evidence from mineralogy, chemistry, and isotopic composition of sulphides at the Lisheen Mine. *Economic Geology*, 100, 63–86.
<https://pubs.geoscienceworld.org/segweb/economicgeology/article-abstract/100/1/63/151075>

Young, M.E. and Donald, A.W. (eds.) (2013). *A guide to the Tellus data*. Geological Survey of Northern Ireland, Belfast.

Young, M.E. (2016) The Tellus geoscience surveys of the north of Ireland: context, delivery and impacts. In Young, M.E. (ed.) *Unearthed. Impacts of the Tellus Surveys of the North of Ireland*. Royal Irish Academy, Dublin, 3-10.

